Application of Game Theory to Interactive Lane Change Decision Making for Autonomous Driving

by

Zejian Deng

A thesis

presented to the University of Waterloo

in fulfillment of the

thesis requirement for the degree of

Doctor of Philosophy

in

Mechanical and Mechatronics Engineering

Waterloo, Ontario, Canada, 2022

© Zejian Deng 2022

Examining Committee Membership

The following served on the Examining Committee for this thesis. The decision of the Examining Committee is by majority vote.

External Examiner	Dr. Fengjun Yan Associate Professor, Department of Mechanical Engineering, McMaster University
Supervisor	Dr. Amir Khajepour Professor, Department of Mechanical and Mechatronics Engineering, University of Waterloo
Internal Member	Dr. Soo Jeon Associate Professor, Department of Mechanical and Mechatronics Engineering, University of Waterloo
Internal Member	Dr. Zhao Pan Assistant Professor, Department of Mechanical and Mechatronics Engineering, University of Waterloo
Internal-external Member	Dr. Liping Fu Professor, Department of Civil and Environmental Engineering, University of Waterloo

Author's Declaration

This thesis consists of material all of which I authored or co-authored: see Statement of Contributions included in the thesis. This is a true copy of the thesis, including any required final revisions, as accepted by my examiners.

I understand that my thesis may be made electronically available to the public.

Statement of Contributions

This doctoral thesis is accomplished in the manuscript option. Three required manuscripts have been published as refereed conference or journal papers. I was the co-author with major contributions on designing the methods, implementation and writing the papers. I was supervised by Prof. Amir Khajepour. Other co-authors also contributed to the implementation and proofing of these works:

1. **Deng, Z.**, Hu, W., Yang, Y., Cao, K., Cao, D., & Khajepour, A. (2022, October). Lane change decision-making with active interactions in dense highway traffic: A Bayesian game approach. In 2022 IEEE 25th International Conference on Intelligent Transportation Systems (*ITSC*) (pp. 3290-3297). IEEE.

This paper is incorporated in Chapters 3-6 of this thesis.

2. Hu, W., **Deng, Z.**, Cao, D., Zhang, B., Khajepour, A., Zeng, L., & Wu, Y. (2022). Probabilistic Lane-Change Decision-Making and Planning for Autonomous Heavy Vehicles. *IEEE/CAA Journal of Automatica Sinica*, 9(12), 2161-2173.

This paper is incorporated in Chapters 3 and 4 of this thesis.

3. Zhu, X., Hu, W., **Deng, Z.**, Zhang, J., Hu, F., Zhou, R., ... & Wang, F. Y. (2022). Interaction-Aware Cut-In Trajectory Prediction and Risk Assessment in Mixed Traffic. *IEEE/CAA Journal of Automatica Sinica*, 9(10), 1752-1762.

This paper is incorporated in Chapters 4 and 5 of this thesis.

Abstract

The decision-making and motion planning play a critical role in the autonomous driving by connecting the perception to the vehicle control. It aims at generating available paths in the specific driving environment considering vehicle safety and driving efficiency constraints as well as the ride comfort. The complexity of the decision-making depends on the target driving performances and the driving environment.

The complexity of the future driving environment, due to the coexistence of automated and human-driven vehicles, makes the balance between safety, efficiency, and comfort much more challenging. Therefore, the focus of this research is to provide decision-making algorithms for an autonomous vehicle in the interactive driving environment where the surrounding vehicles are driven by human drivers who are unpredictable due to diverse driving behaviors.

To tackle the above problem, tools from game theory are utilized to analyze the interactions between rational players. To consider the driver intentions of the surrounding vehicles, games with complete information and incomplete information are discussed. The driver behavior is learned during the driving process, based on the Gaussian Mixture Model (GMM) trained by the naturalistic driving data. Then the driver behavior of surrounding vehicles is transmitted to the incomplete information game model, so that the human preferences can be estimated and utilized by the ego vehicle to regulate the predictions of the driving environment. Based on the model of incomplete information game, the uncertainty and the variety of the surrounding human-driven vehicles are both focused. The driving decisions can be made adaptively according to the driving styles of the surrounding vehicles.

The lane change scenario on a highway is selected as the research scene to test the performances of the proposed decision-making model. To make the simulation environment more realistic, the motions of the surrounding vehicles are modelled by the Intelligent Driver Model (IDM), whose driving styles are calibrated and classified in an explainable way based on the real driving data. Multiple scenarios are designed with driving style combinations of various surrounding vehicles. Moreover, the two-player game is extended to the multi-player game with the lateral behavior of the vehicles considered. Finally, the proposed model is validated

by comparing the generated driving decisions and trajectories with human drivers' driving profiles under the same driving conditions extracted from the naturalistic driving data. The results show that the driver aggressiveness estimation could help the ego vehicle change lane more efficiently and guarantee safety under the incomplete information model. The developed game-based decision-making model shows high potential to handle the uncertain interaction between the autonomous vehicle and human-driven vehicles.

Acknowledgements

My Ph.D. study at the University of Waterloo has been a great experience for me in the last four years. I am deeply grateful for the support I have received. First and foremost, I would like to thank my supervisor, Professor Amir Khajepour for teaching me how to determine impactful research problems, organize the thoughts, write clearly, give cohesive presentations, and cooperate with others in research.

I would also like to thank my thesis committee members, Prof. Liping Fu from the Department of Civil and Environmental Engineering, Prof. Soo Jeon and Prof. Zhao Pan from the Department of Mechanical and Mechatronics Engineering at the University of Waterloo. They offer insightful comments and valuable feedback on this thesis. Special thanks to Prof. Fengjun Yan from McMaster University for serving as my external committee member.

Besides research, I am thankful to my friends and colleagues in the Mechatronic Vehicle Systems Laboratory, and the teammates who love playing basketball and working out. I can never forget the moment when we won the Champions in the University of Waterloo's intramural basketball match. Their company helps me maintain balance between work and life, and makes the Waterloo region an amazing place for me to study and live.

Finally, I would like to express my heartfelt gratitude to my parents and family. This work could not be finished without their endless love and support.

Dedication

This thesis is dedicated to my parents.

Table of Contents

List of Figures

List of Tables

Chapter 1

Introduction

1.1 Motivation

Approximately 1.35 million people die each year due to road traffic crashes in the world [1]. Highway-related accidents claimed 37,133 lives in 2017 only in America [2]. A study conducted by the National Highway Transportation Safety Administration (NHTSA) found that human error causes 94% of serious crashes [3]. The automated driving technology and Advanced Driving Assistance Systems (ADAS) have the potential to reduce and eventually eliminate human driving errors resulting in reducing road fatalities, increasing traffic efficiency and improving driving comfort.

Since human-driven vehicles cannot be replaced in a short time period, it is foreseeable that automated and human-driven vehicles will coexist in the **mixed traffic** environment in a the foreseeable. One of the crucial tasks of automated vehicles is to make human-like driving decisions when interacting with human drivers to ensure safety and efficiency.

Given the information about the road and surrounding obstacles, a **decision-making and planning module** is responsible for generating a feasible path that can avoid collisions, save traveling time, and make users feel comfortable. Decision-making algorithms still need significant improvement to be able to deal with **complex interactive scenarios**. Recent reviews show that Google cars cannot plan future trajectories and speed profiles when facing unpredictable actions of other human traffic participants [4], [5]. A human driver can understand the intentions of other drivers in decision-making especially in complex scenarios.

It can be observed that most drivers can understand the intentions, predict the driving behaviors of other drivers, and make proper decisions in the strongly interactive scenarios. Therefore, the goal of this project is to enable the autonomous vehicles behave in a socially compliant way in highway lane change scenarios, which are common but highly interactive. Different from the non-interpretable methods, such as end-to-end, neural networks, and deep learning, the

interpretabilities are stressed in the proposed decision-making model. In fact, a well-established **game theoretical framework** has been utilized to describe such active interactions in multiple disciplines, such as economics [6], biology [7], and computer science [8]. Game theory is equipped with solid mathematical foundations to analyze the interactions between players. To effectively utilize the collected driving data, GMM is trained and utilized to determine the human drivers' aggressiveness during the interactive driving. With human preferences learned, the proposed model can make adaptive decisions when interacting with drivers with different driving styles. Meanwhile, the generated paths can capture the patterns of human drivers.

1.2 Research question

Most decision-making models ignore or unreasonably simplify the interaction. The interactive behavior is a pervasive and complex behavior in human driver decision-making. Therefore, how to make safe and efficient driving decisions and enable the autonomous vehicles behave in a socially compliant way is the research question when interacting with other real human traffic participants.

1.3 Objectives

Compared with urban scenarios, highway driving is much simpler with respect to the types and numbers of traffic participants, traffic scenarios, and driving behavior. In highway traffic, car following (CF) and lane changing (LC) are two primary driving tasks. Considering the highly interactive characteristics of lane changing, developing the game theoretic decision-making model for interactive highway lane changing is the focus of this Ph.D. research. Hence, the research objectives are:

Interactive lane change decision-making modeling based on game theory

The lane change process will be analyzed first to determine the components under the framework of game theory. Meanwhile, the human behavior will be investigated, and some behavior patterns can be found for lane change modeling. The knowledge domain of the players is important in the game. Thus, the game with complete information and incomplete information will be discussed. The driver intentions of the surrounding vehicles will be studied and integrated in the game-based decision-making model, to consider the varieties of human

driving behaviors.

Model tuning using real driving data

To capture the driving behavior patterns of real human drivers, the physical motion model is utilized to mimic the human driving behavior from the naturalistic driving data. The model parameters are tuned based on the selected single-vehicle and interactive features. These decision patterns can be analyzed to obey the multi-dimensional Gaussian distribution. Then the connections are made between the driving features and learning-based parameters tuning. Upon such tuning, the proposed model could show optimal preferences defined by the users when interacting with different drivers.

Validation of the decision-making model

The proposed model will be evaluated and validated in different lane change scenarios first in a simulation environment and then using real driving data. The performances of the proposed decision-making model will be compared with other traditional models in different complex cases. Synthetic assessment criteria will be established to evaluate the decision-making model in terms of safety, speed efficiency, and lane change success rate.

1.4 Thesis outline

This research thesis is structured as follows. In the second chapter, the literature is reviewed regarding game theory based driving decision-making methods. In the third chapter, the proposed interactive lane change decision-making model is developed in terms of two-player game and multi-player game. The fourth chapter introduces the naturalistic driving data that are connected to the motion modeling of the environment vehicles and driver identification model. In the fifth chapter, the motion models of the surrounding vehicles and the driver type identification method are developed based on the human driving data. The sixth chapter shows simulation results and analysis. The human-driven vehicles are programmed to drive aggressively or cautiously, and the interaction results are used to assess the performance of the developed decision-making model. In the seventh chapter, the main findings in this study are concluded, and future work is highlighted.

Chapter 2

Literature Review

This chapter reviews the decision-making methods for autonomous vehicles, focusing on the issue of interactive behavior in the presence of other moving vehicles. Existing studies on conventional decision-making methods are reviewed first in Section 2.1. Then Section 2.2 discusses the vehicles' interactions in the highway lane change. The game-theoretical models are then reviewed to formalize the vehicle-vehicle interactive driving decision-making behavior in Section 2.3. The literature review is concluded in Section 2.4.

2.1 Autonomous driving decision-making methods

From the perspective of responding to the surrounding environment, driving decision-making can be divided into three stages, i.e., strategic, tactical and operational levels [9]–[12], or in other expressions, strategic, maneuvering and control levels, as shown in Fig. 2.1 [13].

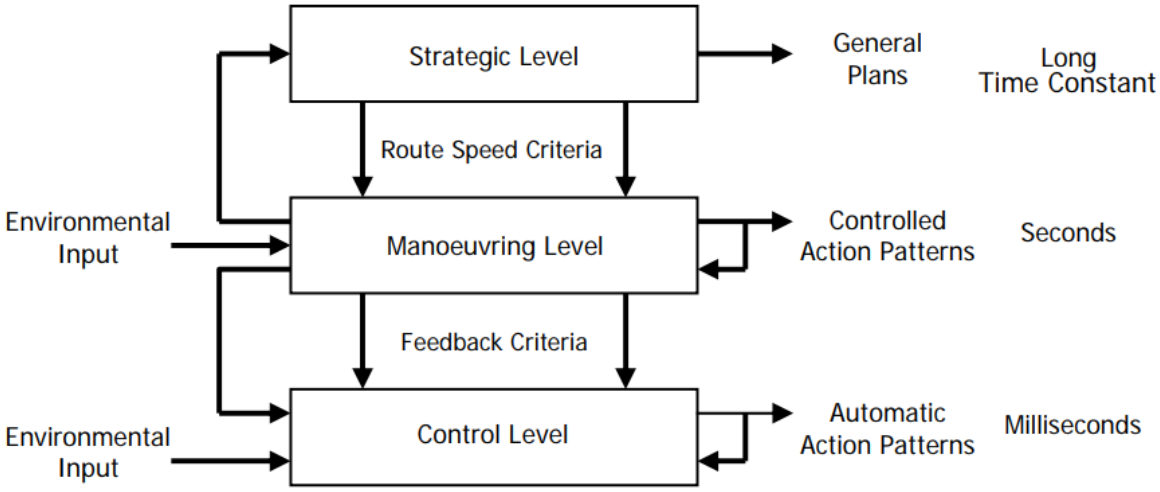

Figure 2.1. The hierarchical structure of the driving tasks [13]

Strategic decisions are responsible for the choice of destination and global route, which take minutes or even hours to make [9][10]. Examples of tactical decisions include keeping lane, changing lane, accelerating, turning right, [11][12] etc. The strategic decision is composed of a series of tactical decisions, which take 5 to 30 seconds to complete [14]. In the operational

stage, the main issue is to decide when to execute the decisions and how to complete the required maneuvers with time scale of a short term [15]. According to this classification, the driving decision-making methods reviewed here is mainly focused on the tactical level.

2.1.1 Rule-based methods

State machine

An intuitive solution for making decisions is the rule-based method, which is encoded with rules according to human experiences. In fact, most teams that finished the game in the 2007 DARPA Urban Challenge utilized the State Machine to release the driving decisions, switching between predefined behaviors [16]–[18]. These predefined driving behaviors are selected in real time based on the current driving environment and vehicle states. This type of model mainly includes Finite State Machine (FSM) and Hierarchical State Machine (HSM).

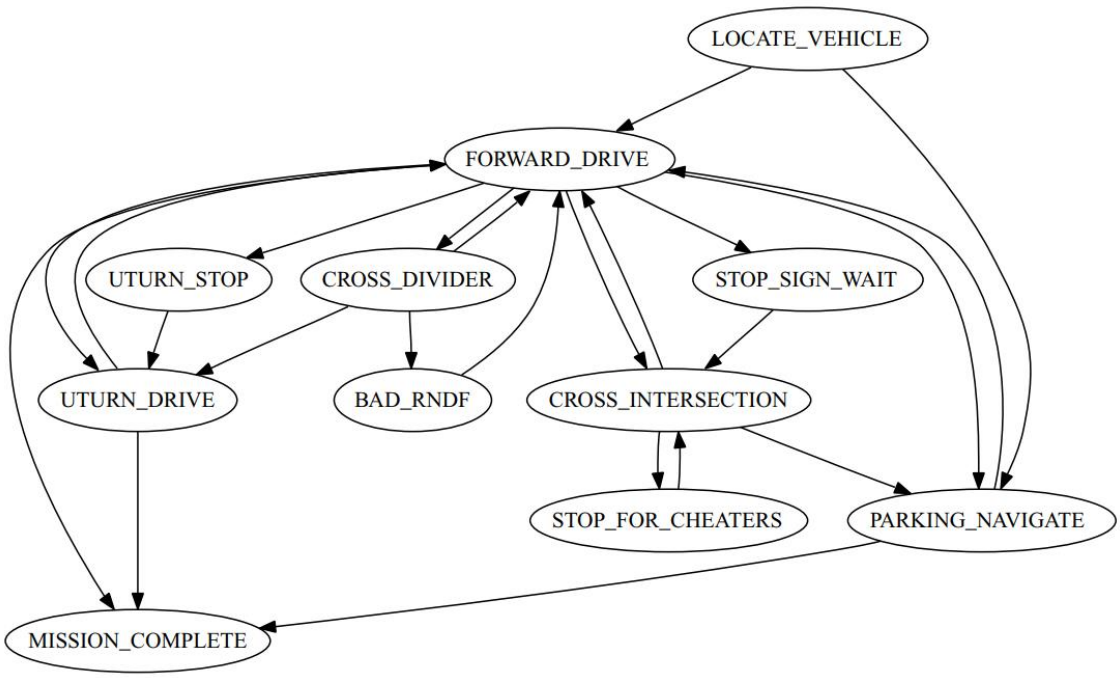

Figure 2.2. FSM that governs the robot's behavior [18]

FSM is a mathematical model that describes systems with discrete input-output, consisting of events, states, and state transitions. Fig. 2.2 shows the FSM model of Stanford's robot "Junior" [18], which consists of 13 states (only 11 are shown), including initial state, lane keeping, crossing intersection, mission complete, etc. Because of its simple structure and clear control

logic, FSM has been adopted by the Champion Team A1 of the AVC in Korea in 2012 [19] and the Vislab's robot "Terramax" [20].

When the driving states increase, the structure of the FSM becomes messy and difficult to modify. To deal with this problem, HSM defines the high-level and low-level states. Fig. 2.3 shows the HSM-based decision structures for the parking zone context of the Knight Rider autonomous vehicle in the DAPRA competition in 2007. When the top state (parking area driving state) is activated, the state machine starts working. HSM not only describes the driving state hierarchically but also limits the switch path of the state machine [21]. HSM was adopted by CMU's BOSS and OSU-ACT in the 2007 DAPRA competition [16], [22].

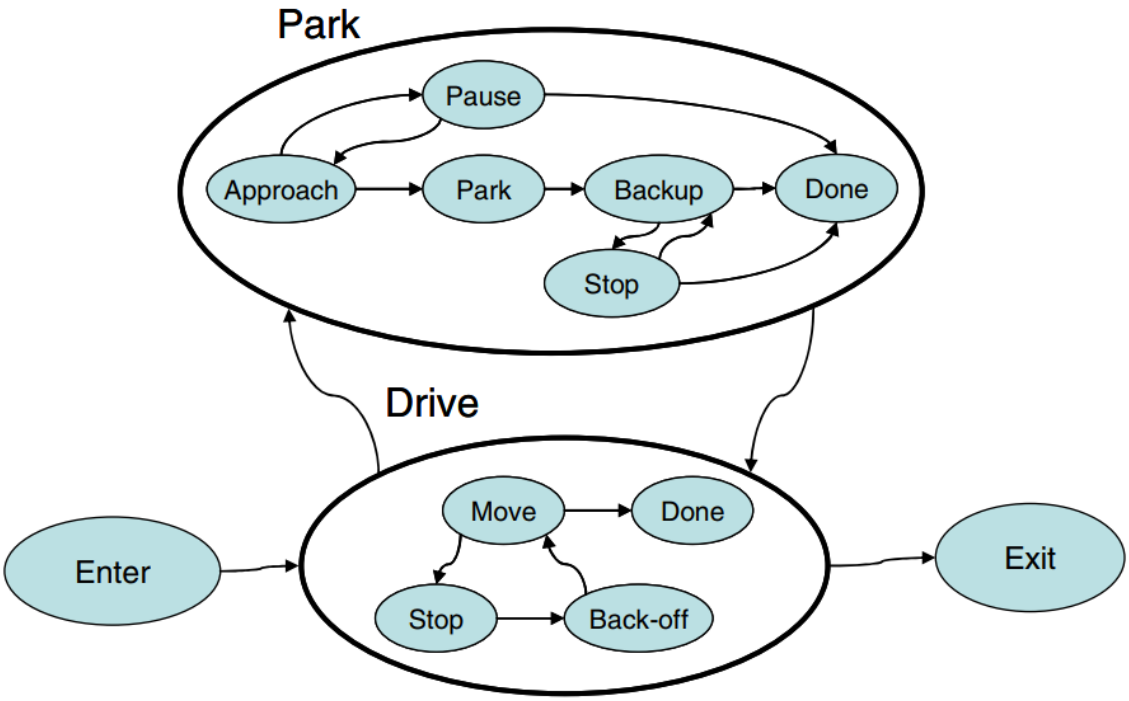

Figure 2.3. HSM that governs the robot's behavior [21]

Decision tree-based methods

A decision tree is composed of internal nodes and leaf nodes that can be used for classification and decision-making purposes. Claussmann et al. [23] planned a finite set of deterministic candidate driving decisions of right lane change, left lane change and keeping the same lane under the framework of binary decision diagrams. Team Cornell's Skynet [24] in the DARPA Challenge adopted the decision tree to check the feasible passing maneuver in the face of other

moving vehicles. Li et al. [25] proposed an explicit decision tree approach to improve the performance in computational effort and state transition accuracy for a case study of autonomous driving on a two-lane highway. It was utilized as a benchmark to be compared with the method of the Stackelberg game theoretic decision-making process in terms of collision rates [26].

2.1.2 Knowledge-based models

The knowledge-based reasoning decision-making model mimics the behavioral decision-making process of human drivers through the mapping from scene features to driving actions.

Neural network-based methods

The mapping relationships between driving scene features and driving actions are automatically obtained by supervised learning in the neural network, which avoids the trivial work of manual feature extraction and strategy modifications. Dating back to 1989, the model adopted by Carnegie Mellon University consists of three layers of back propagation neural network, where the input is camera and lidar data, and the output is the direction control commands to the vehicle [27]. In recent years, deep learning has also been applied to the behavioral decision-making system of autonomous vehicles. Bojarski et al. [28] used the convolutional neural network (CNN) to learn the mapping function from the pixel-level features of perceived images to specific control commands to mimic the driving behavior of human driver. Similar approaches have been adopted by some other researchers [29].

Bayesian network and its extensions

Bayesian network (BN) is a kind of probabilistic graph model that stores the driving knowledge in the form of causal links between nodes based on probabilistic transitions. Ulbrich et al. [30] presented BN-based situation assessment approach in tactical behavior planning to determine the benefits and possibilities for lane changes. Schubert et al. [31] used an extended Bayesian network to derive lane-change maneuver decisions for highly automated driving. Kasper et al. [32] detected the lane change decisions based on the object-oriented Bayesian network (OOBN).

Dynamic Bayesian network (DBN) specifies causal relationships and temporal dependencies simultaneously. As Fig. 2.4 shows, Schulz et al. [33] modelled the interaction-aware behavior of drivers based on the constructed DBN. With the interaction-aware motion predictions, the autonomous vehicle is supposed to make proper decisions considering the uncertainty in measurements and human behavior. Hierarchical DBN integrates the physical relationships with the driver behaviors in [30], [31]. The interactions are considered through the intention predictions that are regarded as prior information for decision-making.

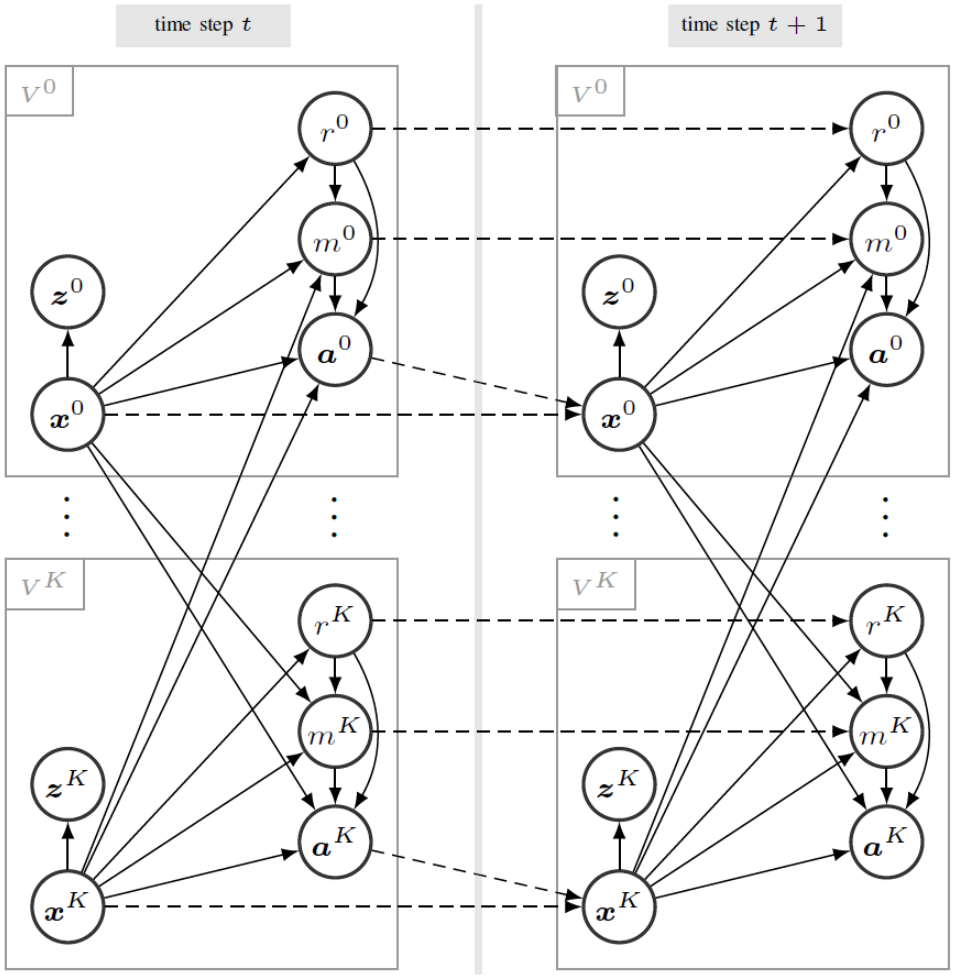

Figure 2.4. Interaction-aware behavior of drivers based on the constructed DBN [33]

2.1.3 Utility-based models

The majority of the aforementioned behavioral decision-making methods employ heuristics to determine the best driving strategy based on prior driving experience. It is necessary for these methods to specify a driving strategy for each driving scenario, which is based on state

transition, rules generation or mapping relationships.

Action evaluation based on predefined cost function

According to the maximum utility theory, the basic idea of a utility/value-based decision model is to select the optimal driving action among multiple alternatives based on the selection criteria [34]. Furda et al. [35] proposed a multi-criteria decision-making to select the optimal one from the candidates. The behavioral decision system of the Caroline automated vehicle in the 2007 DAPRA Challenge [36] is based on the distributed architecture for mobile navigation scheme (DAMN). A cluster of candidate driving trajectories was first generated, and then the votes were given based on multiple criteria. Similar to the scheme, the behavioral decision model based on Prediction-and-Cost-function (PCB) is proposed by Carnegie Mellon University. After the prediction of the surrounding traffic scenarios, the optimal strategy is obtained through evaluating the candidate strategy using the predefined cost function [37].

Markov decision process-based models

A Markov decision process (MDP) is models the decision-making process based on the Markov property. Guan et al. [38] modelled the driving task as MDP, considering safety, efficiency and comfort in a dynamic traffic environment. Since reinforcement learning (RL) is capable of finding optimal solutions to problems modelled by MDP, it is widely used in the autonomous driving decision-making issues. Loiacono et al. [39] trained the agent with simple RL to overtake the surrounding vehicles. Li et al. [40] compare the overtaking policies from Q-learning and the expert system, and find that the former always obtains a higher reward under a series of traffic conditions. The results indicate that Q-learning performs better to ensure safety but is approximately the same in efficiency. Ngai et al. [41] propose a multiple-goal reinforcement learning (MGRL) framework to instruct the autonomous vehicle to overtake other cars when there are a large number of surrounding vehicles at different and varying speeds.

As the number of states increases, standard Q-learning algorithms cannot find a feasible policy solution due to the computational effort. Another option is to use a Q-function approximator to output the Q values, which normally rely on the neural networks. Wang et al. [42] made the agent change lane automatically through a deep Q-learning algorithm that reduced the

computation in both continuous state space and action space.

Table 2.1 Taxonomy of autonomous driving decision-making methods

Algorithm group	Technique	Technique description	How is interaction involved	Implemented in
Rule-based methods	State machine	Finite State Machine (FSM)	The interaction is specified by the transitions among states and modules	[18]–[20]
		Hierarchical State Machine (HSM)		[16], [21], [22]
	Decision tree	The optimal path is selected by the attribute test with internal node, branch and leaf node	The root node contain information with most interactions and the goal is to generate leaf nodes with less interaction information	[23]–[26]
Knowledge-based methods	Neural network	The actions are executed according to the existed driving experience materialized to the network	Interaction information is contained in the features and how they jointly predict the outcomes	[27]–[29], [43]
	Bayesian network family	The driving knowledges are stored in the form of causal links between nodes in the probabilistic graph	The causal links model the interactions as probability	[30]–[33]
Utility-based models	Multi-criteria decision-making	Each candidate driving action is evaluated by the utility in terms of safety, comfort, driving efficiency, etc.	The interaction term is evaluated in the utility	[35], [36]
	Prediction-and-cost-function	Optimal strategy is obtained through evaluating the candidate strategy using the cost function	Cost function quantifies the interaction	[37]
	Markov decision process (MDP)	Utilizing RL to solve it with unknown reward and transition functions	Interaction can be included in the state transitions and reward function	[38]
		Utilizing dynamic programming when the environment model is known		[39]–[42], [44], [45]

Using Long Short-Term Memory (LSTM), they applied DRL in the on-ramp merge scenario, where the states contain historical driving information [44]. Hoel et al. [45] investigated fully connected neural networks (FCNN) and temporal convolutional neural networks (CNNs) to approximately calculate the optimal value function, and generate driving decisions for a truck-trailer, which is also known as Deep Q-Network (DQN).

In summary, the decision-making methods for autonomous driving are classified into three groups in terms of the principles that lead to the driving decisions from the goal setting, internal states, and environment information, as shown in Table 2.1. Each group can be further divided into specific algorithms or models. When reviewing these models, interactions become increasingly important, from traditional methods to the most recent studies.

2.2 Vehicles interactions in the highway lane change

Interaction, by definition, requires communication between the participants. Interacting agents make responses according to the observed information and the orders of the decision system, affecting the states of each agent. The literature is classified according to the **intelligence level** of the surrounding vehicles.

2.2.1 Unidirectional reactive interaction

For the unidirectional reactive interaction, the surrounding vehicle is supposed to follow a specific physics law, and does not consider the behavior of the autonomous vehicle (ego vehicle). Under this circumstance, the autonomous vehicle can achieve perfect accuracy if the physics law of the surrounding vehicle is captured. Some assumptions constrain the ego or surrounding vehicles to move straight, such as the Constant Velocity (CV) [46] and Constant Acceleration (CA) [47] models. To consider the planar motion, the yaw angle and yaw rate are introduced in the models such as Constant Turn Rate and Velocity (CTRV) and Constant Turn Rate and Acceleration (CTRA), where the parameters in the longitudinal and lateral directions are decoupled [48][49]. Furthermore, the Single-track Model (STM) [50] integrates the yaw rate and velocity to the state variables, while the bicycle model replaces the yaw rate with the steering angle.

As is presented in Fig. 2.5, the autonomous ego vehicle (EV) is affected by the surrounding vehicles, but the EV itself does not have any effects on the surrounding vehicles. The surrounding vehicles then follow the predefined motion laws without considering the EV's current or future states, such as CA in car-following scenarios and CTRV in lane change cases. Simultaneously, the EV is required to predict the future states of the surrounding vehicles and make driving decisions. Therefore, the interaction is bidirectional and reactive.

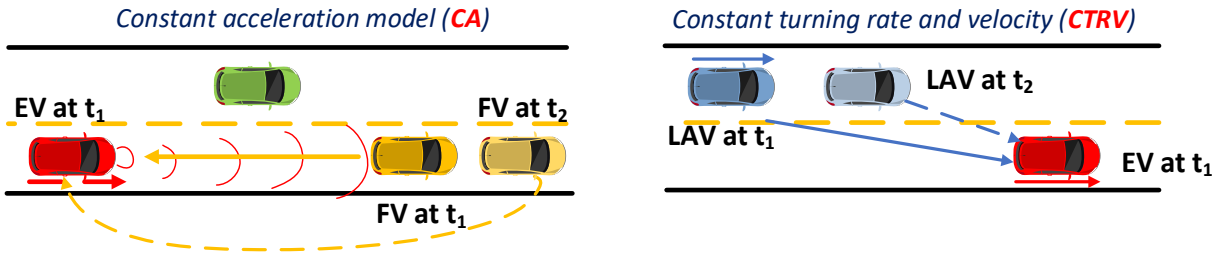

Figure 2.5. The illustrative scenarios of unidirectional reactive interaction

These single-vehicle feature-based prediction methods are often used for vehicle tracking control. When the surrounding vehicles are dominated by these physical models, the interaction only exists in the ego vehicle's reaction to their motions. The complexity is greatly reduced when there is no coupling relationship between the autonomous vehicle and surrounding vehicles.

2.2.2 Bidirectional reactive interaction

The prediction and decision-making based on the unidirectional reactive interaction do not account for the effects of the surrounding vehicles. This prediction model can be utilized for model-based state estimations and vehicle tracking control, but is too simple when there are other vehicles surrounding it. More recently, the bidirectional reactive interaction has attracted the attention because the mutual effects exist in real traffic. For the bidirectional reactive interaction, the surrounding vehicle is supposed to react to its driving environment, which means the connection is built from the ego vehicle to the surrounding vehicle.

Potential field model is widely used to analyze the interactions between the autonomous vehicle and other traffic participants [51][52]. It can consider the vehicle types and road structures by

assigning different potential functions, so that the path can be generated depending on the driving environment. Obviously, the interactions are contained in the mutual effects of these potential functions. One important advantage of this pure physics-law-based method is that the calculation cost is low, and it can be applied to online decision-making.

Since the main considerations for the surrounding vehicles are their longitudinal motions, the car-following models are used to capture the interactions between the lag vehicle and the lane change vehicle. Gazis-Herman-Rothery (GHR) model [53]–[55] considers the velocity difference between the subject vehicle and the preceding vehicle as the stimulus for generating the corresponding longitudinal acceleration, which is aimed at balancing the velocities and keeping a safe distance between two vehicles. Besides, there is a sensitivity parameter to regulate the value by introducing constant parameters, relative distance, lag vehicle's speed, etc. Newell [56] proposed a car-following model whose output is the velocity of the following vehicle, where the maximum speed and the minimum space headway are included. Also, the spacing between the vehicles is an important parameter in this model. Intelligent driver model (IDM) is a typical reactive model that generates longitudinal acceleration according to the driver's desire and driving environment [57]. This model is popular because it considers the driver's desired driving states, and is thus adaptive by tuning the corresponding parts. More importantly, these parameters are interpretable.

These models are essentially physics-laws-based models, while the parameters extend from the single-vehicle features to the interactive features. The interactions are formulated between the surrounding vehicles with those motion models and the ego autonomous vehicle with the proposed decision-making model in the literatures. Therefore, the human drivers are not required to participate as the surrounding vehicles to validate the proposed decision-making model, and this type of interaction is popular in the validation part of the literature that requires a large number of training episodes.

2.2.3 Bidirectional active interaction

The active interaction implies that the surrounding vehicles can predict future states and are aware of the ability to change those states through their actions. The active interaction involves

two aspects. The first one is the current states and future states. The second is between the ego and surrounding vehicles. What's more complicated, these two issues can also be coupled. However, this type of interaction is what the real traffic shows.

According to the definition of the bidirectional active interaction, the surrounding vehicle should have the ability to predict and consciously use this ability to interact with others. Dynamic Bayesian networks (DBN) describe the interactions in the form of probability and directed acyclic graphs. In the fully connected DBN, the actions and states of the ego and its surrounding vehicles are connected, representing the mutual effects between each other. Besides, the temporal dependencies and measurement uncertainties can also be considered. Schulz et al. [33] predict the behavior of other vehicles based on DBN, where the intentions of drivers and the trajectories interdependencies are considered. The results show that the interaction-aware model performs better than both CTRV and map-based models. Gonzalez et al. [58], [59] model the multi-vehicle dependencies based on DBN, where the surrounding vehicles' maneuvers are sampled from the posterior distribution of each traffic participant, given the observations of all vehicles, while the ego vehicle's action is determined by minimizing the cost after listing all the possibilities. Gindele et al. [60], [61] explicitly modeled the interactions between traffic participants using DBN. The vehicle behavior is estimated by evaluating the driving environment. However, graph models like DBN are actually intractable in most cases if the number of vehicles increases. The complexity of inference grows exponentially with the number of considered agents and possible intentions.

Another option is to predict all the possible results, considering the reactions of the other drivers before making decisions. Game theory is a well-developed theoretical framework that can determine the solutions when the coupled relationships existed. The utilities can be determined assuming the decisions have been made. Since the combinations of each player's actions are all considered, the active interactions are contained in the utility functions. For the static game, the interactions between merging and through vehicles are quantified by anticipating the other's action [62], [63]. Also, the utility functions can be modelled with the cumulative rewards if the lane change is considered as a repeated game [64], [65]. For the dynamic game, the players are recognized as leader and follower, and the normal game is

switched to the game tree [66]. However, the transitions can be made so that the equilibriums can be solved in the same way.

In summary, most research focuses on the unidirectional reactive interaction and bidirectional reactive interaction in the lane change modeling and later validation experiments. Game theory is found to be applicable in the scenarios with bidirectional active interaction. Many game theory models have been developed for highway lane change scenarios, however, lacking the considerations of the human drivers' varieties, which are critical for human-like decision-making.

2.3 Game theory based driving decision-making methods

As the aforementioned sections state, human drivers are not reactive agents, which means that they are able to observe the surrounding traffic participants, predict the future states of others, and make decisions considering the potential actions of other agents. More importantly, human drivers would have the same expectations from others, which makes it paradoxical to explain the human decision-making process solely using prediction-based methods because the predictions can be changed given the ability of active agents to predict others' intentions.

In fact, a well-established game theoretical framework has been utilized to describe such active interactions in multiple disciplines, such as economics [6], biology [7], and computer science [8]. Game theory is equipped with solid mathematical foundations to analyze the interactions between rational players with their anticipations of other players' behavior considered. Compared with reactive models, the game theoretic frameworks can be utilized to describe the active interactions in the driving decision-making process.

2.3.1 Static game-based driving decision-making

In the static game, players are assumed to move simultaneously. A payoff matrix lists the players of a game, their strategies and related payoffs. As an earlier application of a static game in the highway merging scenario, Kita [62], [63] developed a game-based model to consider the interactions between merging and through vehicles, as shown in Fig. 2.6. The driving goal

of Vehicle 1 is to merge onto the main road within a limited distance, or the crash will happen. To achieve this goal, it needs to interact with other surrounding vehicles and decide when and how to change lanes. This process is modelled as a non-cooperative static game with complete information. The results indicate the capability to explain merging and give-way behaviors in the real world.

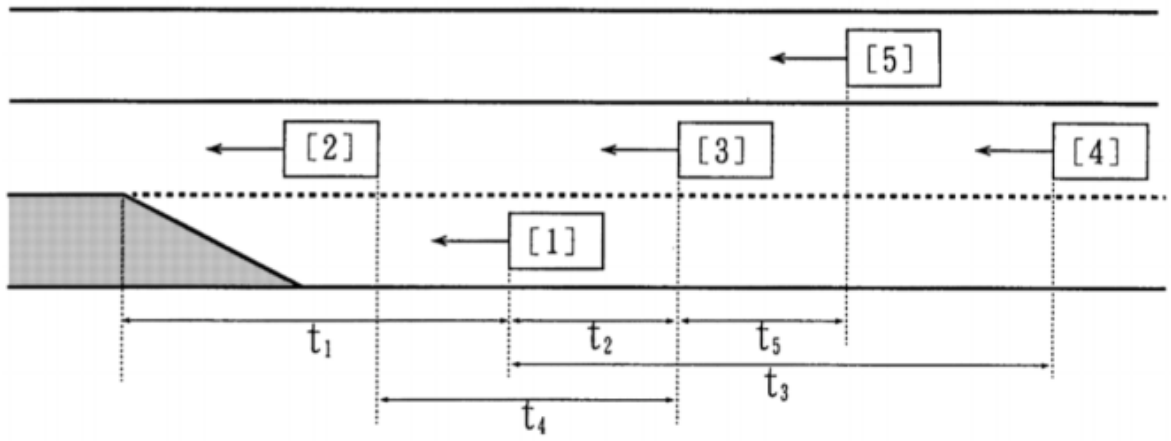

Figure 2.6. Highway ramp merging scenario

After Kita, Liu et al. [67] modelled the merging behavior at the highway on-ramp as a two-player non-cooperative game. An important contribution is that the payoffs contain the predicted states and actions of both vehicles, which are conformed to the decision-making paradigm of human drivers. Kang et al. [68] first modelled the merging behavior as a one-time game that begins when the ego vehicle enters the merging lane. The merging vehicle can overtake the leading vehicle besides waiting for the lag vehicle and merging between the lead and lag vehicles. Safety and speed efficiency are two factors that each vehicle considers in their payoff functions. The proposed method avoids the potential difficulties of determining the exact decision time and position, however, it is not adaptive to the dynamic surrounding environment.

Lane changing is another common and challenging driving behavior which includes rich interactions between lane changing vehicle and lag vehicle. Talebpour et al [69] presented a game-theoretical lane change model with two game types, where the difference is whether to know the driving intentions of the others through V2V communication. For the lane-changing vehicle, the payoff functions mainly consider safety and speed efficiency. To strictly guarantee

lane change safety in a dynamic environment, Meng et al. [70] introduce the concept of Receding Horizon Control (RHC) to handle uncertainties of the surrounding vehicles through reachability analysis. The reachable set is utilized to conduct safety assessments in autonomous driving. Instead of assuming the exact future information is known [68], upper and lower bounds are determined for the interested parameters in terms of the ranges of current states. By introducing RHC, new information is taken into account when making driving decisions, which is important for a safe and smooth lane change.

2.3.2 Dynamic game-based driving decision-making

The aforementioned game models assume both players should act simultaneously, while some other researchers believe there exists a leader who acts first, and the follower makes decisions according to both observations and the actions of the leader. Therefore, the game becomes dynamic, with the payoffs in the form of a game tree.

In Kang's later work, a repeated game was utilized to model the driver merging behavior by introducing successive decision-making, assuming driving decisions are made repeatedly to adapt to the dynamic surrounding environment. The payoffs are then calculated cumulatively over time period $\boldsymbol{T}$ rather than instantaneously. The model is evaluated using the NGSIM data, and the results show prediction accuracy is over 75% in terms of mean absolute error (MAE). Similarly, Ali et al. [71] modelled the merging behavior in the connected environment as a dynamic game. The difference is that the driving environment is determined with probability $\boldsymbol{p}$ to be a traditional environment, and $\boldsymbol{1\text{-}p}$ to be a connected environment, which becomes another variable that can affect the driving decisions.

Yoo et al [72], [73] modelled highway ramp merging as a Stackelberg game because it is similar to the hierarchical decision-making process in highway driving, in which information is transferred backward. For the utility design, positive and negative utilities are defined for merging and acceleration games, however, with different inputs. It is worth noting that the authors begin by considering the driver characteristics, which have a significant impact on utility determination and parameter setting, and thus influence driving decisions. Yu et al. [66] utilized game theory to determine when and how to change lanes with possible interaction

between vehicles, as shown in Fig. 2.7. The payoff functions consist of safety and space payoffs. Since the drivers' driving behaviors are various, the aggressiveness of competing vehicles is introduced as the indicator for driving style evaluation, which is used for weighting the safety and space payoffs. Specially, the aggressiveness of the competing vehicle is estimated and updated based on the interaction behavior. Therefore, the Stackelberg equilibrium would also change as the aggressiveness of competing vehicles changes at each time step, which explains human lane changing behavior in the real driving to some extent.

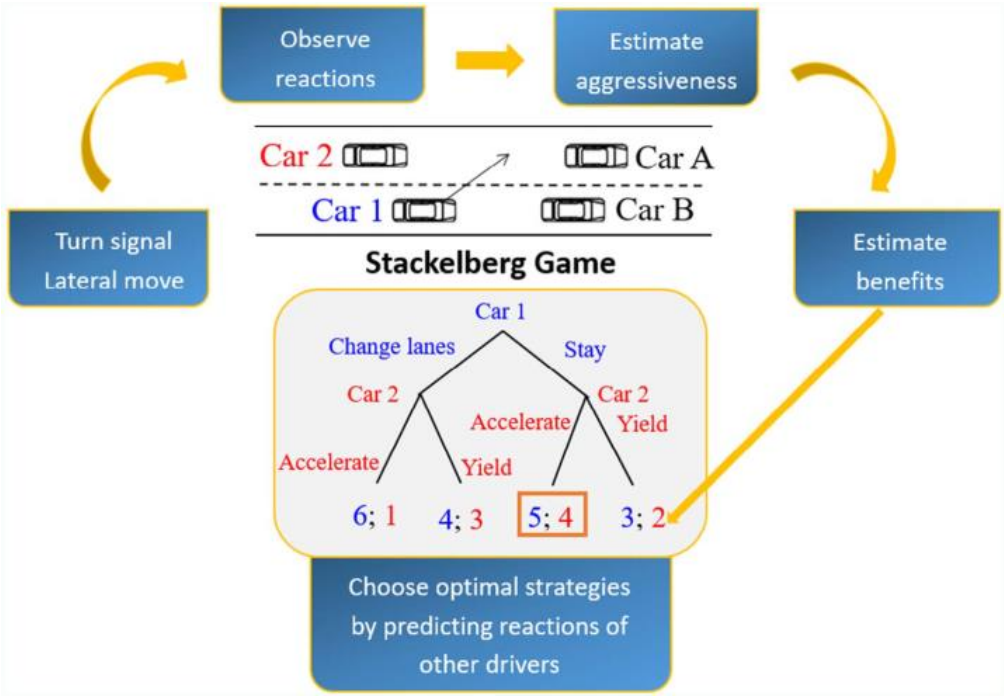

Figure 2.7. Schematic diagram of Stackelberg game based lane change interaction model [66]

2.3.3 Deep coupling of game theory and control module

One disadvantage of hierarchical framework-based decision-making is that the decisions are discrete, which means that they can differ from one another many times in a short period of time. Some studies directly integrate the high-level decision-making and low-level control modules by combining game theory and control algorithms. In fact, this kind of idea has been applied in the area of engineering, such as in shared control [74], [75], where the cost function of Player A contains the interaction terms that are affected by Player B. The task is to solve the transformed optimization problem and generate the control variables under the constraints [76].

Wang et al [77] combined the high-level lane change decisions and low-level controllers to determine the discrete lane change sequences and continuous accelerations, where the interactions can be considered through the cost functions. The joint cost function considers comprehensive factors that are composed of safety cost, equilibrium cost and control cost. The game theory-based model is proved to generate optimal lane change decisions in various scenarios.

Other examples include the ramp merging and intersection left turn behaviors, where the cost functions are learned from data [76], [78], which avoids the complex induction of human preferences and their dependent relationship with each other. However, the learning-based reward functions are less interpretable compared with the rule-based ones.

Table 2.2 Taxonomy of game theory-based decision-making models in traffic scenarios

Game type	Scenarios	Information integrity	Driver type recognition	References
Static game	Ramp merging	Complete	No	[62], [63], [67], [68]
	Lane change	Complete	No	[69]
		Incomplete	No	[70]
Dynamic game	Ramp merging	Complete	No	[64], [65], [71]
		Incomplete	Yes	[72], [73]
	Lane change	Incomplete	Yes	[66]
Coupled with control variable	Ramp merging	Incomplete	Yes	[76]
	Lane change	Incomplete	No	[127]
			Yes	[77]
Behavioral game	Ramp merging	Complete	No	[79]
	Lane change	Complete	No	[80]

The game models applied in the interactive driving decision-making are summarized in Table 2.2. In summary, game theory has been applied to describe the microscopic interaction behavior with different game types in the previous studies. The forms are also evolving from a hierarchical decision-making and planning framework to one that is deeply coupled with control variables and the cost function bridge. Some other game types, such as behavioral game theory, have also been developed and revised for making driving decisions with new assumptions in recent years [79], [80]. However, these assumptions and game models have not been verified in the on-field test and are not explained from the aspect of interaction

mechanisms. Therefore, the interaction mechanism needs further study to propose more reasonable assumptions and accurate game models.

Driver characteristics or driver types are important when making lane change decisions [81][82]. Aggressive drivers move more drastically at the operational level, and are willing to taking higher driving risks when making decisions in the tactical level than cautious drivers. However, driving styles are not adequately reported with respect to many game theory-based decision-making models. Therefore, driver recognition methods need further investigation and will be indispensable in future game theory-based models.

2.4 Summary

Current decision-making methods for autonomous vehicles can be classified in terms of multiple perspectives, including rule-based, knowledge-based and utility-based methods. While the interaction is an important factor that determines the complexity of decision-making problem, the types of interaction are not well clarified. As the assumptions of the interaction level differ, the decision-making framework will vary greatly.

It is clear that the bidirectional active interaction is what the autonomous vehicles have with human-driven vehicles in the real mixed traffic. Also, the competing vehicles type can influence the interaction results to some extent. Game theory is appropriate to obtain the human-like strategies when interacting with human drivers. Furthermore, human drivers are not homogeneous, leading to various decisions even under the same situation. Therefore, how to connect the decision-making model to the real driving data, and adaptively make human-like decisions through data training is to be investigated.

Chapter 3

Autonomous Lane Change Modeling Based on Game Theory

In this chapter, the lane change behavior is firstly analyzed by dividing the stages into intention generation, preparation, and execution. The vehicle states, actions, goals and strategies are then formulated as the essentials for lane change decision-making. After that, the lane change decision process is modelled under the framework of game theory, and two types of games are presented as the assumptions for the information availability differ. Moreover, the two-player game is extended to a multi-player game with the lateral behavior of the players considered. The preliminary simulation results validate the proposed decision-making model.

3.1 Lane change behavior analysis

3.1.1 Lane change phase divisions

Lane changing is a routine but complex and risky behavior in highway driving. As is shown in Fig. 3.1 (a), there are 4 surrounding vehicles after the ego vehicle (**EV**) determines which lane to change to. EV driver needs to observe the states of surrounding vehicles, including the front vehicle (**FV**) in the current lane, the leading vehicle (**LEV**) and the lag vehicle (**LAV**) in the target lane, and make decisions.

The lane change process can be divided into three stages. The first stage is the lane change intention formation process. The motivations may include the speed efficiency and safety space in discretionary lane change, and ramp merging in mandatory lane change. In the stage 2, the driver would not execute a lane change immediately but hold the lane change intention and observe the surrounding traffic conditions to determine whether it is safe to change lane. In the third stage, the driver makes sure that the conditions are safe enough to change lane, and then the executions are conducted.

For the first stage, it is difficult to measure the driver's intentions level for lane change from the observations. Essentially, the human intention changes without any observable motion pattern and human themselves are sometimes not sure whether the intention is lane change or lane keeping, regardless of the quantitative degree of intention. During this period, drivers are focused on pursuing better driving conditions which are mainly determined by FV and LEV. The turning signal should be turned on when the intention level exceeds a certain threshold value, which happens at time point T_0 in Fig. 3.1. (b).

For the second stage, the EV driver needs to observe the traffic conditions carefully to determine the object lane and the appropriate time point for lane change. In this stage, EV is required to adjust its longitudinal and lateral states to create a safe condition for future successful lane change. EV should consider the constraints of FV and LEV. Meanwhile, it is possible for EV to create safety gap between LAV through active interactions.

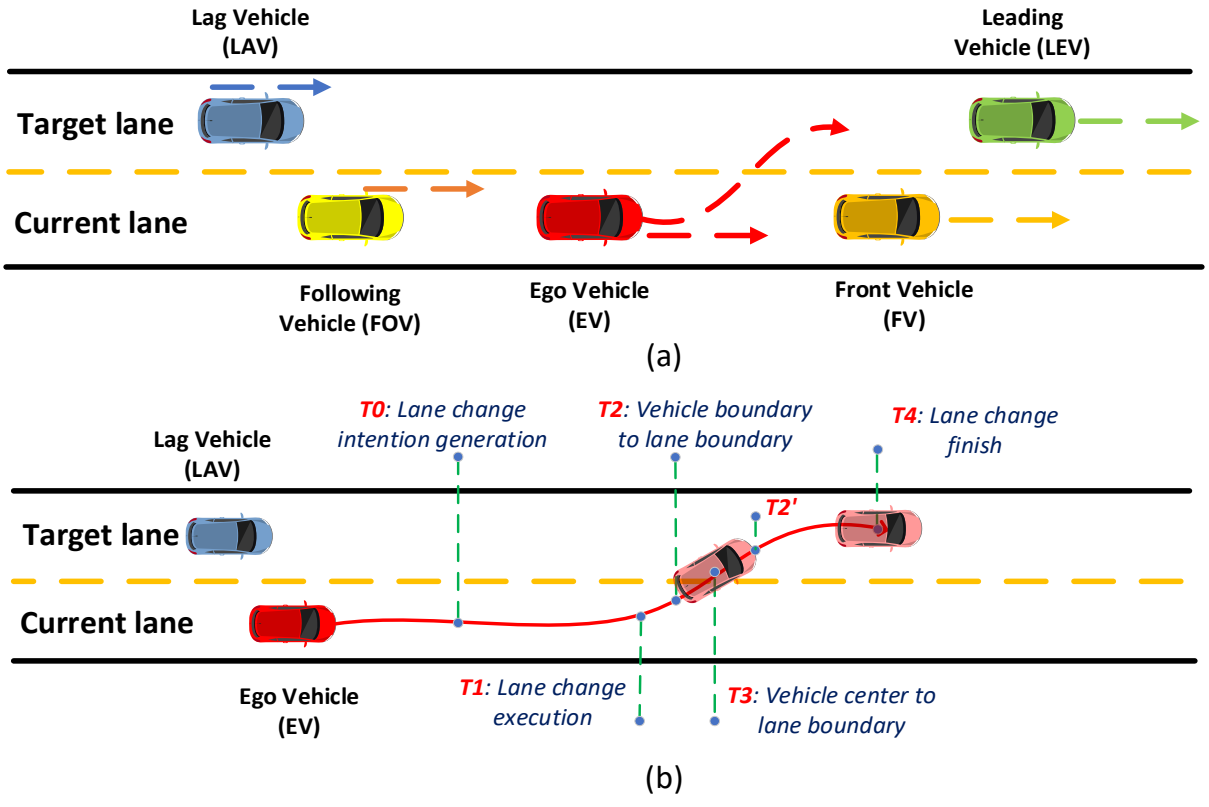

Figure 3.1. Schematic diagram of lane change scenario: (a) traffic environment, (b) lane change process division

After the safe gaps have been created, the EV driver needs to execute lane change behavior in

the third stage. Defined by the time point when lateral speed is over 0.35 m/s [83], EV starts to change lane at T_1, as is shown in Fig. 3.1. (b). There are three critical time points during vehicle crossing, which are T_2, T_3 and $T_{2'}$, when the vehicle's left boundary, center and right boundary cross the lane boundary. During vehicle crossing period [T_2, $T_{2'}$], the EV should maintain a safe distance to LAV. Once the entire vehicle body crosses the lane line, it becomes the LAV's task to keep a safe distance from the EV, which shows the sudden responsibility transition in the lane change. Finally, the lane change finishes when the lateral speed decreases to 0.2 m/s at T_4.

3.1.2 Lane change process formalization

Aiming at protecting the right-of-way of each participant [84], the rules-of-thumb in this traffic act are explained as follows:

(1) For the car-following scenarios, the following car should be able to stop behind the front vehicle even if it suddenly brakes.

(2) For the lane change scenarios, the lane change vehicle should not affect the normal driving of other vehicles in the target lane.

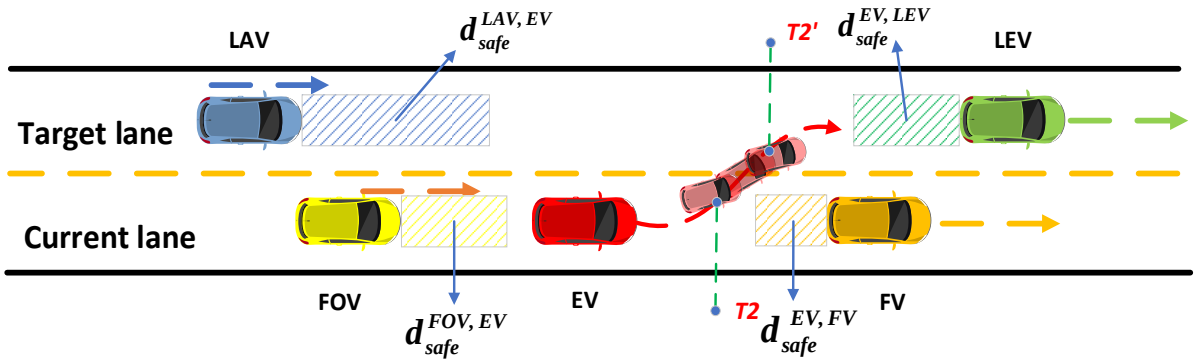

Figure 3.2. Safe distances in the lane change

According to the traffic rules, EV should be careful to avoid approaching the safe distance area in different stages, as shown in Fig. 3.2. Before T_2, EV follows FV, so it is only required to be cautious of $d_{safe}^{EV,FV}$. During vehicle crossing period of [T_2, $T_{2'}$], EV should keep three safe distances from LAV, LEV and FV. After $T_{2'}$, EV enters the target lane and follows LEV, so it

only needs to keep a safe distance $d_{safe}^{EV,LEV}$ from LEV.

Goals and constraints

Drivers care about three aspects of goals in normal driving, namely driving safety, efficiency and comfort, so do they in lane change scenarios. Then the goal is modeled as a linear combination of driving safety, efficiency and comfort with corresponding weighting factors.

$$J_{EV} = \omega_s^{EV} J_s^{EV} + \omega_e^{EV} J_e^{EV} + \omega_c^{EV} J_c^{EV} \tag{3.1}$$

where ω_s^{EV}, ω_e^{EV} and ω_c^{EV} are the weighting coefficients of the safety, efficiency and comfort costs.

For **lane change safety**, the risks come from the surrounding vehicles if their positions overlap in both longitudinal and lateral directions simultaneously. There are sudden responsibility transitions in the lane change process when the ego vehicle finishes lane change. The previous LAV becomes the new following vehicle (FOV), and the responsibility to avoid collisions is transferred from the EV to the LAV. Therefore, the safety cost is related to the measured distance and the safe distance:

$$\begin{aligned} J_s^{EV} &= f_1(t) \cdot g\left(\frac{d_{safe}^{EV,FV} - \left(X_{FV}(t) - X_{EV}(t)\right)}{d_{safe}^{EV,FV}}\right) + f_2(t) \\ &\cdot g\left(\frac{d_{safe}^{LAV,EV} - \left(X_{EV}(t) - X_{LAV}(t)\right)}{d_{safe}^{LAV,EV}}\right) + f_3(t) \\ &\cdot g\left(\frac{d_{safe}^{EV,LEV} - \left(X_{LEV}(t) - X_{EV}(t)\right)}{d_{safe}^{EV,LEV}}\right) \end{aligned} \tag{3.2}$$

where functions $f(\cdot)$ are used to indicate the risks from surrounding vehicles according to the lane change stages,

$$f_1(t) = \begin{cases} 1, & t \le T_{2'} \\ 0, & else \end{cases}, f_2(t) = \begin{cases} 1, & T_2 \le t \le T_{2'} \\ 0, & else \end{cases}, f_3(t) = \begin{cases} 1, & t \ge T_{2'} \\ 0, & else \end{cases} \tag{3.3}$$

The indicator function $g(\cdot)$ ensures the risk range [0, 1]

$$g(x) = \begin{cases} 0, & x \leq 0 \\ x, & 0 < x \leq 1 \\ 1, & x \geq 1 \end{cases} \tag{3.4}$$

For the definition of safe distance, the model of Responsibility Sensitive Safety (RSS) is recently proposed by Intel on the premise of rigorous assumptions about the actions of other road users [85].

$$d_{safe}^{r,f} = \left[v_r \rho + \frac{1}{2} a_{max,acc} \rho^2 + \frac{\left(v_r + \rho a_{max,acc}\right)^2}{2a_{min,brake}} - \frac{v_f^2}{2a_{max,brake}} \right]_+ \tag{3.5}$$

where subscripts r and f represent rear and front vehicles, separately. The notation $[x]_+ := max\{x, 0\}$. The rear vehicle is assumed to accelerate with maximum acceleration when the front vehicle suddenly brakes with maximum deceleration. After ρ seconds, the rear vehicle starts to decelerate with minimum deceleration to avoid collisions with front vehicle. RSS model can guarantee safety in such a scenario, which indicates its conservation and potential to be a benchmark for absolute safety in the car-following scenario.

The longitudinal speed is selected as the feature to model the **travel efficiency** goal, which is

$$J_e^{EV} = \left[v_x^{EV}(t) - v_{x,desired}^{EV} \right]^2 \tag{3.6}$$

where

$$v_{x,desired}^{EV} = \min\left(v_{x,max}^{EV},\ v_x^{LEV}\right) \tag{3.7}$$

The cost term on **ride comfort** is related to longitudinal and lateral jerks, which can be written as

$$J_c^{EV} = \alpha_{x,j_x}^{EV} (j_x^{EV}(t))^2 + \alpha_{y,j_y}^{EV} \left(j_y^{EV}(t)\right)^2, \tag{3.8}$$

where α_{x,j_x}^{EV} and α_{y,j_y}^{EV} are weighting coefficients; $j_x^{EV}(t)$ and $j_y^{EV}(t)$ are longitudinal and lateral jerks.

The **constraints** come from the driving safety, efficiency and comfort. For driving safety, the distance between EV and other surrounding vehicles cannot be shorter than the corresponding

safe distances. Then the **safety constraints** for collision avoidance are

$$\begin{cases} X^{FV}(t) - X^{EV}(t) \geq d_{safe}^{EV,FV}, & t < T_2 \\ X^{FV}(t) - X^{EV}(t) \geq d_{safe}^{EV,FV} \wedge X^{EV}(t) - X^{LAV}(t) \geq d_{safe}^{LAV,EV} \\ \wedge X^{LEV}(t) - X^{EV}(t) \geq d_{safe}^{EV,LEV}, & t \in [T_2, T_{2'}] \\ X^{LEV}(t) - X^{EV}(t) \geq d_{safe}^{EV,LEV}, & t > T_{2'} \end{cases} \tag{3.9}$$

Also, **vehicle stability** is considered a part of driving safety, which is constrained by the vehicle system, including acceleration, front wheel steering angle, and their increments.

$$\begin{cases} |a_x^{EV}(t)| \leq a_x^{max} \\ |a_y^{EV}(t)| \leq a_y^{max} \\ |\delta_f^{EV}(t)| \leq \delta_f^{max} \\ |\Delta a_x^{EV}(t)| \leq \Delta a_x^{max} \\ |\Delta a_y^{EV}(t)| \leq \Delta a_y^{max} \\ |\Delta \delta_f^{EV}(t)| \leq \Delta \delta_f^{max} \end{cases} \tag{3.10}$$

For **travel efficiency constraints**, EV is supposed to drive within an interval,

$$v_x^{min} \leq v_x^{EV}(t) \leq v_x^{max} \tag{3.11}$$

Driver comfort is mainly affected by the jerk, so it is formulized as

$$\begin{cases} |j_x^{EV}(t)| \leq j_x^{max} \\ |j_y^{EV}(t)| \leq j_y^{max} \end{cases} \tag{3.12}$$

To summarize, the lane change task of EV is modelled as an optimization problem with constraints from driving safety, vehicle dynamics, travel efficiency and driver comfort. Especially, for lane change decision-making, EV should consider the surrounding traffic conditions over the next few seconds so that the planned path is optimal without breaking the constraints. For each time point, the cost function is an accumulation of all time points in the prediction horizon.

3.2 Lane change modeling as a two-player game

The above analysis shows that the lane change vehicle has its own objective functions and constraints, which are related to the motions of surrounding vehicles. However, the interactions result in coupled effects between the EV and other surrounding vehicles, and the optimization-

based decision-making model cannot handle it. For example, the lane change vehicle's safety J_s^{EV} is closely related to the safety distance between it and other vehicles, which is determined by the behavior of both sides. Moreover, perfect predictions of other vehicles' trajectories are impossible because there are time-dependent mutual effects between the EV's action and other vehicles' responses. Therefore, directly generating the motion profiles based on the defined objective functions and constraints is difficult.

To avoid this situation, a hierarchical structure is adopted in this study, which is divided into decision-making, path planning and tracking control. The interaction is considered in the part of high-level game-based decision-making, where all the possibilities are listed and analyzed with the coupled effects considered. After the decision is made, the optimal trajectory will be selected from the candidate paths. The following section discusses the lane change interactions between two players, i.e., the ego vehicle and the lag vehicle.

3.2.1 Interactions with complete information

Fig. 3.3 depicts the lane change game. Different from the assumption in [66], where the ego vehicle acts first and the surrounding vehicle responds, both players have the same information and move simultaneously.

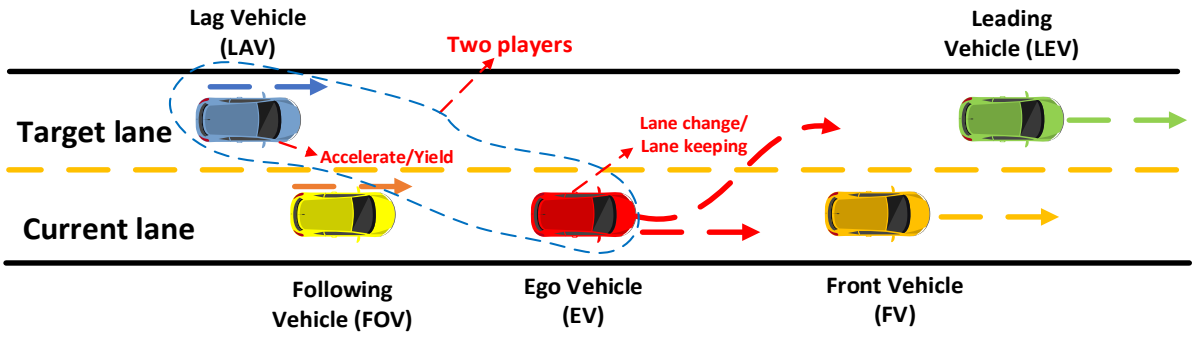

Figure 3.3. Lane change game played by EV and LAV

A Nash equilibrium is a strategy profile in which no actor can increase its utility by unilaterally altering its strategy. S_i denotes the strategy set of player i, and $u_i(s)$ is the utility function for player i. $s_i \in S_i$ stands for the strategy profile of player i, while s_{-i} means the strategy profile of all other players. We use (s_i, s_{-i}) to emphasize that player i only has direct

influence over s_i, whereas s_{-i} represents the decision variables of other players.

A strategy profile $s^* = (s_1^*, s_2^*, \dots, s_n^*)$ is a Nash equilibrium if

$$\boldsymbol{s}_i^* = \arg \max_{s_i \in S_i(s_{-i}^*)} u_i(\boldsymbol{s}_i, \boldsymbol{s}_{-i}^*), i = 1, \dots, n. \tag{3.13}$$

In our settings of the lane change game, the ego vehicle in the current lane and the lag vehicle in the target lane are considered as the players 1 and 2, respectively, and the other vehicles are environment vehicles. Then the strategy spaces for two players are $S_1 = (LC, LK)$ and $S_2 = (Yield, Acc)$.

The factors that influence decisions for the utility functions of the players are primarily safety and speed efficiency costs. When the players choose different strategies, the utilities will differ. Therefore, the player i's utilities in each scenario are essentially the function of the other player's actions, which is formally described as $u_i(a_i', s_{-i})$.

The safety utility of two vehicles is related to three basic traffic indexes, i.e., relative distance, relative velocity and the absolute velocity of the following vehicle. The combinations of these parameters derive many surrogate safety measures [86], including THW (Time Headway), TTC (Time To Collisions), DRAC (Deceleration Rate to Avoid the Crash), etc. Besides, the driver response time also affects driving safety. To comprehensively consider these factors, the index "required deceleration" is proposed based on the revised RSS model [RSS], where the minimum and maximum parameters are replaced by the real time values, and the conditions will not be that strictly conservative in terms of safety. The revised RSS model is

$$d_{safe}^{r,f} = \left[v_r \rho + \frac{1}{2} a_r \rho^2 + \frac{(v_r + \rho a_r)^2}{2a_{r,brake}} - \frac{v_f^2}{2a_{max,brake}} \right]_+ \tag{3.14}$$

Compared with Eq. (3.5), the rear vehicle is supposed to maintain its motion instead of accelerating at maximum acceleration when the front vehicle suddenly decelerates during response time. The rear vehicle would decelerate with its comfortable deceleration instead of minimum deceleration once it realizes the front vehicle's braking. If the current distance $d_{r,f}$ is given between front and rear vehicles, the required deceleration can be determined by

$$a_{req,brake} = \frac{1}{2}(v_r + \rho a_r)^2 / \left[\left(d_{r,f} + \frac{v_f^2}{2a_{max,brake}}\right) - ((v_r\rho + \frac{1}{2}a_r\rho^2))\right] \quad (3.15)$$

After the determination of safety index, the safety utility functions can be determined according to the following and leading vehicles in different situations. For example, in the {Lane change, Yield} case, the safety utility of LAV is determined by the states of LAV and EV because EV will be its leading vehicle. The EV's safety utility is determined by EV, LAV and LEV because the LEV is the expected leading vehicle of EV if making lane change. Also, the lane change vehicle should consider the effects on the lag vehicle.

A pure strategy denotes the available choice of from the action space in games [87]. Suppose player 1 has K pure strategies, and player 2 has J pure strategies. Then the strategy spaces of two players are $S_1 = (s_{11}, \cdots, s_{1K})$ and $S_2 = (s_{21}, \cdots, s_{2J})$, respectively. Considering the weighting vector is introduced to balance the parameters range and preferences of different drivers, the safety utilities of players 1 and 2 in the {Lane change, Yield} case are

$$u_{1,safety}(s_{11}, s_{21}) = \alpha_{1,11}\max\left(a_{req,brake,11}^{EV,LAV}, a_{req,brake,11}^{EV,LEV}\right) \quad (3.16)$$

$$u_{2,safety}(s_{11}, s_{21}) = \alpha_{2,11}a_{req,brake,11}^{EV,LAV} \quad (3.17)$$

where the strategy pair (s_{11}, s_{21}) means players 1 and 2 both choose the first strategy from their strategy spaces. The subscript "11" on the right-hand side of the equation means the strategy combinations of two players. The general safety utilities of each player in all possible situations can then be formalized as

$$u_{1,safety}(s_{1k}, s_{2j}) = \alpha_{1,kj}\max\left(a_{req,brake,kj}^{EV,Veh_{1x}}, a_{req,brake,kj}^{EV,Veh_{1y}}\right) \quad (3.18)$$

$$u_{2,safety}(s_{1k}, s_{2j}) = \alpha_{2,kj}a_{req,brake,kj}^{LAV,Veh_{2x}} \quad (3.19)$$

where $k = 1,2,\ldots,K; j = 1,2,\ldots,J$. In the Eq. (3.18), the required braking deceleration of the EV is determined by its actions. If the EV chooses to change the lane, Veh_{1x} will be LAV, and Veh_{1y} will be LEV. If the action is keeping the lane, Veh_{1x} will be FV in the current lane, and Veh_{1y} will not exist. For the LAV in the Eq. (3.19), the Veh_{2x} will be EV and LEV if

EV chooses LC and LK, respectively. When the front and rear vehicles are determined, the required deceleration can be calculated according to Eq. (3.15).

The speed efficiency utility is defined by the expected speed gain. The expected speed should be less than or equal to the front car's velocity in stable traffic. Then the efficiency utilities of players 1 and 2 in the *{Lane change, Yield}* case are

$$u_{1,eff}(s_{11}, s_{21}) = \beta_{1,11}(v_{LEV} - v_{EV}) \tag{3.20}$$

$$u_{2,eff}(s_{11}, s_{21}) = \beta_{2,11}(v_{EV} - v_{LAV}) \tag{3.21}$$

The general efficiency utilities of each player in all possible situations can then be formalized as

$$u_{1,eff}(s_{1k}, s_{2j}) = \beta_{1,kj}(v_{Veh_{1z}} - v_{EV}) \tag{3.22}$$

$$u_{2,eff}(s_{1k}, s_{2j}) = \beta_{2,kj}(v_{Veh_{2y}} - v_{LAV}) \tag{3.23}$$

where $k = 1,2,\dots,K; j = 1,2,\dots,J$. For the EV in the Eq. (3.22), the Veh_{1z} will be LEV and FV if EV chooses LC and LK, respectively. For the LAV in the Eq. (3.23), the Veh_{2y} will be EV and LEV if EV chooses LC and LK, respectively.

The lane change penalty is introduced to avoid the situation where the EV changes lanes when there is enough space to accelerate. Therefore, the lane change cost is defined as

$$f_{LC}(\Delta x_{EF}) = \begin{cases} 0 & \Delta x_{EF} < d_{th1} \\ \left(\frac{1}{d_{th2} - d_{th1}}\Delta x_{EF} - \frac{d_{th1}}{d_{th2} - d_{th1}}\right) & d_{th1} < \Delta x_{EF} < d_{th2} \\ 1 & \Delta x_{EF} > d_{th2} \end{cases} \tag{3.24}$$

where Δx_{EF} is the distance between EV and FV in the current lane; d_{th1} and d_{th2} are the threshold distances that determine the lane change cost. If the EV changes the lane when the EV-FV distance exceeds d_{th1}, the lane change penalty will be effective. The general lane change penalty in all possible situations can then be formalized as

$$u_{1,LC}(s_{11}, s_{2j}) = \gamma_{1,1j} f_{LC}(\Delta x_{EF}) \tag{3.25}$$

The lane change cost only exists for the player 1 (lane change vehicle) when it chooses to

change lane, and the actual distance is bigger than the threshold value d_{th1}.

The comprehensive utility functions of each player are defined as the linear combinations of safety and speed costs. Therefore, the utility functions of each player in all the possible situations are

$$u_1(s_{1k}, s_{2j}) = u_{1,safety}(s_{1k}, s_{2j}) + u_{1,eff}(s_{1k}, s_{2j}) + u_{1,LC}(s_{11}, s_{2j}) \tag{3.26}$$

$$u_2(s_{1k}, s_{2j}) = u_{2,safety}(s_{1k}, s_{2j}) + u_{2,eff}(s_{1k}, s_{2j}) \tag{3.27}$$

In the pure strategy based game, the Nash equilibrium may not exist, which cannot be applied in our decision-making framework. Therefore, the mixed strategies are introduced in this study. Then the decisions of each player in any scenario is determined by the strategy with higher probability in the Nash equilibrium. The utilities function in the pure strategy based game will be revised to the expected utilities with the probability distribution σ_i over S_i introduced. The element σ_{1k} is the probability that the player 1 selects the pure strategy s_{1k}. The expected utility of player 1 when choosing $\sigma_1 = (\sigma_{11}, \cdots, \sigma_{1K})$ is

$$v_1(\sigma_1, \sigma_2) = \sum_{k=1}^{K} \sigma_{1k} \sum_{j=1}^{J} \sigma_{2j} u_1(s_{1k}, s_{2j}) = \sum_{k=1}^{K} \sum_{j=1}^{J} \sigma_{1k}\sigma_{2j} u_1(s_{1k}, s_{2j}) \tag{3.28}$$

Similarly, the expected utility of player 2 when choosing $\sigma_2 = (\sigma_{21}, \cdots, \sigma_{2J})$ is

$$v_2(\sigma_1, \sigma_2) = \sum_{j=1}^{J} \sigma_{2j} \sum_{k=1}^{K} \sigma_{1k} u_2(s_{1k}, s_{2j}) = \sum_{k=1}^{K} \sum_{j=1}^{J} \sigma_{1k}\sigma_{2j} u_2(s_{1k}, s_{2j}) \tag{3.29}$$

The Nash equilibrium under the mixed strategies is then defined as

A strategy profile of mixed strategies $(\sigma_1, \ldots, \sigma_n)$ *for an n-player normal form game* $(I, (S_i), (u_i))$ *is a Nash equilibrium in mixed strategies if for each* i *and any alternative mixed strategy* σ_i',

$$v_i(\sigma_i, \sigma_{-i}) \geq v_i(\sigma_i', \sigma_{-i}) \tag{3.30}$$

In this section, the utility functions of two players are modelled in terms of driving safety and

efficiency. The mixed strategies are introduced, and the discrete decisions are determined by the probabilities over the strategy space in the Nash equilibrium. However, the type of LAV could be various in real traffic, leading to different driving behaviors. EV is required to estimate the driver type of the LAV and calculate the expected utilities with a new theoretical method, which will be discussed in the next section.

3.2.2 Interactions with incomplete information

In the complete information game, the players know the strategy space and utility functions of each other. The assumptions in the complete information game are actually too strong for the lane change interactions. In the lane change scenario, it is probable that the drivers do not know the utility functions without the communications. Even the popularization of V2X technology in future smart transportation could decrease the uncertainty to some degree, the information cannot be fully known by each other. Therefore, the previous model needs to be revised based on the framework of the incomplete information game.

In the lane change scenario, the lane change vehicle EV is assumed to be player 1. For the lag vehicle LAV in the target lane driven by human drivers, it is supposed to be equipped with multiple types, such as aggressive, normal and cautious. The EV does not know the specific type of the LAV, but knows the probability distribution $p(\theta_2 \mid \theta_1)$. This conditional probability distribution is the common knowledge, and each player knows it. If there are finite possible types for player 2 (LAV), then $\Theta_2 = (\theta_{21}, \ldots, \theta_{2L})$, and the sum of the conditional probability is 1

$$\sum_{l=1}^{L} p_1(\theta_{2l} \mid \theta_1) = 1 \tag{3.31}$$

Considering the mixed strategy based utility function with complete information in Eq. (3.31), the expected utility of player 1 with incomplete information will be

$$w_1(\sigma_1, \sigma_2, \theta_1) := \sum_{l=1}^{L} p_1(\theta_{2l} \mid \theta_1) v_1(\sigma_1, \sigma_2, \theta_1, \theta_2) \tag{3.32}$$

where

$$v_1(\sigma_1, \sigma_2, \theta_1, \theta_2) = \sum_{k=1}^{K} \sum_{j=1}^{J} \sigma_{1k}(\theta_1)\sigma_{2j}(\theta_2)u_1(s_{1k}, s_{2j}) \tag{3.33}$$

If the player 2 has continuous types $\theta_2 \in \Theta_2$ and take $\Theta_2 = [0, 1]$ without loss of generality, then the integration of the conditional probability over Θ_2 is 1

$$\int_0^1 p_1(\,\theta_2 \mid \theta_1\,)\, d\theta_2 = 1 \tag{3.34}$$

The expected utility of player 1 with incomplete information will be

$$w_1(\sigma_1, \sigma_2, \theta_1) := \int_0^1 p_1(\,\theta_2 \mid \theta_1\,) v_1(\sigma_1, \sigma_2, \theta_1, \theta_2)\, d\theta_2 \tag{3.35}$$

According to the definition of the Bayesian equilibrium in Eq. (A.4), player 1 will choose the strategy that maximizes $w_1(\sigma_1, \sigma_2, \theta_1)$. The integration range $\Theta_2 = [0, 1]$ denotes that the LAV's type is continuous given the EV belongs to type θ_1. $v_1(\sigma_1, \sigma_2, \theta_1, \theta_2)$ the utility of the EV over the mixed strategy space under different types of two players. Through the integration of $v_1(\sigma_1, \sigma_2, \theta_1, \theta_2)$ over the LAV's type θ_2, the EV's utility will only depends on its own type.

In this section, the lane change is modelled based on the two-player-game under the condition of incomplete information, where the EV is required to consider different types of LAV. The LAV has a continuous aggressiveness whose probability distribution can be extracted from the naturalistic driving data. This information can be encoded to EV's prior knowledge so that the proposed model could make more human-like driving decisions by learning from the driving data. The Bayesian Nash equilibrium based mixed strategy of the EV (player 1) is expected to rely on the LAV's aggressiveness according to Eq. (3.35), which is consistent with our driving experience. The next section will discuss the trajectories generation after the decisions are made.

3.3 Path planning based on quintic polynomial spline

After the high-level lane change or lane keeping decisions are made, the trajectory is generated through candidate trajectories generation and optimal path selection that are processed in the lower-level path planning module. The EV is driving in the middle lane, and the future trajectories can be widely distributed based on the driving decisions and measured kinematics parameters, such as the relative distances, THW, TTC, etc., as is shown in Fig. 3.4.

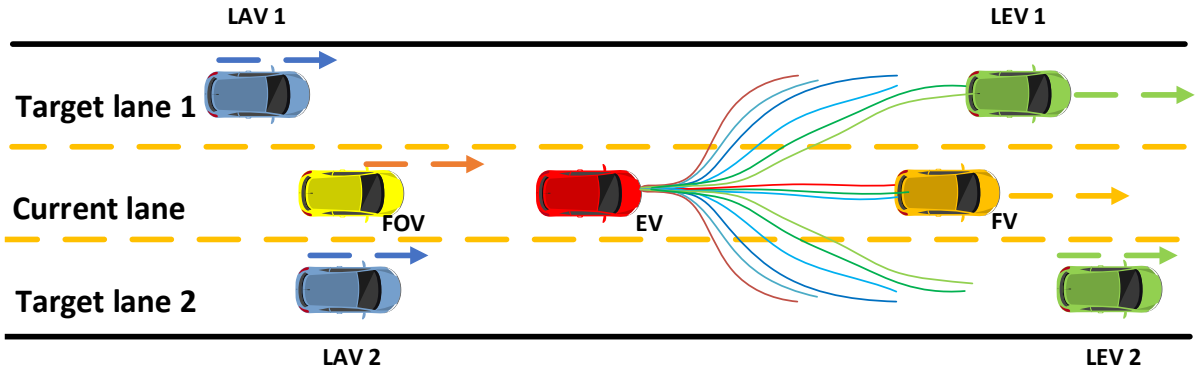

Figure 3.4 Trajectory generation considering surrounding vehicles

After the driving decisions are obtained, the path planning module is designed by assuming the driver can predict the target vehicle states in a short time period. The longitudinal goal speed and future lateral positions can be estimated by the human driver, where the latter is obtained according to the lane keep or lane change decisions. Thus, the polynomial curves are chosen to plan the path in both lateral and longitudinal axis after obtaining the driving decisions

$$\begin{cases} x(t) = a_0 + a_1 t + a_2 t^2 + a_3 t^3 + a_4 t^4 \\ y(t) = b_0 + b_1 t + b_2 t^2 + b_3 t^3 + b_4 t^4 + b_5 t^5 \end{cases} \tag{3.36}$$

where $\{a_0, \dots, a_4\}$ and $\{b_0, \dots, b_5\}$ are coefficients of polynomial functions that are estimated through following boundary conditions.

$$\begin{cases} x(0) = x_0, \dot{x}(0) = v_{x0}, \ddot{x}(0) = a_{x0}, \dot{x}(T) = v_{xT}, \ddot{x}(T) = a_{xT} \\ y(0) = y_0, \dot{y}(0) = v_{y0}, \ddot{y}(0) = a_{y0}, y(T) = y_T, \dot{y}(T) = v_{yT}, \ddot{y}(T) = a_{yT} \end{cases} \tag{3.37}$$

where $\{x_0, v_{x0}, a_{x0}, y_0, v_{y0}, a_{y0}\}$ are the initial states on $t = 0$; T is the lane-change duration. A set of different trajectories are generated through sampling the terminal states space $\{v_{xT}, a_{xT}, y_T, v_{yT}, a_{yT}, T\}$. The centerline of the target lane is set to the future lateral position. Other variables, such as the accelerations and lateral velocity, are assumed zero if the lane change is finished. Therefore, the sample spaces are simplified to cover all possible motions:

$$\begin{aligned} &T \in [T_{\min}, T_{\max}] \\ &v_{xT} \in [\max(v_{xT} - \Delta v, 0), \max(v_{xT} + \Delta v, v_{x\max})] \end{aligned} \tag{3.38}$$

The following multi-objective optimization problem is built to obtain an optimal trajectory from the candidates

$$\xi_{j^*}, j^* = \arg\min_j f(\xi_j \mid S, \boldsymbol{\omega})$$

$$s.t.\ \dot{\boldsymbol{x}}_{\xi_j} = g\left(\boldsymbol{x}_{\xi_j}, \xi_j\right) \tag{3.39}$$

$$\begin{cases} y_j \in [y_{\min}, y_{\max}], f_{collision}(\xi_j) = 0, \\ \boldsymbol{x}_{\xi_j} \in \Omega \end{cases}$$

where f is the cost function with weighting parameters $\boldsymbol{\omega}$ when driving in the environment S; $y_{\min}$ and $y_{\max}$ are the lateral positions of the lane boundaries; Ω denotes the envelope constraints when the vehicle tracks the trajectory ξ_j.

The optimization objectives, i.e., elements of the cost function f, are presented in detail, which consist of safety, vehicle stability, and driving efficiency.

1) Safety: The candidate trajectories that satisfy the constraints are collision-free, while all candidates have different risk levels. We define an exponential function of time headway to select a trajectory with lower risk in terms of the FV, LAV and LEV.

$$f_1(\xi_j) = \max_{t\in(0,T_j)}\left(e^{-THW_i(t)}\right), i = front, lead, lag \tag{3.40}$$

2) Ride comfort: The lateral acceleration is applied to evaluate the passenger comfort for all of the trajectory candidates.

$$f_2(\xi_j) = \frac{1}{T_j}\int_0^{T_j} |a_y(t)|\, dt \tag{3.41}$$

3) Driving efficiency: Human drivers are inclined to complete a lane-change maneuver as fast as possible, which is reflected in higher speed.

$$f_3(\xi_j) = \frac{1}{T_j}\int_0^{T_j} |v_x(t)|\, dt \tag{3.42}$$

Combining the above cost, the cost function is proposed to evaluate the trajectory candidates.

$$f(\xi_j \mid S, \boldsymbol{\omega}) = \sum_{k=1}^{3} \omega_k f_k(\xi_j) \tag{3.43}$$

3.4 Extensions from two-player to multi-player game

In some conditions, the two-player lane change game is necessary to be extended, if the behavior of other vehicles has the influence on the lane change interaction. For example, the EV is intended to change the lane when it approaches the slow moving FV, as is shown in Fig. 3.5.

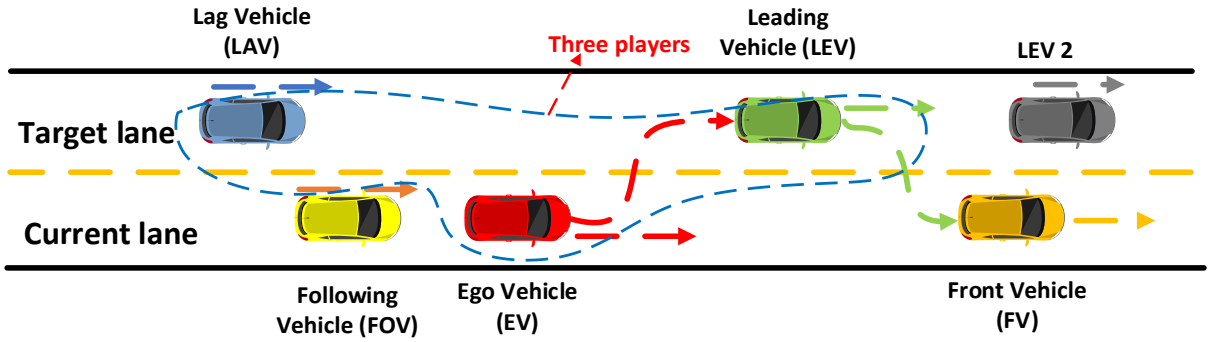

Figure 3.5 Multi-player lane change game considering the LEV's lateral behavior

Simultaneously, the LEV in the other lane is the potential lane change vehicle, observing the gap between EV and FV is long enough for a safe maneuver. Apparently, EV may change lane in advance or decelerate to avoid collisions, if LEV conducts the cut-in behavior. On the other hand, the acceleration behavior of the EV may force the LEV to cancel the lane change intention. Therefore, the EV is required to pay attention to the LEV's lateral behavior when making lane change or lane keeping decisions, besides the longitudinal behavior of LAV. Consequently, the two-player game is extended to the multiplayer game, which covers any possible case in the highway lane change without assuming the simplified motions of other vehicles.

3.4.1 Multi-player complete information game

Following equation (3.13), the strategy of each player is generated according to the Nash equilibrium. The EV, LAV and LEV are regarded as the players 1, 2 and 3, respectively, and the other vehicles are environment vehicles. Then the strategy spaces for three players are $S_1 = (LC, LK)$, $S_2 = (Yield, Acc)$, and $S_3 = (Cut-in, LK)$.

On the basis of the analysis of the utilities in the two-player game, the utilities of the LEV also

include the safety and speed efficiency costs. Suppose player 3 has H pure strategies, then the strategy spaces of three players are $S_1 = (s_{11}, \cdots, s_{1K})$ and $S_2 = (s_{21}, \cdots, s_{2J})$, and $S_3 = (s_{31}, \cdots, s_{3H})$ respectively. Considering the weighting vector is introduced to balance the parameters range and preferences of different drivers, the safety utilities of players 1, 2 and 3 in the {Lane change, Yield, Cut-in} case are

$$u_{1,safety}(s_{11}, s_{21}, s_{31}) = \alpha_{1,111}\max\left(a_{req,brake,111}^{EV,LAV}, a_{req,brake,111}^{EV,LEV2}\right) \tag{3.44}$$

$$u_{2,safety}(s_{11}, s_{21}) = \alpha_{2,111} a_{req,brake,111}^{EV,LAV} \tag{3.45}$$

$$u_{3,safety}(s_{11}, s_{21}, s_{31}) = \alpha_{3,111}\max\left(a_{req,brake,111}^{LEV,FOV}, a_{req,brake,111}^{LEV,FV}\right) \tag{3.46}$$

where the strategy pair $(s_{\mathbf{1}1}, s_{\mathbf{2}1}, s_{\mathbf{3}1})$ means players 1, 2 and 3 all choose the first strategy from their strategy spaces. The subscript "111" on the right-hand side of the equation means the strategy combinations of three players. The general safety utilities of each player in all possible situations can then be formalized as

$$u_{1,safety}(s_{1k}, s_{2j}, s_{3h}) = \alpha_{1,kjh}\max\left(a_{req,brake,kjh}^{EV,Veh_{1x}}, a_{req,brake,kjh}^{EV,Veh_{1y}}\right) \tag{3.47}$$

$$u_{2,safety}(s_{1k}, s_{2j}, s_{3h}) = \alpha_{2,kjh} a_{req,brake,kjh}^{LAV,Veh_{2x}} \tag{3.48}$$

$$u_{3,safety}(s_{1k}, s_{2j}, s_{3h}) = \alpha_{1,kjh}\max\left(a_{req,brake,kjh}^{LEV,Veh_{3x}}, a_{req,brake,kjh}^{LEV,Veh_{3y}}\right) \tag{3.49}$$

where $k = 1,2,\ldots,K; j = 1,2,\ldots,J; h = 1,2,\ldots,H$. In the Eq. (3.49), the required braking deceleration of the LEV is determined by its actions. If the LEV chooses to cut in, Veh_{1x} will be FOV, and Veh_{1y} will be FV. If the action is keeping the lane, Veh_{1x} will be LEV 2 in the target lane, and Veh_{1y} will not exist. When the front and rear vehicles are determined, the required deceleration can be calculated according to Eq. (3.15).

The speed efficiency utility is defined by the expected speed gain. The expected speed should be less than or equal to the front vehicle's speed in the stable traffic. Then the efficiency utilities of players 1 and 2 in the *{Lane change, Yield}* case are

$$u_{1,eff}(s_{11}, s_{21}, s_{31}) = \beta_{1,111}(v_{LEV} - v_{EV}) \tag{3.50}$$

$$u_{2,eff}(s_{11}, s_{21}, s_{31}) = \beta_{2,111}(v_{EV} - v_{LAV}) \tag{3.51}$$

$$u_{3,eff}(s_{11}, s_{21}, s_{31}) = \beta_{3,111}(v_{FV} - v_{LEV}) \tag{3.52}$$

The general efficiency utilities of each player in all possible situations can then be formalized as

$$u_{1,eff}(s_{1k}, s_{2j}, s_{3h}) = \beta_{1,kjh}(v_{Veh_{1z}} - v_{EV}) \tag{3.53}$$

$$u_{2,eff}(s_{1k}, s_{2j}, s_{3h}) = \beta_{2,kjh}(v_{Veh_{2y}} - v_{LAV}) \tag{3.54}$$

$$u_{1,eff}(s_{1k}, s_{2j}, s_{3h}) = \beta_{3,kjh}(v_{Veh_{3z}} - v_{EV}) \tag{3.55}$$

where $k = 1,2, \dots, K; j = 1,2, \dots, J; h = 1,2, \dots, H.$ For the LEV in the Eq. (3.53), the Veh_{1z} will be FV and LEV2 if LEV chooses Cut-in and LK, respectively.

For the lane change penalty, the distance between LEV and LEV2 Δx_{LEF} is selected as the factor for quantification. Then the general lane change penalty of the player 1 and 3 in all possible situations can then be formalized as

$$u_{1,LC}(s_{11}, s_{2j}, s_{3h}) = \gamma_{1,1jh} f_{LC}(\Delta x_{EF}) \tag{3.56}$$

$$u_{3,LC}(s_{1i}, s_{2j}, s_{31}) = \gamma_{3,ij1} f_{LC}(\Delta x_{LEF}) \tag{3.57}$$

The comprehensive utility functions of each player are defined as the linear combinations of safety and speed costs. Therefore, the utility functions of each player in all the possible situations are

$$u_1(s_{1k}, s_{2j}, s_{3h}) = u_{1,safety}(s_{1k}, s_{2j}, s_{3h}) + u_{1,eff}(s_{1k}, s_{2j}, s_{3h}) + u_{1,LC}(s_{11}, s_{2j}, s_{3h}) \tag{3.58}$$

$$u_2(s_{1k}, s_{2j}, s_{3h}) = u_{2,safety}(s_{11}, s_{2j}, s_{3h}) + u_{2,eff}(s_{11}, s_{2j}, s_{3h}) \tag{3.59}$$

$$u_3(s_{1k}, s_{2j}, s_{3h}) = u_{3,safety}(s_{1k}, s_{2j}, s_{3h}) + u_{3,eff}(s_{1k}, s_{2j}, s_{3h}) + u_{3,LC}(s_{1i}, s_{2j}, s_{31}) \tag{3.60}$$

The mixed strategy space and expected utilities are introduced considering the probability

distributions of the players' types. Then the expected utility of player 1 when choosing $\sigma_1 = (\sigma_{11}, \cdots, \sigma_{1K})$ is

$$\begin{aligned} v_1(\sigma_1, \sigma_2, \sigma_3) &= \sum_{h=1}^{H} \sigma_{3h} \sum_{k=1}^{K} \sigma_{1k} \sum_{j=1}^{J} \sigma_{2j} u_1(s_{1k}, s_{2j}, s_{3h}) \\ &= \sum_{k=1}^{K} \sum_{j=1}^{J} \sum_{h=1}^{H} \sigma_{1k} \sigma_{2j} \sigma_{3h} u_1(s_{1k}, s_{2j}, s_{3h}) \end{aligned} \tag{3.61}$$

Similarly, the expected utility of player 2 when choosing $\sigma_2 = (\sigma_{21}, \cdots, \sigma_{2J})$ is

$$\begin{aligned} v_2(\sigma_1, \sigma_2, \sigma_3) &= \sum_{h=1}^{H} \sigma_{3h} \sum_{j=1}^{J} \sigma_{2j} \sum_{k=1}^{K} \sigma_{1k} u_2(s_{1k}, s_{2j}, s_{3h}) \\ &= \sum_{k=1}^{K} \sum_{j=1}^{J} \sum_{h=1}^{H} \sigma_{1k} \sigma_{2j} \sigma_{3h} u_2(s_{1k}, s_{2j}, s_{3h}) \end{aligned} \tag{3.62}$$

Finally, the expected utility of player 2 when choosing $\sigma_3 = (\sigma_{31}, \cdots, \sigma_{3H})$ is

$$\begin{aligned} v_3(\sigma_1, \sigma_2, \sigma_3) &= \sum_{j=1}^{J} \sigma_{2j} \sum_{k=1}^{K} \sigma_{1k} \sum_{h=1}^{H} \sigma_{3h} u_3(s_{1k}, s_{2j}, s_{3h}) \\ &= \sum_{k=1}^{K} \sum_{j=1}^{J} \sum_{h=1}^{H} \sigma_{1k} \sigma_{2j} \sigma_{3h} u_3(s_{1k}, s_{2j}, s_{3h}) \end{aligned} \tag{3.63}$$

In this section, the two-player lane change game was extended to the multi-player complete information game, where the cut-in and lane keeping behavior of LEV is considered to the interaction. The next section will discuss the effects of the player type on the decision-making.

3.4.2 Multi-player incomplete information game

For the driver type distribution, the EV is supposed to know the probability distribution $p(\theta_2, \theta_3 \mid \theta_1)$. The sum of the conditional probability distribution over the driver type space of LAV and LEV is 1

$$\sum\nolimits_{s=1}^{S} \sum\nolimits_{l=1}^{L} p_1(\theta_{2l}, \theta_{3s} \mid \theta_1) = 1 \tag{3.64}$$

Considering the mixed strategy based utility function with complete information in Eq. (3.64),

the expected utility of player 1 with incomplete information will be

$$w_1(\sigma_1, \sigma_2, \sigma_3, \theta_1) := \sum_{s=1}^{S} \sum_{l=1}^{L} p_1(\theta_{2l}, \theta_{3s} \mid \theta_1) v_1(\sigma_1, \sigma_2, \sigma_3, \theta_1, \theta_2, \theta_3) \tag{3.65}$$

where

$$v_1(\sigma_1, \sigma_2, \sigma_3, \theta_1, \theta_2, \theta_3) = \sum_{k=1}^{K} \sum_{j=1}^{J} \sum_{h=1}^{H} \sigma_{1k}(\theta_1) \sigma_{2j}(\theta_2) \sigma_{3h}(\theta_3) u_1(s_{1k}, s_{2j}, s_{3h}) \tag{3.66}$$

If the players' types are continuous, then the integration of the conditional probability over the driver type space is

$$\int_0^1 \int_0^1 p_1(\theta_2, \theta_3 \mid \theta_1) \, d\theta_2 d\theta_3 = 1 \tag{3.67}$$

The expected utility of player 1 with incomplete information will be

$$w_1(\sigma_1, \sigma_2, \sigma_3, \theta_1) := \int_0^1 \int_0^1 p_1(\theta_2, \theta_3 \mid \theta_1) v_1(\sigma_1, \sigma_2, \sigma_3, \theta_1, \theta_2, \theta_3) \, d\theta_2 d\theta_3 \tag{3.68}$$

The player 1 will choose the strategy that maximizes $w_1(\sigma_1, \sigma_2, \sigma_3, \theta_1)$. The integration range $\Theta_2 = [0, 1]$ and $\Theta_3 = [0, 1]$ denotes that the types of LAV and LEV are continuous given the EV belongs to type θ_1. $v_1(\sigma_1, \sigma_2, \sigma_3, \theta_1, \theta_2, \theta_3)$ is the utility of the EV over the mixed strategy space under different types of three players.

In this part, the lane change decision-making is modelled with the multi-player game under the condition of incomplete information, where the EV is required to consider the types of LAV and LEV. The joint probability distribution $p_1(\theta_2, \theta_3 \mid \theta_1)$ given the type of EV can be obtained from the section of driver identification from naturalistic driving data. Then the proposed model could make more human-like driving decisions with this information encoded.

3.5 Simulation results

The performances of the proposed decision-making model are evaluated. In the two-player game simulation, two different types of the lag vehicles are designed to test the adaptivity of the developed decision-making model, including aggressive and cautious driver types. In the multi-player simulation, the combinations of LAV and LEV are designed to evaluate the

proposed model. The simulations are implemented on the MATLAB/Simulink platform.

3.5.1 Simulation environment setup

The simulation scenario in this work is extracted from the highD dataset, which collects the naturalistic vehicle trajectories on the highway with plenty of passenger car data. One typical interactive scenario is selected to verify the proposed model with strong interactions between the EV and the LAV, as is shown in Fig. 3.6. In the dataset, the real drivers' actions can be observed. In the simulation, the EV is replaced by the proposed decision-making model with environment vehicles maintaining their states except the LAV. In this way, the interaction environment is mainly controlled by the EV-LAV relationship, when other surrounding vehicles' states remain unchanged in the two compared scenarios.

The speed limit is 35 m/s, and the perception distances are 200 m. Regarding the candidate trajectories generation, the lane change duration T is sampled from [3, 6] s with an interval of 1s, and the velocity difference range is [-2, 2] m/s with an interval of 0.5 m/s.

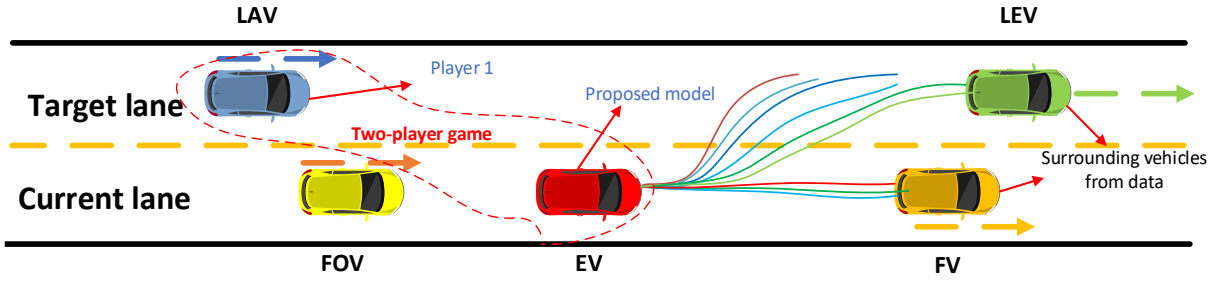

Figure 3.6. Simulation driving environment for two-player complete information game

For the risk assessment, three discrete risk levels are defined as a random variable $\Xi \in \{D, A, S\}$ with respect to the values of the aforementioned metrics vectors, including Dangerous, Alert and Safe. Three risk measures are selected to quantify the driving risks, including TTC, THW and the relative distance between two vehicles. Then two critical values are required to map the observed traffic conditions to the corresponding risk levels. In this work, the following S-shaped membership function is adopted to determine the likelihood function, which generates the probability for each risk measure:

$$P(X = x_m \mid \Xi = \xi_i) = \begin{cases} (2-4\beta)/\left(1+exp\left(-\alpha_{x_m}\left(x_m - \bar{\xi}_i^{cr}\right)\right)\right) + (3\beta - 1), & if\ x_m > \bar{\xi}_i^{cr} \\ (4\beta-2)/\left(1+exp\ \left(-\alpha_{x_m}(x_m - \xi_i^{cr})\right)\right) + (1-\beta), & if\ x_m \le \underline{\xi_i}^{cr} \\ \beta, & otherwise \end{cases} \tag{3.69}$$

where x_m is the measured value of an element in the threat metrics vector $\mathbf{\Phi}$; ξ_i is the inferred risk level; α_{xm} is the shape parameter, representing the uncertainty of the observed threat metrics; β is the regularization factor and is assigned 0.9 in this work; $\bar{\xi}_i^{cr}$ and $\underline{\xi}_i^{cr}$ are upper and bottom thresholds, respectively.

The posterior probability can be determined and normalized with weightings of multiple threat metrics, and then the probability of a certain risk level with all threat metrics measured can be obtained

$$P\left(\Xi = \xi_i \mid X_j = x_m^j\right) = \frac{\sum_{j=1}^{N_0} \omega_j P(\Xi = \xi_i \mid X = x_m)}{\sum_{i=1}^{N_z} \omega_j}, j = 1,2,3 \tag{3.70}$$

For a specific lane change, the risks are from the LAV and LEV. Therefore, the lane change risks probabilities should be a combination of each risk level with a new function.

$$\begin{cases} P(\Xi_l = D) = 1 - \prod_{k=\mathrm{LAV},LEV}\ P\left(\Xi_k = -D \mid X_j^k = x_m^{j,k}\right) \\ P(\Xi_l = S) = \prod_{k=LAV,LLV}\ P\left(\Xi_k = S \mid X_j^k = x_m^{j,k}\right) \\ P(\Xi_l = A) = 1 - P(\Xi_l = D) - P(\Xi_l = S) \end{cases} \tag{3.71}$$

where X_j^{LAV} and X_j^{LEV} are the random variables that represent the threat metrics of LAV and LEV; $x_m^{j,LAV}$ and $x_m^{j,LEV}$ denote their measured values.

The inferred risk level can then be determined by finding the maximum probability of candidate risk levels

$$\underline{\hat{\Xi}}_l = \arg\max_{\Xi_l} P(\Xi = \xi_i) \tag{3.72}$$

Through evaluating the lane change risks, the driving conditions around the ego vehicle are quantified, which quantitatively evaluates the performance of the decision-making model to guarantee the driving safety.

3.5.2 Two-player complete information game

In this part, two cases are presented to evaluate the performances of the lane change decision-making model based on the complete information game.

Interacting with an aggressive driver

The scenario in this case is constructed based on the extracted interactive lane change scenario in the naturalistic real data. The EV is initially located in the leftmost lane, denoted by the red color, as shown in Fig. 3.7 (a).

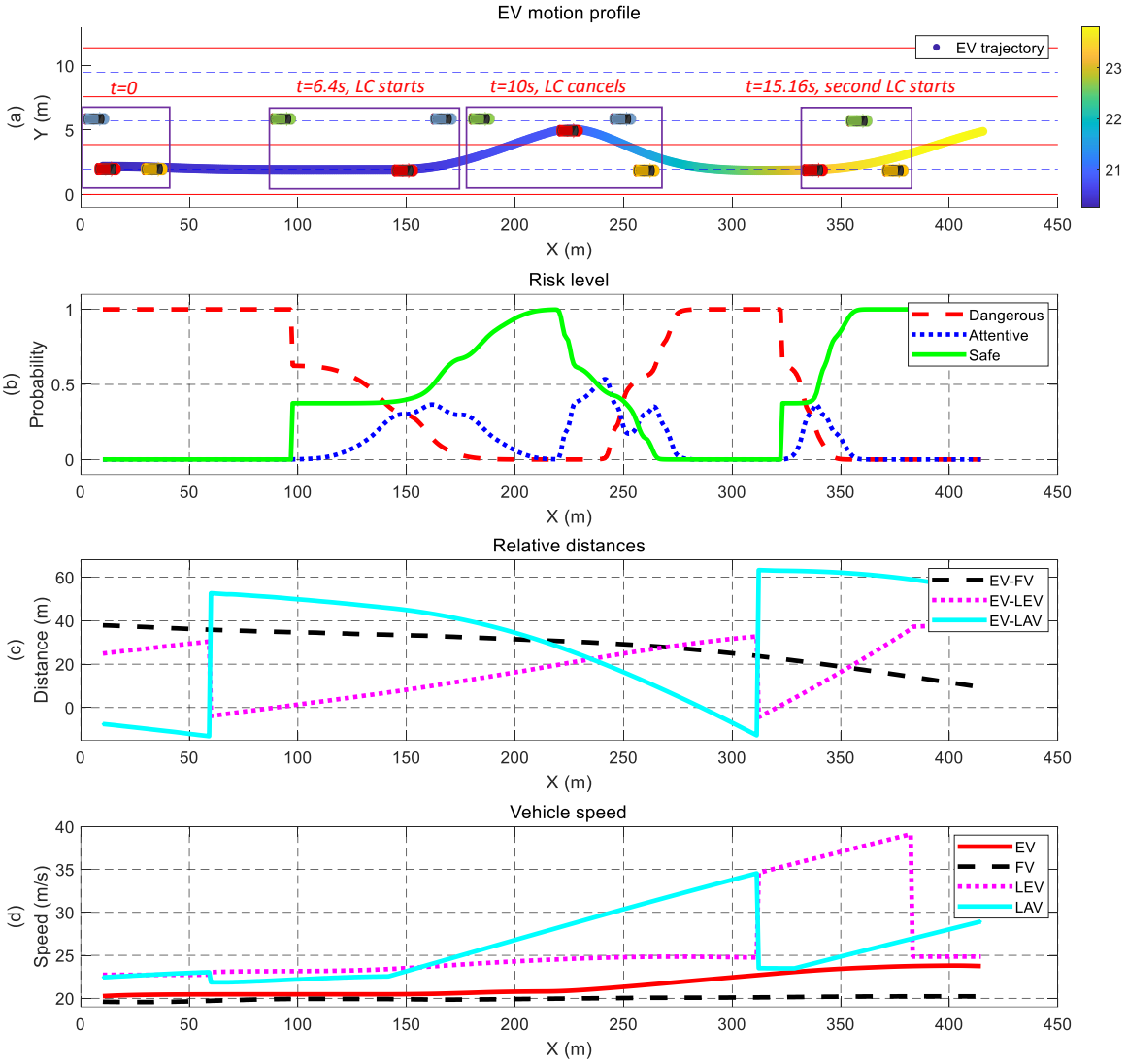

Figure 3.7. The autonomous vehicle interacts with the aggressive lag vehicle driver. (a) EV motion profile. (b) Risk level. (c) Relative distances. (d) Vehicle speed.

Specifically, the probability of each risk level is presented and analyzed according to the risk measures, including TTC, THW and relative distance. Moreover, the relative distances between EV and other surrounding vehicles, and the vehicles' speed are shown to describe the driving process.

The initial position coordinates of EV, FV, LEV, and the LAV are (10.18, 2.19), (59.97, 2.09), (44.05, 5.82) and (9.15, 5.99), separately. Moreover, the initial longitudinal speeds of EV, FV, LEV, and the LAV are 20.25 m/s, 19.6 m/s, 22.73 m/s, and 22.44 m/s, respectively.

It can be seen from the initial condition that the EV drives faster than the FV, but the distance between them is large enough that the EV can accelerate to reach a higher speed. In terms of the left lane, the LAV actually overlaps with the EV and overtakes it in the next few seconds. Therefore, the EV is not motivated to change lane and the driving risk is high in the target lane at the beginning of the period.

The surrounding vehicles drive along the profiles as the real data present until the EV generates the lane change decision based on the noncooperative game played by EV and LAV at 5.4 s, when the risk level is "Safe". The LAV is set to be aggressive and accelerate at 2 m/s^2 if it detects the lane change intention of the EV. Therefore, the LAV's speed increases, and the distance from the LAV to the EV decreases rapidly several seconds after the lane change decision-making time step, as shown in Fig. 3.7 (d) and (c).

Since the LAV keeps accelerating and does not yield to EV, the EV has to cancel the lane change and get back to the original lane at t=10 s, as shown in Fig. 3.7 (a). Although the distances are both over 20 m from the EV to the LAV and LEV, and the probability of being "Safe" is close to the peak value, the EV predicts the worse safety condition because the term is included to estimate the future driving environment. Therefore, the EV successfully avoids the potential collision with the LAV by recognizing the surrounding environment and following Nash equilibrium.

The last decision change happens at t=15.16s when the EV intends to make the second lane change. The EV is expected to change lane successfully because the LAV is over 60 m from EV, and the speed difference is around 0. More importantly, the risk level has stayed "Safe" for

the last several seconds. However, the result is unknown because of the limit range of the data collection.

This noncooperative game begins at $t = 0$, when it is only known by the EV because the LAV follows the motion profile in the real data. At the lane change time step, the game is known to both players, but the LAV does not follow the Nash equilibrium because the test scenario requires the specific driving characteristic for the opponent of the EV. During this process, the EV follows the Nash equilibrium and decides to keep or change lane according to the driving environment. When the LAV drives forward and becomes the LEV, the game ends, and another one starts until the next time the EV generates the lane change decision at t=15.16 s.

Interacting with a cautious driver

For this scenario of interacting with the cautious driver, the states stay the same as the previous one until t=6.4 s. The LAV detects the lane change intention of the EV and decelerates at -0.5 m/s^2.

As the Fig. 3.8 (c) and (d) shows, the relative distance between LAV and EV is around 45 m, and the speed difference is less than 2 m/s although LAV is faster. The LAV cannot overtake EV within such a large distance considering it will decelerate at -0.5 m/s^2. Moreover, the risk level in Fig. 3.8 (b) shows that the probability of being “Safe” is increasing after the EV makes lane change.

After the EV successfully changes lane, the dense traffic flow in the leftmost lane results in a high probability of the “Dangerous” risk level. Therefore, the EV keeps the lane and follows the new FV until the end of the data collection range.

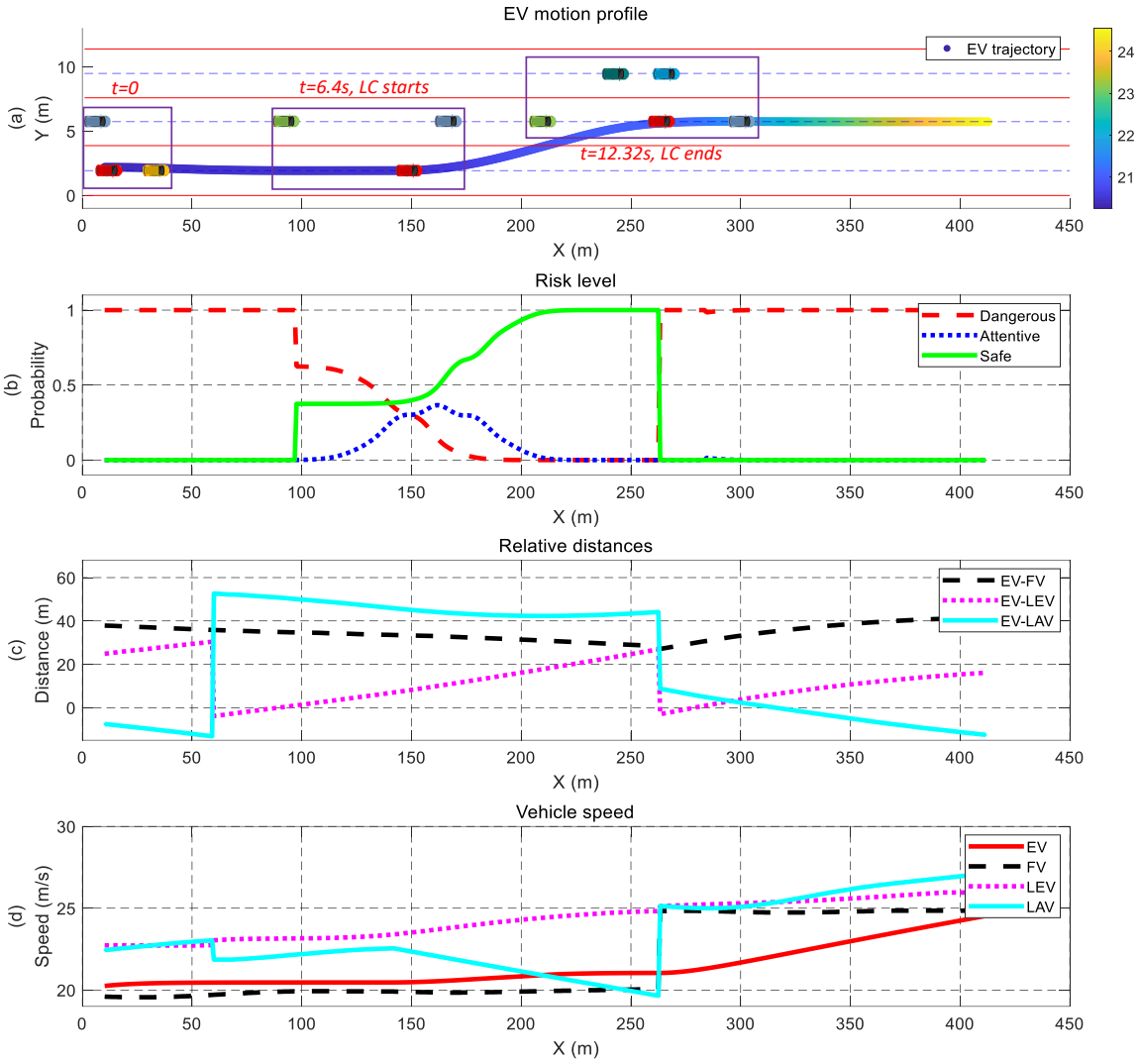

Figure 3.8. The autonomous vehicle interacts with the cautious lag vehicle driver. (a) EV motion profile. (b) Risk level. (c) Relative distances. (d) Vehicle speed.

3.5.3 Multi-player complete information game

This section introduces how the multi-player game is used in the conditions where the LEV cuts in.

LEV cuts in and LAV accelerates

The environment vehicles and the states in this case are kept as same as them of the two-player game, except for the controlled vehicles, including LEV, EV and LAV. As is shown in Fig. 3.9 (a), the brown vehicle in this scenario is initially overlapped with the red EV and identified as

the LAV at $t = 0$. Because it travels much faster than an EV, it is quickly identified as a LEV and performs the cut-in behavior when it reaches around 100 meters. At $t = 5.16\ s$, the LEV crosses the lane boundary, and it is recognized as the front vehicle (FV) by EV. Thus, the EV starts to change lane for a larger safety space and higher efficiency when the probability of being "Safe" in the target lane is 1. The critical time steps in the cut-in process of the LEV are marked by the squares along with its trajectory, while the corresponding points are marked by the star for the EV. The EV stays a relatively safe distance from the LEV during the whole process, which is indicated in Fig. 3.9 (c).

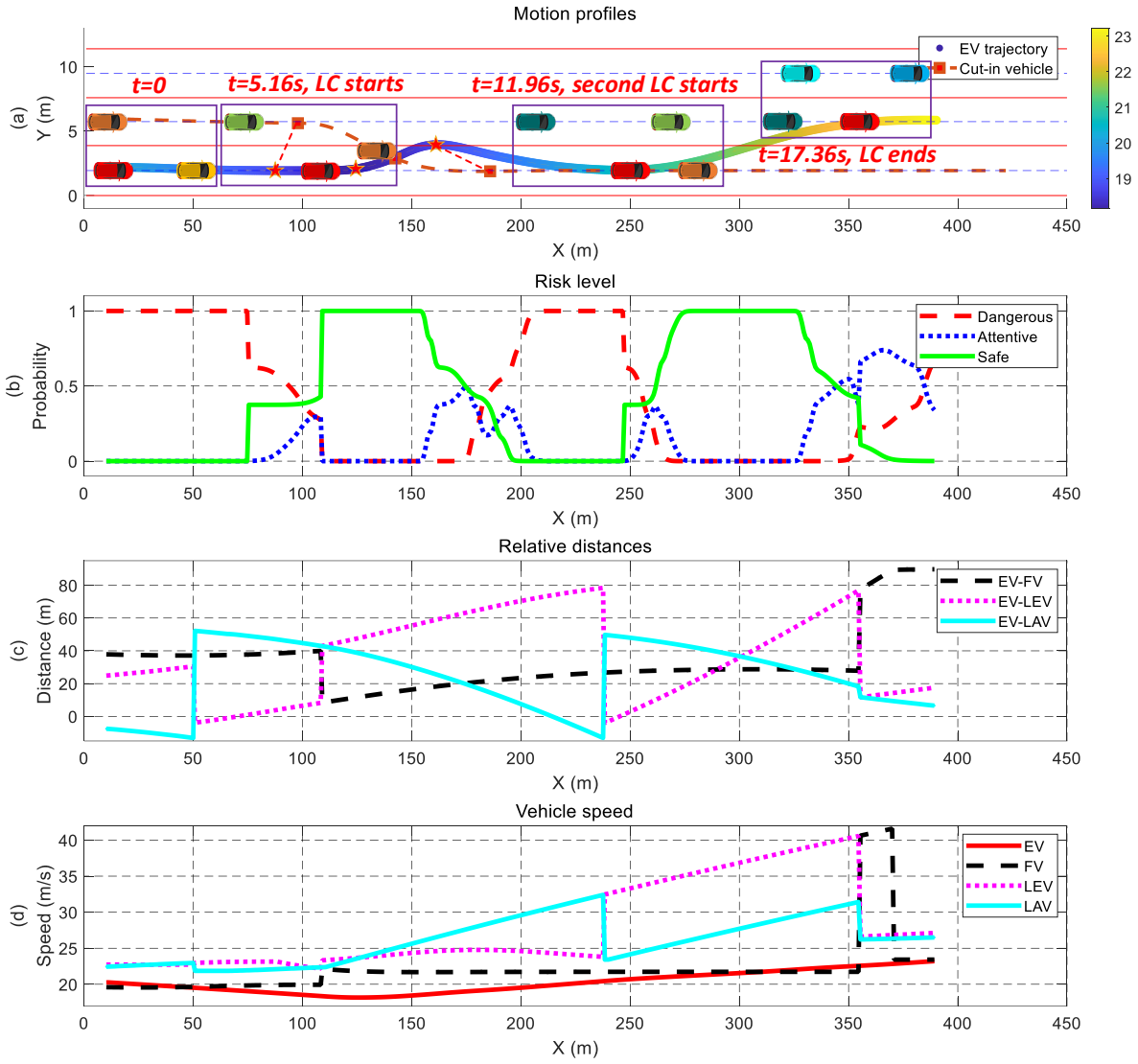

Figure 3.9. The autonomous vehicle interacts with the aggressive lag vehicle driver when LEV cuts in. (a) Motion profiles. (b) Risk level. (c) Relative distances. (d) Vehicle speed.

The light green LAV is set to accelerate at 1.5 m/s^2 if it detects the lane change intention of the EV. Therefore, the LAV's speed increases, and the distance from the LAV to the EV decreases rapidly, as shown in Fig. 3.9 (d) and (c). Since the LAV does not yield to the lane changing EV and the distance from EV to the currently identified EV is not large, the EV cancels the lane change at around 160 meters, and drives at nearly constant speed. After the LAV overtakes EV and EV is approaching to the FV at $t = 12.56\ s$, EV starts its second lane change. Although the current risk level of being "dangerous" occupies the highest probability due to the small relative distance between the light green LEV and EV, the probability of being "safe" increases rapidly because the LEV drives much faster than the EV with their speeds being 32 m/s and 20 m/s, separately, presented in Fig. 3.9 (c). Moreover, the ego vehicle crosses the lane boundary after driving over 50 meters, when the distance between EV and LEV is nearly 40 meters. Therefore, the EV changes lane safely at the appropriate time.

After the EV successfully changes lane and switches to the middle lane, the dense traffic flow in the leftmost lane and large space in the current lane make the EV accelerate until the end of the data collection range.

LEV cuts in and LAV yields

Instead of accelerating and overtaking the EV, LAV in this scenario detects the lane change intention of the EV and decelerates at -0.5 m/s^2. As Fig. 3.10 (a) shows, the motion states of all the vehicles stay the same until the EV changes lane at $t = 5.16\ s$, when the EV-FV distance drops to less than 10 meters because of the cut-in of the LEV. The EV changes lane without the disturbance of the LAV. In terms of the risk level for EV in the target lane, the probability of being "Safe" is 1 during whole lane change process, as shown in Fig. 3.10 (b). The distances in Fig. 3.10 (c) between EV and other vehicles are all more than 20 meters and do not decrease too much until the EV finishes a lane change.

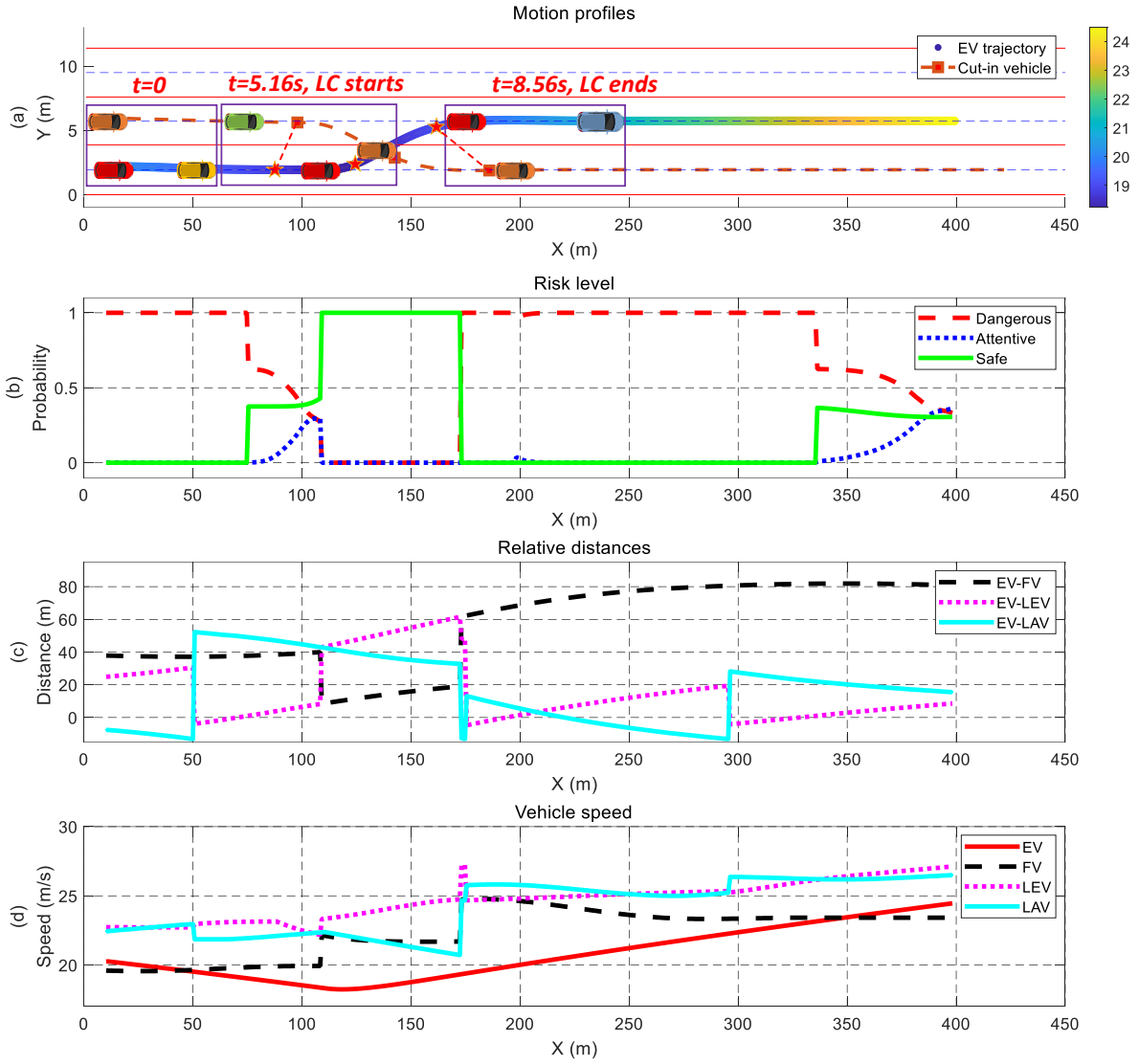

Figure 3.10. The autonomous vehicle interacts with the cautious lag vehicle driver when LEV cuts in. (a) Motion profiles. (b) Risk level. (c) Relative distances. (d) Vehicle speed.

Compared with the two-player game scenario, the ego vehicle's driving decisions are affected by both LEV and LAV in the multi-player game scenarios. The lateral behavior of the LEV is considered to affect the EV's driving space, and the lane change behavior is triggered in advance compared with two-player game scenarios. In some cases, the driving conditions are safety-critical, such as when the LEV cuts in from a short distance and the LAV accelerates simultaneously. The ego vehicle can either cancel the lane change or brake hard to guarantee driving safety.

3.6 Summary

In this chapter, the lane change behavior was analyzed and modelled under the framework of game theory. The game model was classified to complete and incomplete information game based on the information availability in real traffic. In particular, the incomplete information game with mixed strategies was emphasized accounting for the uncertainty of the enviroment vehicles in real traffic. After that, the optimal path was generated after candidate trajectory generation and path selection considering some important driving indexes based on the polynomial splines. Moreover, the two-player lane change game was extended to the multi-player game with the LEV's lateral behavior considered. Finally, the developed model was validated in the case of both two-player and multi-player games.

Chapter 4

Lane Change Model Training Based on Naturalistic Driving Data

In this chapter, the proposed decision-making model is trained by the naturalistic driving data so that it becomes as close as possible to the human decision. To achieve this goal, the interactive driving data are firstly extracted to ensure the interactions. Next, the connection from driving data to the motion modeling of the environment vehicles and driver identification model is introduced.

4.1 Dataset selection

4.1.1 Naturalistic datasets investigation

Naturalistic and simulation driving data

To let the model learn from the data, the driving data should be collected first. There are two types of data, namely naturalistic data and simulation data. The naturalistic data can be collected by the real vehicle traveling in the traffic roads equipped with multiple sensors, and monitoring equipment that records the traffic flow in several fixed road segments. Collecting simulation data requires human drivers to operate the driving simulator and finish several driving tasks. The driving behaviors in the driving simulator are not as authentic as real driving. Also, the surrounding vehicles in the driving simulator are set by the researchers instead of intelligent human drivers, so the recorded behaviour would be skewed and would leave out the rare occurrences that occur in the real world. Interaction related studies require the driving behavior to be as naturalistic as possible. Therefore, the naturalistic driving data are investigated for dataset selection.

(a)

(b)

Figure 4.1. Description figures of KITTI dataset [88]. (a) Recording platform. (b) Example scenarios.

Perception and trajectory datasets

Naturalistic datasets can be divided into two categories: perception and trajectory. For perception datasets collected by a real vehicle with sophisticated sensors, the raw data include multiple formats, including video, lidar point cloud and GPS positions. Road user trajectories are not included in datasets like KITTI [88] (see Fig. 4.1) or the Waymo Open Dataset [89], and can only be derived in a limited and difficult way from perception data. Accurate

environment information sensing requires highly advanced technologies of computer vision, information fusion and data filtering, while it is the biggest challenge for current AV research. Furthermore, some problems cannot even be solved due to the limitations of sensors. Therefore, the trajectory datasets are the focus for the research.

The earliest trajectories dataset NGSIM [14] is published to the public in 2006 and is intended for traffic flow related research. The data were collected with a sampling frequency of 10 Hz, which recorded the traffic flow on U.S. Highway 101 and the Interstate 80 (I-80) Freeway. Multiple kinematics information of the vehicles was collected, including position, speed, acceleration, etc. However, the raw data of the NGSIM trajectories cannot be utilized for further analysis due to large amount of noise, especially the speed and acceleration data. One reason is the trajectory data are extracted based on the video data while the computer vision technology at the beginning of the 21st century was not as advanced as it is now. Also, the filter is not adopted to the speed and acceleration when they are derived from position data using derivation equations. Researchers proposed methods [90], [91] to reduce the errors, but they could only work for a small part of the dataset.

Other trajectories datasets inspired by NGSIM are recorded from a bird's-eye view to clearly record the information of surrounding road users. The Stanford Drone Dataset [92] was released in 2016, and it contains data collected from road users using a drone on the Stanford University campus. Bicyclists (1748) and pedestrians (1036) make up the majority of traffic participants, with vehicles (260) accounting for a small share. The low resolution of the recorded videos and inaccurate detections result in noisy trajectory data. Because there are many walkers and bicyclists on campus, the recorded driving behavior is likely to differ from that on public highways. The same drawbacks happen in the CITR dataset and DUT dataset [93], which were published by the Control and Intelligent Transportation Research (CITR) Lab at The Ohio State University (OSU) in 2019. The *highD* dataset [94] is one of the large-scale trajectory databases based on the videos collected by the aerial drone. Descriptions of the INTERACTION [95], *inD* [96], and *rounD* [97] datasets were released during the construction of the *openDD* dataset. The INTERACTION dataset contains data from 11 intersections, including 5 roundabouts, 3 unsignalized intersections, 2 merging and lane change scenarios,

and 1 signalized intersection, and lasts roughly 16.5 hours. The *inD* dataset [96], which includes 10 hours of data captured by a drone, distinguishes walkers, bicycles, vehicles, trucks, and buses.

The *rounD* dataset includes three recording sites in and around Aachen, Germany's westernmost city, with almost 6 hours of footage and 13746 road users. The naturalistic trajectory datasets are summarized as Table 4.1.

Table 4.1. Overview of naturalistic trajectory datasets published in recent years.

Dataset Name	**Length**	**Scenarios**	**# locations**	**# tracks**	**Road User Types**
NGSIM [14]	2.5 h	Freeway and arterial road	4	16557	Cars, trucks, motorcycles
Stanford Drone [92]	9 h	Campus	8	10240	Pedestrians, bicycles, cars, buses, skateboards, carts
highD [94]	16.5 h	Highway	6	110000	Cars, trucks
CTTR [93]	0.21 h	Parking lots	1	340	Pedestrians
DUT [93]	0.16 h	Urban intersections, shared space	2	1793	Pedestrians
inD [96]	10 h	Urban intersections	4	11500	Pedestrians, bicycles, cars, trucks, buses
rounD [97]	Over 6 h	Roundabouts	3	13746	cars, vans, trucks, buses, pedestrians, bicycles, motorcycles
INTERACTION [95]	16.5 h	Urban intersections, highway, roundabouts	11	40054	Cars, pedestrians

In summary, current naturalistic trajectory datasets are mostly focused on scenarios in urban traffic, such as intersections and roundabouts. The researchers intend to include as many road user types as possible such that the dataset seems more comprehensive. However, for the microscopic interaction mechanism study between two vehicles, the scenarios should not be

very complicated without the disturbances caused by other types of road users. The driving environment should be structured public roads so that the driver can behave naturally. Also, the mechanism may be different while the driver interacts with more than one driver during a complete driving task. Therefore, *highD* dataset is chosen as the objective data for interaction mechanism study.

4.1.2 HighD dataset

HighD dataset [94] contains 16.5 hours records of naturalistic driving data from six German highways around Cologne with 110,000 vehicles during 2017 and 2018. Sixty recordings were made along a 420-meter stretch of road at six different locations, with an average length of 17 minutes (16.5 hours total). The computer vision technologies were utilized to extract the vehicles from the raw video data and the infrastructure were annotated manually.

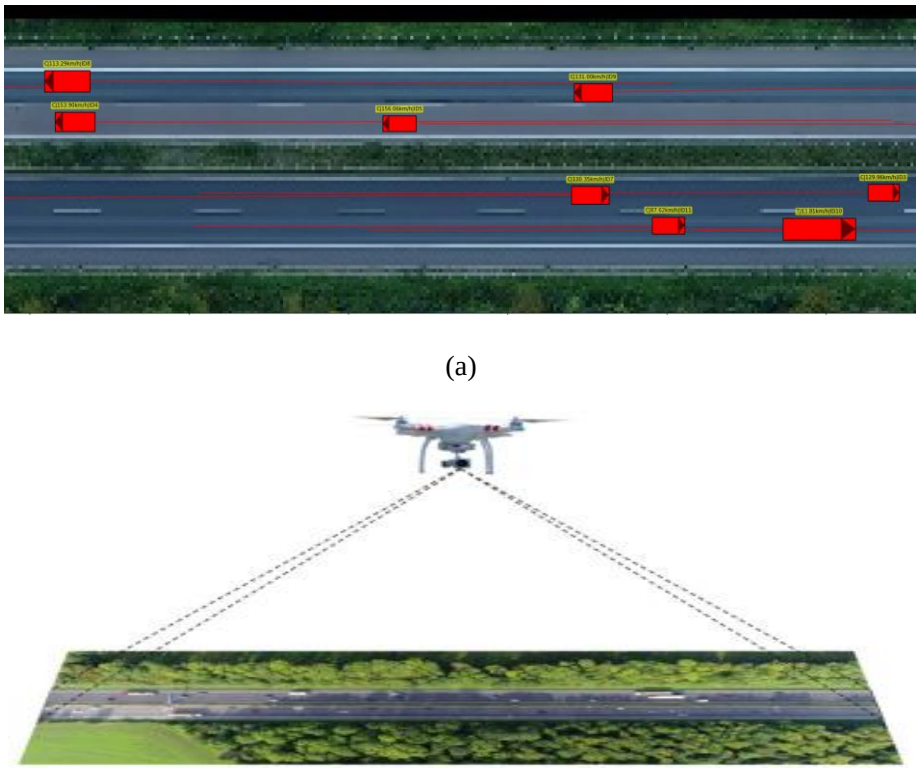

(a)

(b)

Figure 4.2. Description figures of the highD dataset. (a) Example of a recorded highway. (b) Bird's eye view of the highway road section. [94]

To get all the information required by the many scenario-based validations, a drone was used

to record 4K 25 frames per second videos to capture every vehicle's movements from a bird's eye view. Each recording has four files in the dataset, i.e., three CSV files with location, vehicle, and trajectory data, as well as an aerial view of the specified highway area. The first file contains information about the site's location, driving lanes, traffic signs, and lane speed limits. A summary of each track is included in the second file, which includes vehicle size, vehicle class, driving direction, and average speed. Each track's specific information, such as speeds, accelerations, lane locations, and a description of neighboring vehicles, is included in the last file.

Fig. 4.2 is an illustration of the dataset. Red boxes with different labels and the red lines show the trajectories, vehicle classes and id, as well as the velocity. By using some state-of-the-art computer vision algorithms, the dataset achieves decimeter accuracy.

4.2 Interactive driving data extractions

From the analysis above, the uncertainties in the surrounding vehicles are major sources of the lane change complexity. Specially, for the LEV and FV, EV is not able to change their future behavior but reactively act according to the prediction information due to the responsibility division criteria by the traffic law. However, EV can negotiate with LAV and change its future action to create a chance for lane change in dense traffic, which is not handled well in current methods. To emphasize this problem, the interactive lane change scenarios should be first defined so that the interactions can be analyzed. The research goal is to investigate the bidirectional active interaction between EV and LAV.

Interaction range limitation

To guarantee the EV and LAV can interact with each other, an intuitive idea is to set a limited gap distance when the EV starts to change lanes. However, as driving velocities differ, the interaction range should not be fixed. Therefore, time headway (THW) is introduced to define the interaction range, which is defined by the gap distance and the speed of following vehicle:

$$THW = \frac{\Delta X}{V_{following}} \tag{4.1}$$

where ΔX is the gap distance between two vehicles, and $V_{following}$ is the speed of following vehicle. Time headway defines the collision risks in the form of time. Two-second rule [98] states that drivers should at least stay "two seconds" behind the front vehicle for a good space cushion, which indicates the interaction level is high enough when THW is within two seconds. Therefore, interactive lane changes are firstly filtered by excluding those scenarios where THW is over 2 seconds at $\boldsymbol{T_1}$.

Looking into the reactions of lag vehicle during a lane change, it can choose to accelerate/decelerate in the longitudinal dimension or change to the other lane and adjust longitudinal velocity simultaneously. These behaviors are conducted because the ego vehicle has effects on the lag vehicle through interactions. The scenarios where LAV changes lanes are excluded considering the majority of LAV drivers respond by staying in their lane. More importantly, increasing the action dimension of the lag vehicle from one to two dimensions will lead to analytical difficulties and increase the complexity of the problem.

4.3 Applications of real data on motion modeling and driver identification

4.3.1 Physical motion model of surrounding vehicles

For the validation of the proposed decision-making model, the behaviors of the surrounding vehicles are critical. The traffic environment is required to be like real-world traffic, where the surrounding vehicles should drive like real human drivers. Therefore, the motion model should be various to represent the driving behaviors of different types of drivers. Moreover, human behavior is essentially stochastic. The uncertainty always exists which is affected by the traffic environment and their internal behavior generation. To meet this requirement, the real driving data are essential.

A general motion model for a specific surrounding vehicle SV_i can be formulized as

$$\boldsymbol{x}_i(t: t + T_f) = f(\boldsymbol{x}_{1:N}(t - T_h: t - 1), \varepsilon_i) \tag{4.2}$$

where $\boldsymbol{x}$ is the state vector that can include position, velocity, yaw angle, etc.; T_f is the prediction horizon; T_h is the history horizon; ε_i represents the uncertainty of SV_i; N is the

number of vehicles that influence the behavior of SV_i; $x_{1:N}(t-T_h:t-1)$ is the model input, i.e., the history states of the involved vehicles related to SV_i; $\boldsymbol{x}_i(t:t+T_f)$ is the model output, i.e., the future states of SV_i during the prediction horizon.

In some conditions, Eq. (4.2) can be revised as

$$\boldsymbol{a}_i(t-1) = f(\boldsymbol{x}_{1:N}(t-T_h:t-1), \varepsilon_i) \tag{4.3}$$

where $\boldsymbol{a}_i(t-1)$ is the action of SV_i at time step $t-1$, and the future states $\boldsymbol{x}_i(t:t+T_f)$ can be updated iteratively according to

$$\boldsymbol{x}_i(t) = f(\boldsymbol{x}_i(t-1), \boldsymbol{a}_i(t-1), \varepsilon_i) \tag{4.4}$$

For the motion model Eq. (4.2), the parameters can be calibrated according to the designer's experience. However, this model may not represent the driving behavior features of the real human drivers. The resulted vehicle motions can be unrealistic and do not conform to the social attributes when interacting with other human-driven vehicles in the real traffic.

The introduction of the naturalistic driving data can help to calibrate the motion model parameters reasonably. To specifically demonstrate how the parameters are determined, the observations $y_{t_1:t_2}$ during a period $[t_1, t_2]$ are firstly extracted. Then the mean square error (MSE) is utilized to represent the loss function

$$\text{MSE} = \frac{1}{n}\sum_{i=1}^{n}(y_i - \tilde{y}_i)^2 \tag{4.5}$$

where n is the number of steps during $[t_1, t_2]$; y_i is the actual observations; $\tilde{y}_i$ is the motion model output. The calibrated parameters are obtained by minimizing the MSE

$$\boldsymbol{\theta} = argmin\frac{1}{n}\sum_{i=1}^{n}(y_i - \tilde{y}_i)^2 \tag{4.6}$$

where $\boldsymbol{\theta} = (\theta_1, \theta_2, \dots, \theta_k)^T$ is the parameters set or vector in the motion model. If this group of drivers can represent the majority of all the human drivers, we can use their driving data to model the driving behavior of the normal drivers. In terms of the variety of the driving styles in the dataset, an option is preparing several parameters set or setting up other parameters to

control the driving style. The latter method requires the prior knowledge about the statistical law of the different extent to the aggressiveness of the driving behavior. For the former method, the only extra step is to classify the drivers. After that, the parameters can be sampled randomly from the probability distribution.

From the analysis above, the physical motion model of the surrounding vehicles is more human-like and can represent the various driving styles of the real human drivers after the calibration based on the naturalistic driving data. Then the simulation results of the proposed decision-making model are more realistic because the interactions are generated by the vehicles that capture the human-likeliness and variety of human drivers. The performances are then analyzed to evaluate the proposed decision-making model.

4.3.2 Driver identification model

To interact with the surrounding vehicles effectively and safely, the ego autonomous vehicle is required to identify their driving styles and make decisions adaptively. For example, the ego vehicle is more likely to keep the lane even if its front vehicle drives slowly, if the lag vehicle in the target lane drives fast. In other words, the ego vehicle recognizes that the lag vehicle is aggressive and chooses to keep lane considering the driving safety, even the driving efficiency decreases due to the slow front vehicle. Conversely, the ego vehicle is likely to change the lane if the lag vehicle drives cautiously under the same driving conditions. The driver recognitions show the future expectations of the ego vehicle to the possible driving behavior of surrounding vehicles.

We can learn from the examples above that the driver types of the surrounding vehicles greatly affect the driving decisions of the ego vehicle. The utilities or rewards are directly related to the driver types in the decision-making model. This factor shows how the ego vehicle adaptively makes decisions when interacting with different drivers.

The driver identification can be formulated as a classification problem, where $\boldsymbol{x}$ is a sample including n driving features, and Y is a label set that contain k labels. The driving data are consisted of the sequence $X = \{\boldsymbol{x}_1, \boldsymbol{x}_2, \dots, \boldsymbol{x}_T\}$. The objective of the classification is to

determine the label of a specific driver according to the observed driving data X, i.e., $argmax(p(y_i \mid X))$.

Discriminative model or generative model can be adopted to deal with the classification problem. For the generative model, the posterior probability is calculated by

$$p(y_i \mid X) = \frac{p(y_i)p(X \mid y_i)}{\sum_Y p(y_i)p(X \mid y_i)} \tag{4.7}$$

where $p(y_i)$ is the prior probability of label that can be assigned to normal distribution or uniform distribution based on the experience; $p(X \mid y_i)$ is the likelihood probability function that needs to be estimated. In the generative model, the label set Y is open, where the new data can be supplemented, while all drivers' data are required to retrain the model parameters using the discriminative model. This is because the discriminative model directly estimates the posterior probability $p(y_i \mid X)$. Therefore, very complicated and non-interruptible models are utilized to minimize the designed loss function based on the numerical optimization method, such as deep neural network.

Both classification models require the training process based on the driving data. For the driver identification modeling, the driving data are needed to learn the knowledge from the demonstrations of real human drivers. The real driving data can offer the feature distribution so that the statistical law can be learned.

4.4 Summary

In this chapter, the interactive driving data were extracted from the naturalistic driving data, i.e., the highD dataset, so that the interactions were guaranteed between the lane change vehicle and lag vehicle. Then the applications of the real driving data were introduced on the motion modeling of the environment vehicles and driver identification model, which would be realized in the next chapter.

Chapter 5

Motion modeling and identifications of the surrounding vehicles

In this chapter, the motion models of the surrounding vehicles are presented, including the car-following behavior of the lag vehicle in the two-player game and the lateral cut-in behavior of the leading vehicle in the multi-player game. The naturalistic driving data are utilized for driving style classification and model calibration so that the driving behavior of the surrounding vehicles can be more human-like. After the motion modeling, the driver identifications are presented to offer the necessary information to the decision-making of the ego autonomous vehicle. Then the ego vehicle can make decisions adaptively according to the types of other surrounding vehicles.

5.1 Introduction to Intelligent Driver Model (IDM)

A popular rule-based kinetics model to describe human driving behavior is the Intelligent Driver Model (IDM) [57]. Following this model, the objective car can be controlled to drive at a desired speed and keep a specific distance from the front vehicle. It is applied to the microscopic traffic flow under many conditions, such as on-ramp, off-ramp, lane change, etc. This model is used to simulate the driving behavior of real drivers combing with other decision-making models. For example, the lane change model MOBIL [99], another rule-based model, is adopted with IDM to simulate the multilane traffic. Eq. (5.1) presents the mathematical formulation of the IDM.

$$a_{\mathrm{IDM}}(s, v, \Delta v) = \frac{\mathrm{d}v}{\mathrm{d}t} = a\left[1 - \left(\frac{v}{v_0}\right)^{\delta} - \left(\frac{s^*(v, \Delta v)}{s}\right)^2\right] \tag{5.1}$$

where

$$s^*(v, \Delta v) = s_0 + vT + \frac{v\Delta v}{2\sqrt{ab}} \tag{5.2}$$

The model contains the acceleration strategy in the free traffic flow

$$\dot{v}_{free}(v) = a\left[1 - \left(\frac{\dot{v}}{v_0}\right)^4\right] \tag{5.3}$$

toward a desired speed v_0 under the constraints of the maximum acceleration a. Meanwhile, the braking strategy also exists in this model

$$\dot{v}_{brake}(s, v, \Delta v) = -a\left(\frac{s^*}{s}\right)^2 \tag{5.4}$$

where $s(t)$ is the current gap, $s^*(v, \Delta v)$ is the desired minimum gap:

$$s^*(v, \Delta v) = s_0 + vT + \frac{v\Delta v}{2\sqrt{ab}} \tag{5.5}$$

The minimum distance s_0 and desired time headway T are always positive, and the second term vT in Eq. (5.5) is adaptive according to the driving speed of the following car. For the driving speed difference, if the following car drives faster than the preceding car, the Δv is positive and $s^*(v, \Delta v)$ is large to increase the weightings in deceleration. The comfortable deceleration b is designed to limit the braking decelerations, while however, the car brakes harder than b if current gap is too small. All IDM parameters v_0, T, s_0, a, and b, are defined by positive values.

The model can be used to describe the longitudinal behavior of various drivers after being calibrated based on the real driving data. However, it does not, 1) show real human driving behavior because the parameters are determined subjectively according to the individual driving experience, and 2) consider personal driving behavior, which requires multiple sets of parameters. The parameters determination relies on the predefined rules and cannot be generalized to the diverse scenarios. Thus, the individual variations should be accounted by introducing the real driving data. The IDM model can be extended to the personalized model that shows the driving preferences. In the next sections, the cut-in scenarios will be extracted, and the car-following data of the lag vehicle in the target lane during the cut-in period are expected to analyze the longitudinal driving behavior of real human drivers and calibrate the IDM model.

5.2 Driving style classification based on an explainable way

To capture the variety of responses in the cut-in scenarios, the car-following driving style of the LAV is classified during the interactive lane changes. The information can be utilized to model the driving behavior of different lag vehicles, so that the motion model of surrounding vehicles can be human-like, and the simulation traffic environment is diverse and realistic. Moreover, the driver identification model can also be trained by learning the corresponding parameters from real data. The identification results can help the decision-making model generate more adaptive decisions according to the observations of other vehicles.

The interactive lane change is defined in Section 4.2. The THW between the lane change vehicle and the lag vehicle should be lower than 2 seconds, so that the interactions are guaranteed. The responses of the LAV are worth studying when the EV conducts a lane change behavior. The LAV type can then be estimated by learning the prior knowledge from real data. Therefore, the data from T_3 to T_4 are collected and analyzed to classify the car-following style when there is a cut-in behavior, as is shown in Fig. 5.1. The lane change intent or behavior is assumed to be completely known by the LAV at T_3 when the center of EV crosses the lane line. The observations end when the ego vehicle finishes the lane change at T_4.

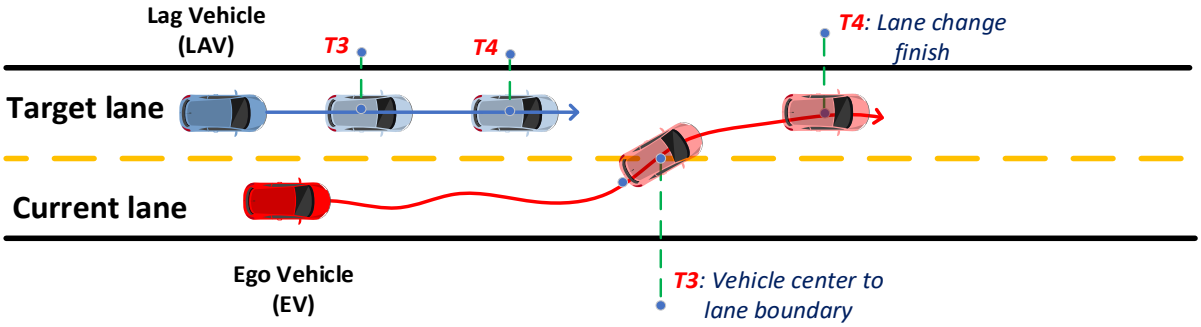

Figure 5.1. The diagram of the cut-in scenario

Different from the machine learning or deep learning-based driving style classifications, the car-following style is classified based on an explainable way in this work. Considering there are measurements of relative distance and relative velocity in the IDM model, the parameters set can be calibrated respectively according to the clustering or classification based on the observation of these data. The differences between each set will be significant. Therefore, the

relative distance and relative velocity are introduced as the features to represent the environment risk. For the longitudinal responses, acceleration is the most relevant term to show the driving behavior. Moreover, the output of the IDM model happens to be the longitudinal acceleration. Therefore, the remaining parameters can be determined with significant differences with these three terms involved.

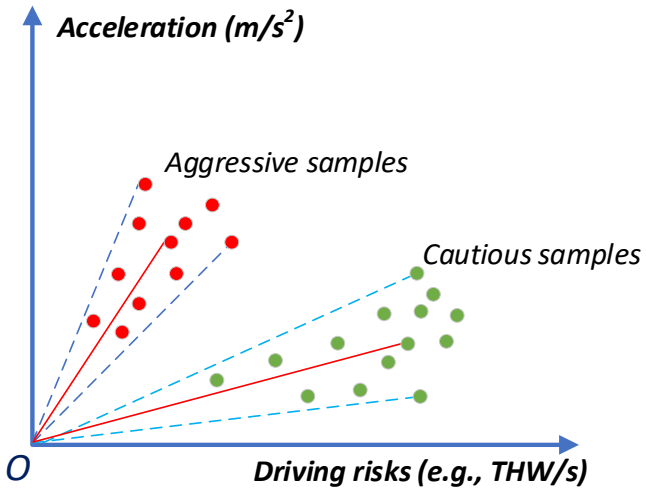

Figure 5.2. Diagram of the classification rule

The driver type plot is then constructed by taking the driving environment risk as the X-axis and the longitudinal vehicle behavior as the Y-axis. The slope of each data point is the driver aggressiveness, as shown in Fig. 5.2. If the vehicle drives in a risky environment and shows acceleration behavior, then the driver's longitudinal driving is aggressive. Conversely, if the vehicle slows down even in the relatively safe driving environment, then the driver aggressiveness is low. Following this criterion, the driving risk and longitudinal driving behavior are introduced to quantify the driving style of a specific driver. The area division in Fig. 5.3 can be expressed with the following mathematical formulation

$$\underline{\varepsilon_{ij}} \leq f_{ij} \leq \overline{\varepsilon_{ij}} \tag{5.6}$$

where $\underline{\varepsilon_{ij}}$ and $\overline{\varepsilon_{ij}}$ are the upper and lower percentile of the driving features; f_{ij} is the jth feature of the ith driving style; $i = 1,2,3$ represents the three different driving styles, including cautious, moderate and aggressive drivers; $j = 1,2,3$ is the driving features extracted from real data, including relative distance, relative speed and measured longitudinal

acceleration.

The participant drivers are classified into cautious, moderate, and aggressive styles. It can be seen from figures 5.3 and 5.4 that the cautious drivers have a longer relative distance, a lower relative speed, and less acceleration, compared with the moderate and aggressive drivers. The moderate drivers account for roughly 60% in the whole driver group. The aggressive drivers have the shortest relative distance, the highest relative speed, and greatest acceleration. The results in Fig. 5.4 show that all the cautious drivers decelerate when the driving risks are relatively low, with a larger relative distance and a lower relative speed. More than 50% of aggressive drivers choose to accelerate when their driving risks are widely higher than those of cautious drivers. Therefore, the driving style classification is reasonable and meets the original design requirement.

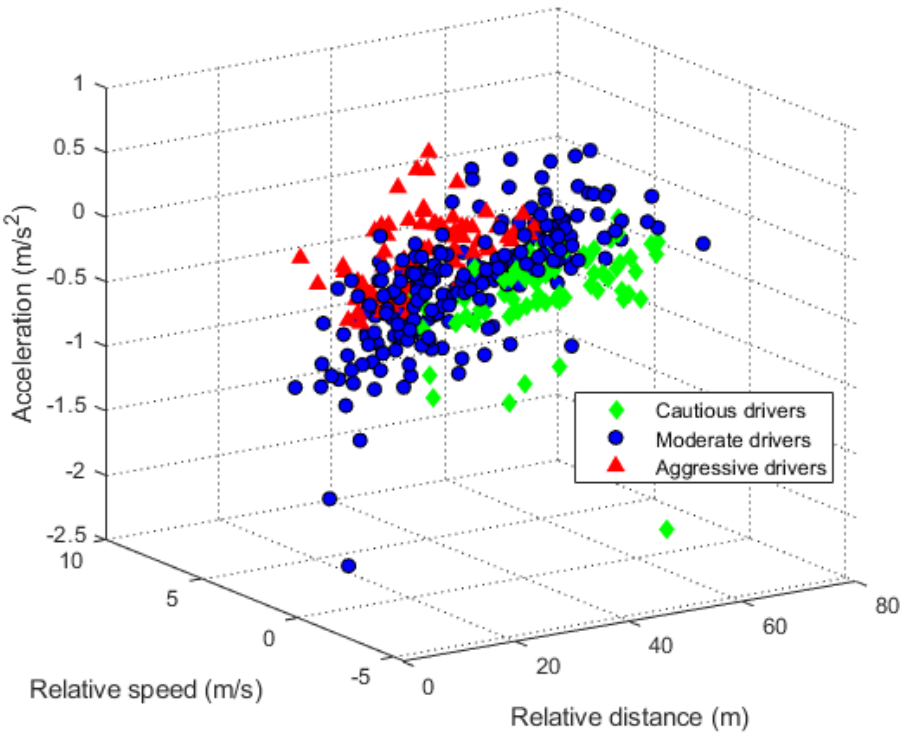

Figure 5.3. Classification results of the driver samples

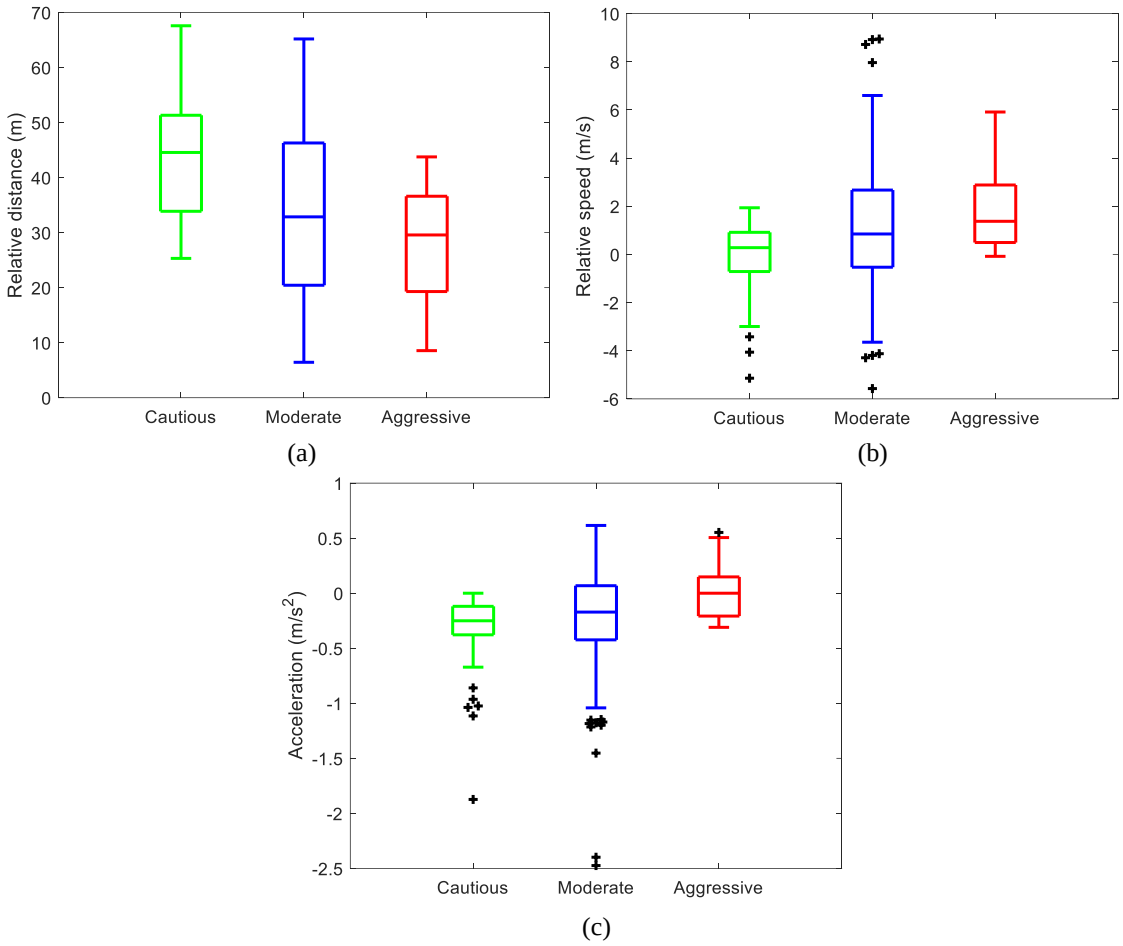

Figure 5.4. Boxplots of the driving features for three different driving styles

5.3 IDM parameters calibration based on the real data

After the classification, the parameters in the IDM can be calibrated for each type of driver, separately. The results show the variation of real drivers in terms of the car-following behavior. The data to be used are introduced in Section 5.2. The estimated model acceleration is generated by the IDM model with the measured input, including relative distance, the speed of lag vehicle and relative speed. Simultaneously, the actual accelerations are available in the real data. Therefore, the IDM parameters of a specific driver k can be calibrated using the metric of mean square error based on time series driving data

$$\boldsymbol{\theta}_k = \underset{\boldsymbol{\theta}_k}{\operatorname{argmin}} \frac{1}{N} \sum_{i=1}^{N} (y_i - \tilde{y}_i(\boldsymbol{\Omega}|\boldsymbol{\theta}_k))^2 \tag{5.7}$$

where i is the ith time step, and N is the number of observations in the trajectory; $\boldsymbol{\theta}_k = (v_0, T, s_0, a, b)^T$ is the parameters vector in the IDM model; $\boldsymbol{\Omega} = (s(i), v(i), \Delta v(i))^T$ is the measurement vector at ith time step. Because the parameter vector to be estimated is highly dimensional, dimension reduction is implemented while keeping the model's generalization and simplicity in mind, without affecting its accuracy in describing human car-following behavior.

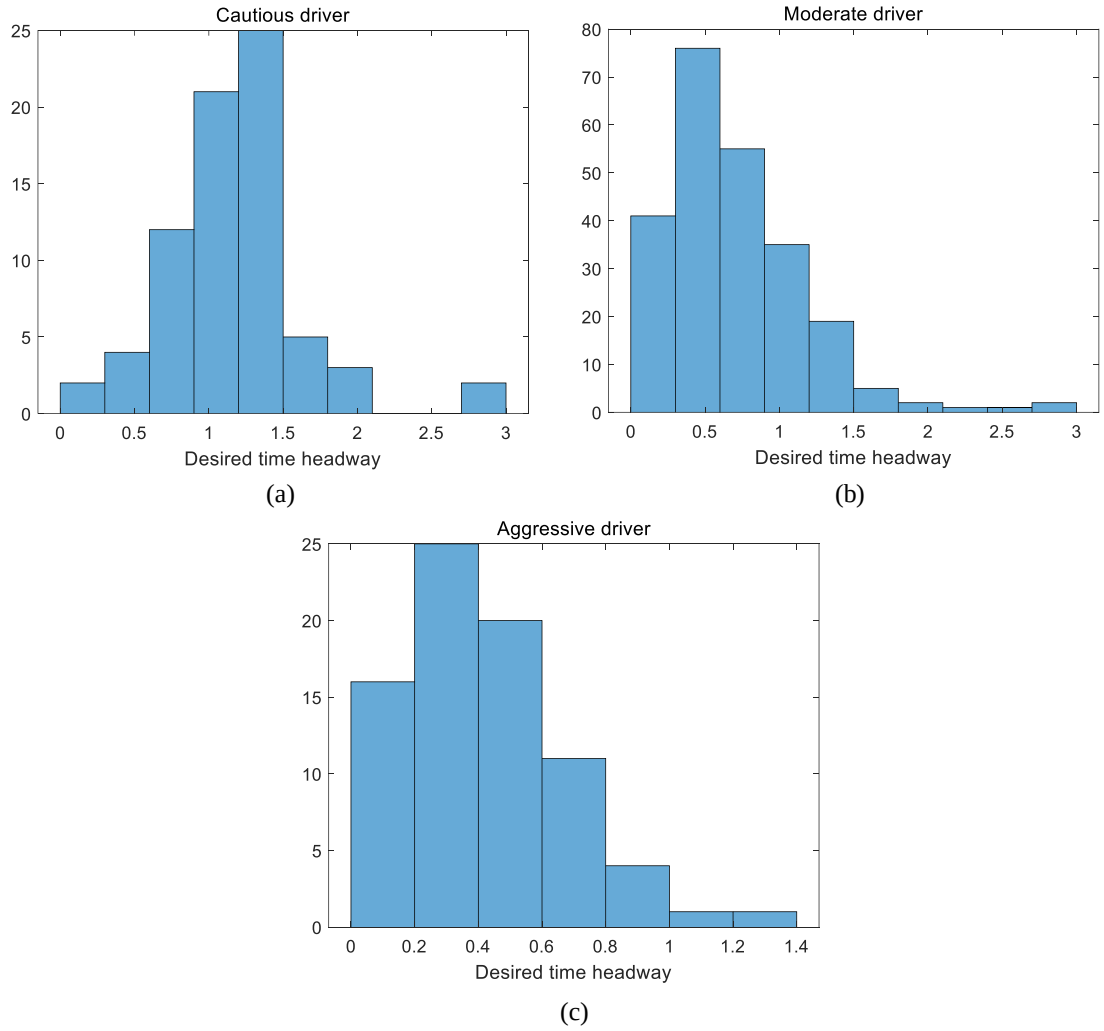

Figure 5.5. Histograms of the desired time headway for different driving styles

In the published literature, the desired time headway T and maximum acceleration a are two promising parameters that affect the car-following behavior in terms of the platoon oscillation stability [100] and variance contributions in the analysis of variance (ANOVA). Furthermore, both papers demonstrated that adjusting the desired time headway T is the most contributing

factor in their corresponding research. Therefore, in this study, T is calibrated to replace the previous parameter vector $\boldsymbol{\Omega}$.

The calibration results are shown in figures 5.5 and 5.6. It is shown that the calibrated T in three driver groups follow the normal distribution with mean values of 1.17 s, 0.7 s, and 0.41 s, separately. The results show that over 75% of the cautious drivers have a higher desired time headway than it of 75% of moderate drivers and nearly 100% of aggressive drivers. The significant differences exist between cautious drivers and the other two groups of drivers. This result will be used in the behavior model of the surrounding vehicles through setting up various driving styles, so that the model can be validated in the real traffic environment to some extent. Corresponding simulations will be conducted in the next chapter.

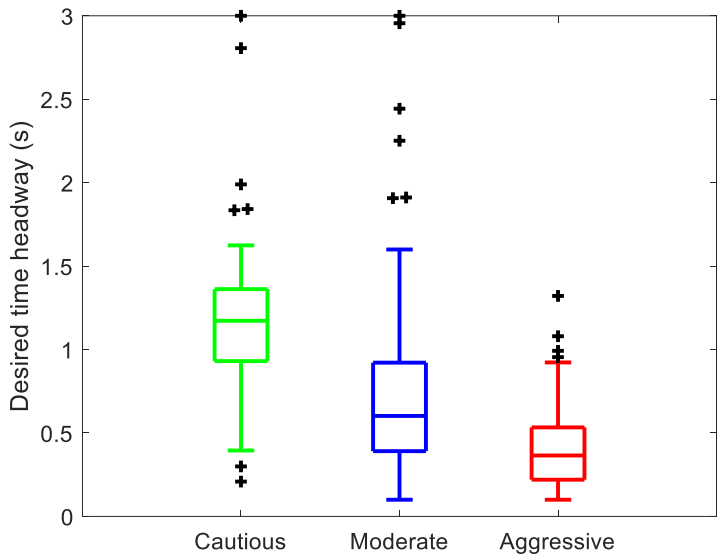

Figure 5.6. Boxplot of the desired time headway for different driving styles

5.4 GMM based driver aggressiveness determination

5.4.1 GMM-based LAV trajectory predictions

The naturalistic driving data help determine the driver type of the surrounding vehicles. In this study, the driver identification is conducted by predicting the future trajectories based on the naturalistic driving data. The Gaussian mixture model (GMM) combines multiple Gaussian distributions, and has great strength to address and model problems with uncertainty due to its

excellent approximation properties [101]. Therefore, it is chosen here to construct the relationship between the past driving states and the probability distributions of the future motion trajectory.

To predict the motion of the LAV from the aspect of the EV, several features are considered. Firstly, the historical motion information of the LAV itself is critical for the prediction. Secondly, the historical information of the longitudinal gap distance and relative speed between it and EV can affect the longitudinal decision. Considering these features can be deduced by the velocities and yaw angles of the LAV and EV, the inputs of the trajectory prediction model are

$$\boldsymbol{s}(\tau) = [v_{LAV}(\tau)\ \ \varphi_{LAV}(\tau)\ \ v_{EV}(\tau)\ \ \varphi_{EV}(\tau)\ \ \Delta d_x(\tau)\ \ \Delta d_y(\tau)], \tau \in [t - T_h, t] \tag{5.8}$$

where Δd_x and Δd_y denote the longitudinal and lateral distances between LAV and EV, separately; T_h is the historical horizon. And the outputs of the model are the future velocity and yaw angle of the LAV:

$$\boldsymbol{z}(\mathrm{T}) = [v_{LAV}(\mathrm{T}) \quad \varphi_{LAV}(\mathrm{T})], \mathrm{T} \in [t, t + T_f] \tag{5.9}$$

where T_h is the prediction horizon. Using the GMM method, the trajectory prediction is equivalent to inferring the following joint probability distribution:

$$\begin{aligned} p(\bar{x}) &= \sum_{k=1}^{K} \pi_k N(\overline{\boldsymbol{x}} \mid \boldsymbol{\mu_k}, \boldsymbol{\Sigma_k}) \\ &\begin{cases} 0 \le \pi_k \le 1 \\ \sum_{k=1}^{K} \pi_k = 1 \end{cases} \end{aligned} \tag{5.10}$$

where $\overline{\boldsymbol{x}}$ is a multi-dimensional random variable and it is represented as $\overline{\boldsymbol{x}} = [\boldsymbol{s}(\tau),\ \boldsymbol{z}(\mathrm{T})]$; K indicates the number of Gaussian components; k indicates a specific Gaussian component; π_k, $\boldsymbol{\mu_k}$, and $\boldsymbol{\Sigma_k}$ are the estimated parameters of GMM, which represent the weighting of components, mean value matrix and covariance matrix.

Given a history feature input $\boldsymbol{s_t}$, the future motion states can be predicted by calculating the following conditional distribution of the estimated output $\boldsymbol{z_t}$.

$$p(\boldsymbol{z_t} \mid \boldsymbol{s_t}) = \frac{p(\boldsymbol{z_t}, \boldsymbol{s_t})}{\int p(\boldsymbol{z_t}, \boldsymbol{s_t})\, d\boldsymbol{z_t}} = \sum_{k=1}^{K} \tilde{\pi}_k N\left(\boldsymbol{z_t} \mid \boldsymbol{s_t}, \tilde{\boldsymbol{\mu}}_k, \widetilde{\boldsymbol{\Sigma}}_k\right) \tag{5.11}$$

where $\tilde{\pi}_k$, $\widetilde{\boldsymbol{\mu}}_k$, $\widetilde{\boldsymbol{\Sigma}}_k$ are the parameters of Gaussian distribution and satisfy the following conditional mixture [101]:

$$\widetilde{\boldsymbol{\mu}}_k = \boldsymbol{\mu}_k^{z_t} + \boldsymbol{\Sigma}_k^{z_t, s_t}\left(\boldsymbol{\Sigma}_k^{s_t, s_t}\right)^{-1}\left(\boldsymbol{s_t} - \boldsymbol{\mu}_k^{s_t}\right) \tag{5.12}$$

$$\tilde{\pi}_k = \frac{\pi_k N\left(\boldsymbol{s_t} \mid \boldsymbol{\mu}_k^{s_t}, \boldsymbol{\Sigma}_k^{s_t, s_t}\right)}{\sum_{i=1}^{K} \pi_i N\left(\boldsymbol{s_t} \mid \boldsymbol{\mu}_i^{s_t}, \boldsymbol{\Sigma}_i^{s_t, s_t}\right)} \tag{5.13}$$

$$\widetilde{\boldsymbol{\Sigma}}_k = \boldsymbol{\Sigma}_k^{z_t, z_t} - \boldsymbol{\Sigma}_k^{z_t, s_t}\left(\boldsymbol{\Sigma}_k^{s_t, s_t}\right)^{-1}\boldsymbol{\Sigma}_k^{s_t, z_t} \tag{5.14}$$

The mean value matrix and covariance matrix are presented as:

$$\boldsymbol{\mu}_k = \begin{bmatrix} \boldsymbol{\mu}_k^{s_t} \\ \boldsymbol{\mu}_k^{z_t} \end{bmatrix} \quad \text{and} \quad \boldsymbol{\Sigma}_k = \begin{bmatrix} \boldsymbol{\Sigma}_k^{s_t, s_t} & \boldsymbol{\Sigma}_k^{s_t, z_t} \\ \boldsymbol{\Sigma}_k^{z_t, s_t} & \boldsymbol{\Sigma}_k^{z_t, z_t} \end{bmatrix} \tag{5.15}$$

where $\boldsymbol{\Sigma}_k^{z_t, z_t}$ and $\sum_{\boldsymbol{k}}^{\boldsymbol{s_t}, \boldsymbol{s_t}}$ denote the auto-covariance matrices regarding $\boldsymbol{s_t}$ and $\boldsymbol{z_t}$ respectively; $\boldsymbol{\Sigma}_{\boldsymbol{k}}^{\boldsymbol{s_t}, \boldsymbol{z_t}}$ and $\sum_{\boldsymbol{k}}^{\boldsymbol{z_t}, \boldsymbol{s_t}}$ denote the cross-covariance matrices; $\boldsymbol{\mu}_{\boldsymbol{k}}^{\boldsymbol{s_t}}$ and $\boldsymbol{\mu}_{\boldsymbol{k}}^{\boldsymbol{z_t}}$ are mean-value matrices.

The parameters set ($\boldsymbol{\Phi} = \{\pi_k, \boldsymbol{\mu}_k, \boldsymbol{\Sigma}_k\}$) related to GMM can be estimated through the standard expectation maximization (EM) algorithm by using the naturalistic driving data.

5.3.2 Driver aggressiveness recognitions

Now that the LAV's trajectories have been predicted, the driver aggressiveness could be obtained from this information. The driver aggressiveness is defined to be determined by two factors, namely the current driving environment and the longitudinal behavior of the vehicle.

If the vehicle drives in a risky environment and shows acceleration behavior, then the driver's longitudinal driving is considered to be aggressive. Conversely, if the vehicle slows down even in the relatively safe driving environment, then the driver aggressiveness is low. Following this criterion, the driving risk and longitudinal driving behavior are introduced to quantify the

aggressiveness of a specific driver. The driving risk is characterized by the normalized THW, and the longitudinal driving behavior is determined by the percentage of the predicted trajectory to the expected trajectory range. The formula for the percentage ratio is

$$ratio = \frac{x_{GMM} - X_{min}}{X_{max} - X_{min}} \tag{5.16}$$

where x_{GMM} is the predicted trajectory based on GMM given the historical information and prediction horizon

$$x_{GMM}(t + T_f) = f_G(\boldsymbol{s}_{t-T_h:t}|\boldsymbol{\Phi}) \tag{5.17}$$

where $f_G(\cdot)$ is the trained GMM model. The minimum and maximum accelerations can be investigated from the existed driving dataset.

The schematic diagram is shown in Fig. 5.7. As can be seen from the figure, the LAV trajectory predicted by GMM is uncertain, and follows the normal distribution. The longitudinal behavior of the LAV is not purely quantified by the acceleration, considering the longitudinal behaviors corresponding to the same acceleration possess great differences if the longitudinal speeds of the vehicle are different. Therefore, the trajectory occupancy ratio is used to quantify the longitudinal behavior of LAV.

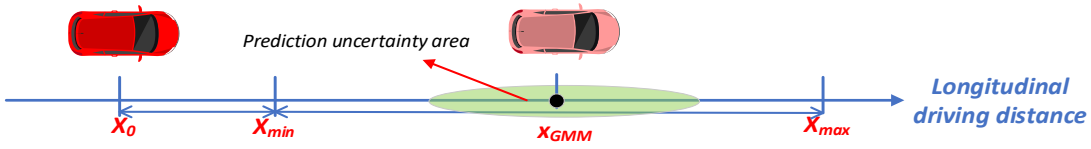

Figure 5.7. Motion prediction based on GMM with uncertainty

The driver type plot is constructed by taking the driving environment risk as the X-axis and the longitudinal vehicle behavior as the Y-axis. The slope of each data point is the driver aggressiveness, as shown in Fig. 5.8. Since the driving environment risk on the X-axis is a determined value, driver aggressiveness is still a random variable following the Gaussian distribution.

After calculating the aggressiveness of all drivers in the dataset, the normalized driver aggressiveness is then determined using the method of maximum-minimum normalization. From the above discussion, the transformation process from the predicted trajectory to the

normalized driver aggressiveness is linear, and the predicted trajectory follows the normal distribution, then the normalized driver aggressiveness also follows the normal distribution

$$\chi_i \sim \mathcal{N}(\mu_i, \delta_i^2) \tag{5.18}$$

where χ_i is the aggressiveness for the ith driver. The driver aggressiveness can interpretably show how the lane change vehicle becomes adaptive when it interacts with the LAV according to its aggressiveness, which is discussed in the next section.

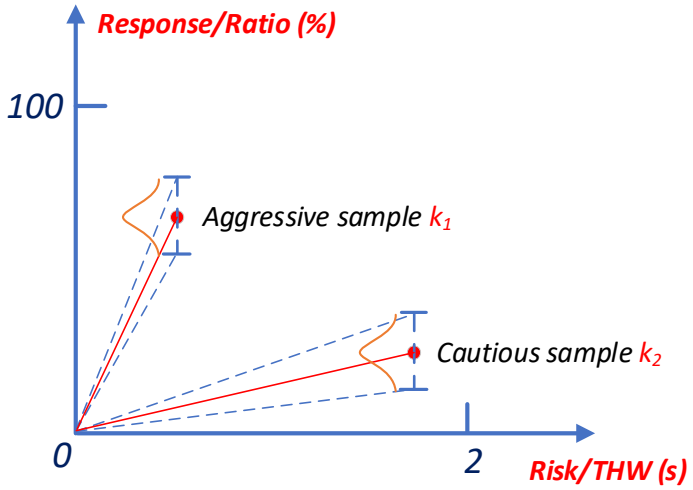

Figure 5.8. Driver aggressiveness definition based on driving environment and driver response

5.3.3 EV utilities modeling considering LAV type

According to the previous discussions, the utilities for the EV decision-making contain both safety and efficiency factors. The definition of incomplete information game states that when the opponent's participant type is uncertain, one's utilities will be given in the form of expectations. Following Eq. (3.35), and the definition of the normalized driver aggressiveness, the utility of EV considering the effects of the LAV's type is

$$w_1(\sigma_1, \sigma_2, \theta_1) := \int_{\mu_i-\delta_i}^{\mu_i+\delta_i} f_{\mathrm{X}_2}(\chi_2) v_1(\sigma_1, \sigma_2, \theta_1, \chi_2)\, d\chi_2 \tag{5.19}$$

where $v_1(\sigma_1, \sigma_2, \theta_1, \chi_2)$ is the expected utility of player 1 when he chooses the mixed strategy $\sigma_1 = (\sigma_{11}, \cdots, \sigma_{1K})$ and player 2 chooses the mixed strategy $\sigma_2 = (\sigma_{21}, \cdots, \sigma_{2J})$, which is shown as

$$v_1(\sigma_1, \sigma_2, \theta_1, \chi_2) = \sum_{k=1}^{K} \sum_{j=1}^{J} \sigma_{1k}(\theta_1)\sigma_{2j}(\chi_2)u_1(s_{1k}, s_{2j}) \tag{5.20}$$

where χ_2 is the LAV's driver aggressiveness, which is a random variable and follows the normal distribution according to Eq. (5.18); σ_1 and σ_2 are the mixed strategies of two players, replacing the pure strategies s_1 and s_2; $f_{\mathrm{X}_2}(\chi_2)$ is the probability density function (*pdf*) of the driver aggressiveness. The LAV's driver aggressiveness affects the expectation of the EV about the possible acceleration or deceleration in different cases, which is represented as

$$a_{exp} = (a_{max} - a_{min})\chi_2 + a_{min} \tag{5.21}$$

$$b_{exp} = (b_{max} - b_{min})\chi_2 + b_{min} \tag{5.22}$$

where a_{exp} and b_{exp} are the acceleration and deceleration of the LAV that are predicted by the EV after the prediction horizon T_p; a_{max} and a_{min} are the maximum and minimum positive accelerations; b_{max} and b_{min} are the maximum and minimum decelerations, separately. The estimated parameters a_{exp} and b_{exp} are substituted into Eq. (3.15), and the safety indicator $a_{req,brake}$ can be obtained. Finally, $v_1(\sigma_1, \sigma_2, \theta_1, \chi_2)$ becomes the function of the LAV's driver aggressiveness, with the safety utility affected by it.

5.5 Summary

In this chapter, the motions of the surrounding vehicles are modelled by the IDM. The driving styles are classified in an explainable way based on the real driving data. After that, the IDM model is calibrated separately to show the variances of surrounding vehicles in the simulation. Moreover, the driver identification model is realized relying on the trajectory predictions based on the GMM model and real driving data. The results in this chapter will be applied in the simulation and validation, which is the content of the next chapter.

Chapter 6

Simulation and Validations

In this chapter, the performances of the developed lane change decision-making model are evaluated based on the incomplete information game model. Two other models, namely the game model without driver identification and the rule-based model MOBIL are presented and compared with the proposed model in various scenarios. Moreover, the surrounding vehicles are extended to change lanes to test the model performances in the multi-player case. For the validations, the lane change scenarios are extracted from the real driving data. The lane change decisions and trajectories generated by the proposed model are compared with those of human drivers

6.1 Two-player incomplete information game simulations

In the two-player incomplete information game, the EV does not know the exact type of LAV, but can estimate the probability distributions of the driver type according to the equipped driver identification module. As is shown in Fig. 6.1, the LAV follows the IDM with different driving styles, which were discussed in Sections 5.2 and 5.3.

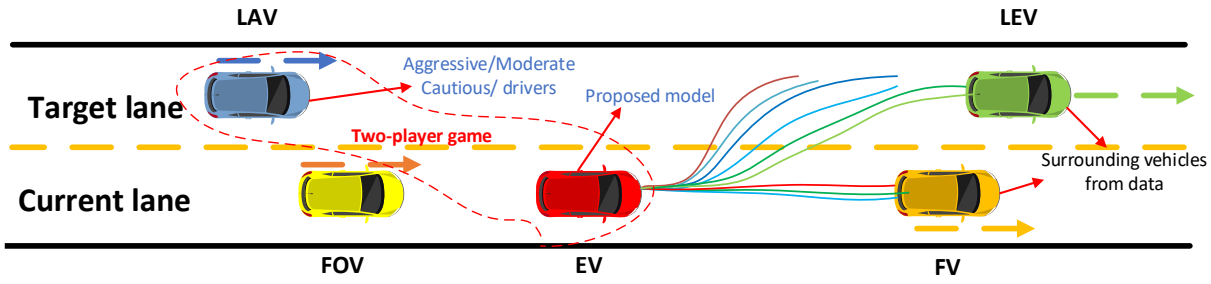

Figure 6.1. The two-player lane change game with incomplete information

The red ego vehicle (EV) drives in the rightmost lane when the simulation starts, surrounded by the slower yellow front vehicle (FV) in the current lane, green leading vehicle (LEV) and blue lag vehicle (LAV) in the target lane. The lane width is set to 4 m. The length and width of each vehicle are set to 5 and 2.2 meters, separately. When the simulation starts, the LAV is moderate and follows the EV at a normal distance. If the EV generates the lane change intention

and plans to change lane, the signal will be sent to the LAV and the car-following style will be switched to the target one.

For each scenario, the initial positions of EV, FV, LEV, and LAV are (60, 2), (85, 2), (70, 6) and (35, 6), respectively. The initial longitudinal speeds of EV, FV, LEV, and the LAV are 25 m/s, 24 m/s, 26 m/s, and 25 m/s, respectively. For the simulation in each scenario, the EV is controlled to keep the lane, and the driver aggressiveness is at its maximum in the first 3 seconds. This is because the aggressiveness prediction model requires the historical data for 3 seconds. After that, the driver aggressiveness can be estimated and the decision-making model generates the lane keeping or lane change decision adaptively with the aggressiveness considered. Therefore, the simulation results are plotted from the third second, when the EV is located at around 130 m. The critical time steps are marked with the light-colored bars in each figure.

For the model comparisons, two benchmark models are introduced. The first one is the rule-based lane change model, namely the MOBIL model. This model is widely accepted by the researchers through considering the brake decelerations differences between the LAV and EV itself. The model defines the lane change criterion as

$$\tilde{a}_{EV} - a_{EV} > p[\tilde{a}_{LAV} - a_{LAV}] + a_{thr}$$

where a_{EV} and a_{LAV} are the actual IDM accelerations of EV and LAV; $\tilde{a}_{EV}$ and $\tilde{a}_{LAV}$ are the accelerations after possible lane change; p is the politeness factor; a_{thr} is the minimum net acceleration required to avoid unnecessary lane changes for marginal advantages.

The other benchmark model is the game model without a driver identification module. In this case, the EV assumes the LAV as the moderate style without any updates. The simulation results are analyzed to show the performances of the proposed lane change model.

6.1.1 Interacting with a cautious driver

In this scenario, the EV drives faster than the FV, but the distance between them is big enough that the EV can accelerate to reach a higher speed. Therefore, the EV is not motivated to change lane in the beginning. The FV and LEV drive at constant speed, and the LAV switches from

moderate to cautious driving style when the EV is supposed to show its lane change intention by the turning signals because the EV-FV distance is not big enough for the EV to pursue higher speed.

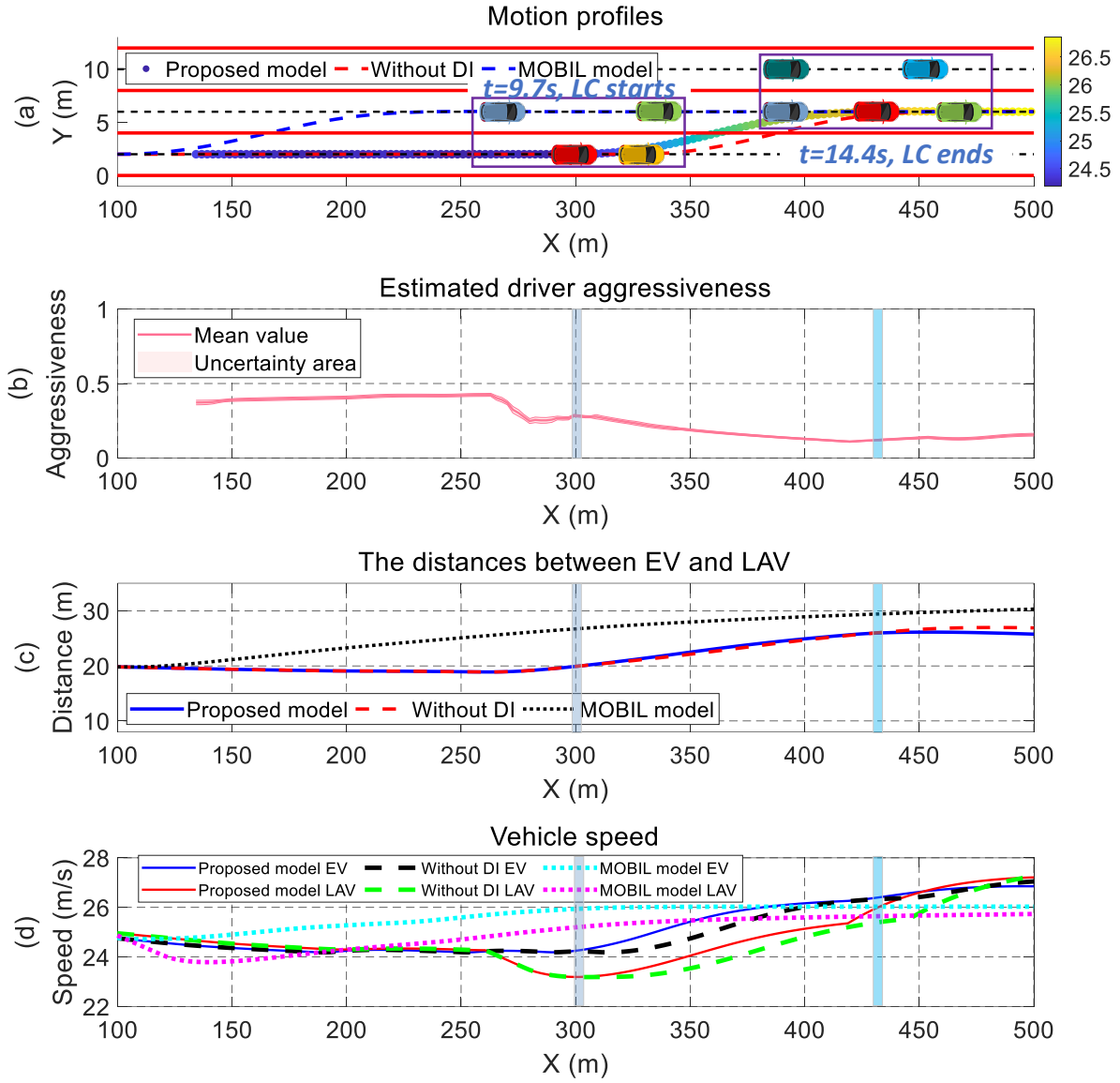

Figure 6.2. The simulation results when interacting with the cautious driver. (a) Motion profiles. (b) LAV's driver aggressiveness. (c) The distances between EV and LAV. (d) Vehicle speeds

As is shown in Fig. 6.2 (a), the EV generates the lane change decision based on the noncooperative game played by EV and LAV at 9.7 s, when their relative distance is 20 m (shown in Fig. 6.2 (c)), and their speeds are 24.2 and 23.2 m/s (shown in Fig. 6.2 (d)), respectively. Therefore, the safety risk is decreasing, and the EV changes lane successfully.

When the lane change ends, the new LAV in the leftmost lane is set to be in the same state as the old one, and the new LEV is set to be several meters before the EV. Therefore, the EV keeps following the new FV until the simulation finishes.

It can be seen from Fig. 6.2 (b) that the LAV's aggressiveness is around 0.42 in the first several seconds of simulation, where the aggressiveness varies from 0 to 1. This is because the LAV follows the IDM with moderate driving style. At t=8.3 s, the LAV starts to decelerate and the EV-LAV distance increases because the IDM style switches to cautious driving. Consequently, the estimated driver aggressiveness decreases and stabilizes at 0.25. Then the EV conducts the lane change safely until t=14.4 s, when the lane change ends.

Considering the aggressiveness helps to generate more efficient decisions. For the EV controlled by the game model without driver identification (DI), it starts to change lane at 10.8 s although the risk is acceptable 1 s ago. This is because the aggressiveness is not recognized, resulting in the conservative decision. For the MOBIL model, it changes lane very early when the EV-LEV distance is big enough for acceleration. This is because the MOBIL model makes lane change decisions based on the deceleration differences, instead of the actual driver requirements, such as safety and efficiency.

6.1.2 Interacting with an aggressive driver

Fig. 6.3 shows the results when the EV interacts with the aggressive LAV. The initial driving condition is set the same as the last scenario. The LAV switches to the aggressive car-following style when the EV generates the lane change intention at t=8.3 s. Then the LAV accelerates and the EV-LAV distance decreases slowly. As the driver aggressiveness keeps increasing from around 0.5 to a higher value, the EV recognizes the driving style of the LAV is aggressive. Therefore, the EV does not change lane but follows the FV at a constant speed. It is shown that the proposed model can avoid collisions by determining the driver type of surrounding vehicles.

For the benchmark model without DI, the controlled EV keeps lane all the time because it assumes the LAV is moderate, and the driving conditions does not allow the lane change even if the driver recognition is inaccurate. For the EV controlled by the MOBIL model, it keeps

lane for a while in the beginning, and changes lane although the risk is high when the EV-LAV distance is around 13 m. This is because the LEV in the target lane drives far from EV, and the lane change profit surges compared with following a slow moving FV in the current lane. The collision does not happen because the LAV is designed to follow the EV, although the car-following distance is short. It can be inferred that the collision risks are unacceptable if the LAV has the intention to overtake the EV.

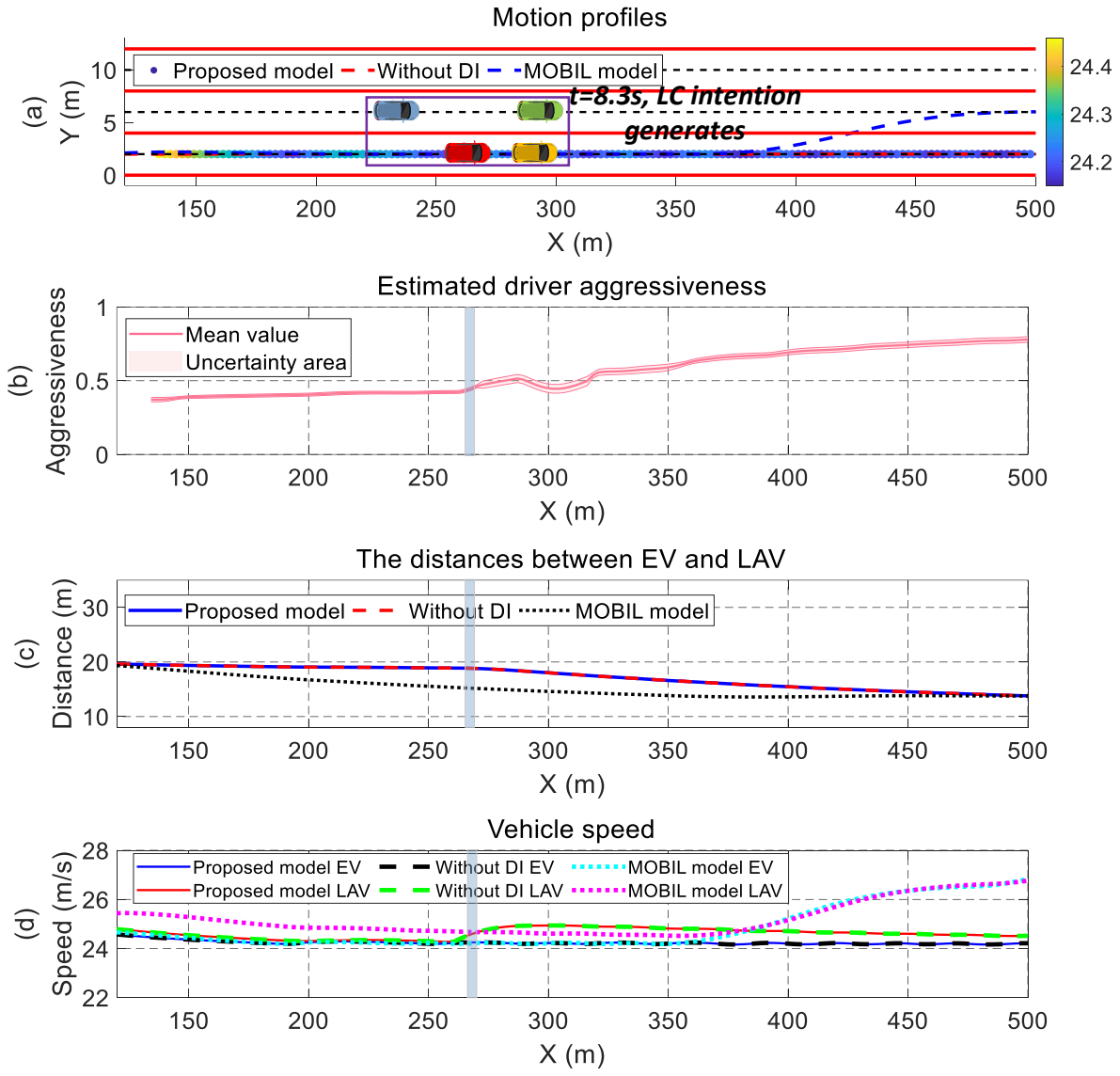

Figure 6.3. The simulation results when interacting with the aggressive driver. (a) Motion profiles. (b) LAV's driver aggressiveness. (c) The distances between EV and LAV. (d) Vehicle speeds

6.1.3 Interacting with an overtaking car

In this scenario, the LAV is designed to overtake the EV when detecting the lane change intention. Different from the previous scenarios, the LAV is controlled manually to not follow the car-following rule but accelerate slowly. This is because the overtaking behavior cannot be conducted in the IDM.

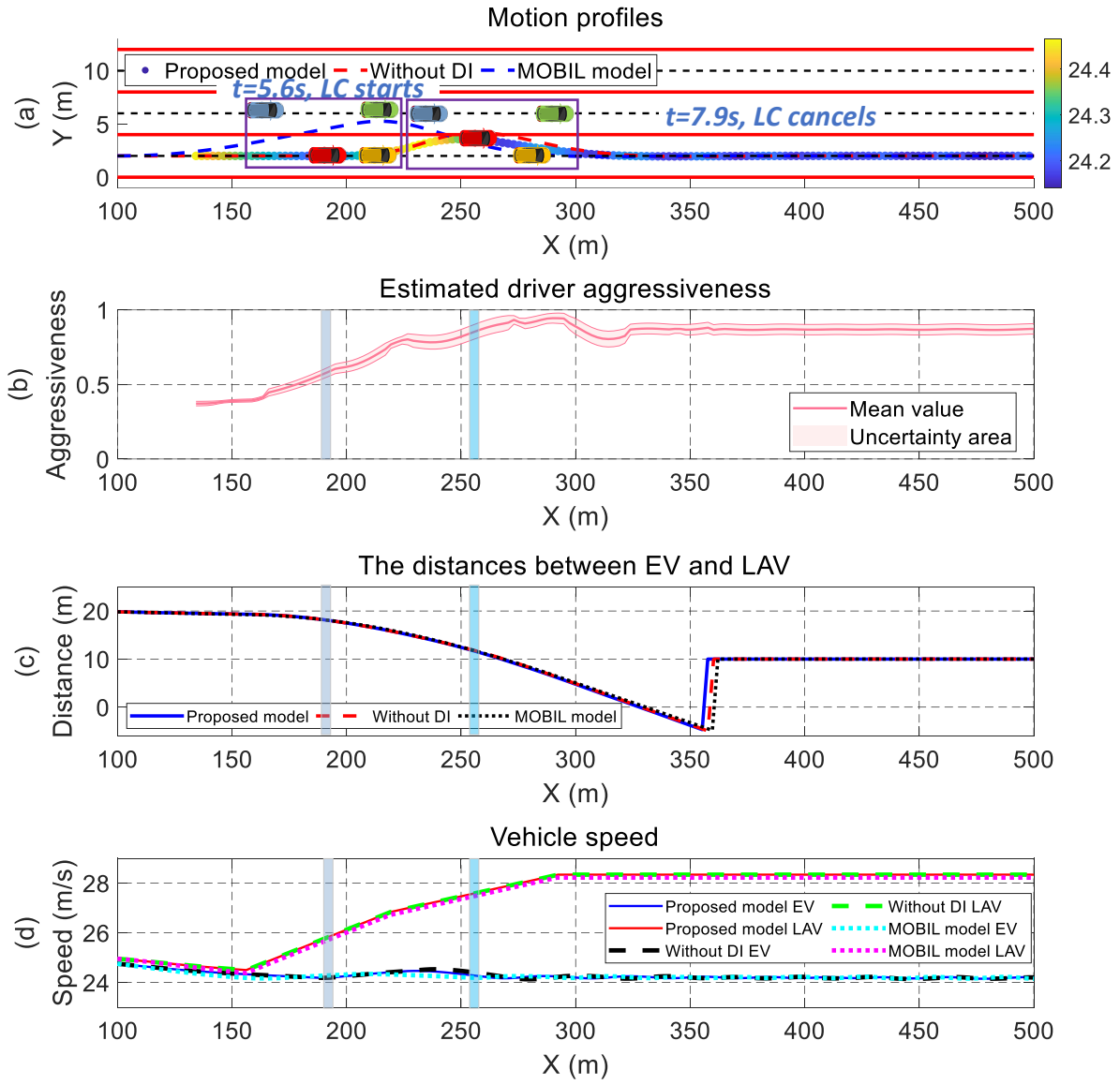

Figure 6.4. The simulation results when the LAV overtakes EV. (a) Motion profiles. (b) LAV's driver aggressiveness. (c) The distances between EV and LAV. (d) Vehicle speeds

As is shown in Fig. 6.4 (a), the EV starts to change lane at t=5.6 s when the EV-LAV distance

is around 18 m, and the driver aggressiveness is 0.55, showing moderate driving style. After that, the speed difference between LAV and EV increases continuously, and the driver aggressiveness increases to 0.8 at t=7.9 s, when the EV cancels the lane change. The LAV drives almost 4 m/s faster than EV, and their distance gap decreases to 10.5 m. The driving risks are high with the TTC of 2.6 s and the THW of 0.38 s. Therefore, the aggressiveness recognition in the proposed model helps the EV avoid the potential collision with the LAV.

In terms of the benchmark models, the game model without DI cancels the lane change with a lateral deviation of 4.2 m, which is larger than the 3.6 m of the proposed model. This result shows that the driver identification helps detect collision risks and respond. For the MOBIL model, the derivation is much higher than the game models and reaches 5.2 m, indicating its reckless driving style and higher driving risks, because returning back to the safe lane requires more time in this case. Compared with the benchmark models, the proposed model could recognize the intention of the LAV and responds to the driving environment change more quickly.

6.2 Multi-player incomplete information game simulations

In the multi-player game, the LEV in the target lane is required to cut into the current lane and affect the decisions of the ego vehicle, as is shown in Fig. 6.5. The player LAV is deigned to behave differently with yielding to the EV's lane change or accelerate to compete for the right of way. The LEV 2 is located in front of the LEV as the constraints of the EV's infinite acceleration.

For each scenario, he initial positions of EV, FV, LEV, LEV 2 and the LAV are (60, 2), (95, 2), (80, 6), (95, 6) and (45, 6), separately. The initial longitudinal speeds of EV, FV, LEV, LEV 2 and the LAV are 25 m/s, 25.5 m/s, 26 m/s, 26 m/s, and 25 m/s, respectively. The LEV is controlled to change lane in the same time. The LAV follows the IDM motion rule when it yields to the EV. In the case of accelerating, LAV is manually controlled because IDM cannot generate overtaking behavior.

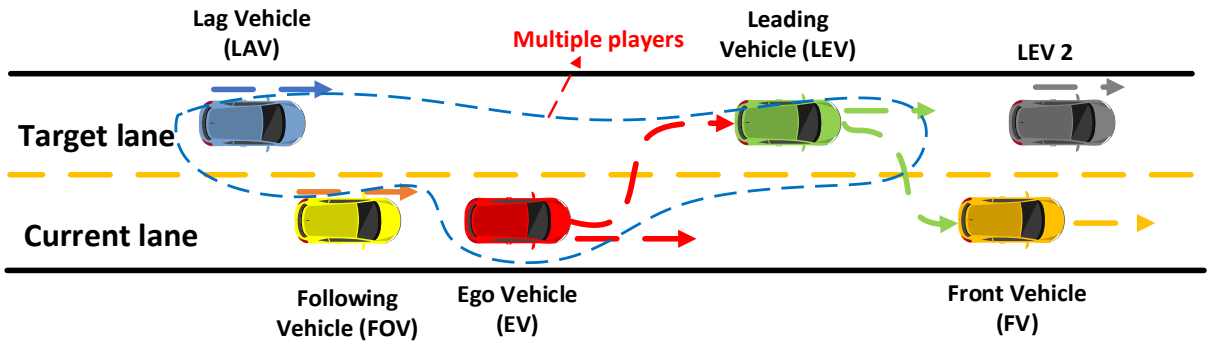

Figure 6.5. The multi-player lane change game with incomplete information

6.2.1 LEV cuts in and LAV yields

The motion profiles of the lane change EV and cut-in LEV are shown in Fig. 6.6. Specifically, the cut-in process of the LEV is labelled by the square marker, and the corresponding positions of the EV are marked by the pentagram. It is shown that the cut-in LEV makes the EV change lane in advance since there is enough space for it to accelerate in the current lane. The risk level in the target lane suddenly changes due to the variation of FV and LEV. The EV-FV distance drops from 25 m to around 12 m. Therefore, the lane change desire surges. Simultaneously, the LAV switches from moderate to cautious driving style, and the EV-LAV distance keeps increasing. The EV changes lane successfully from t=4.4 s to t=10.1 s.

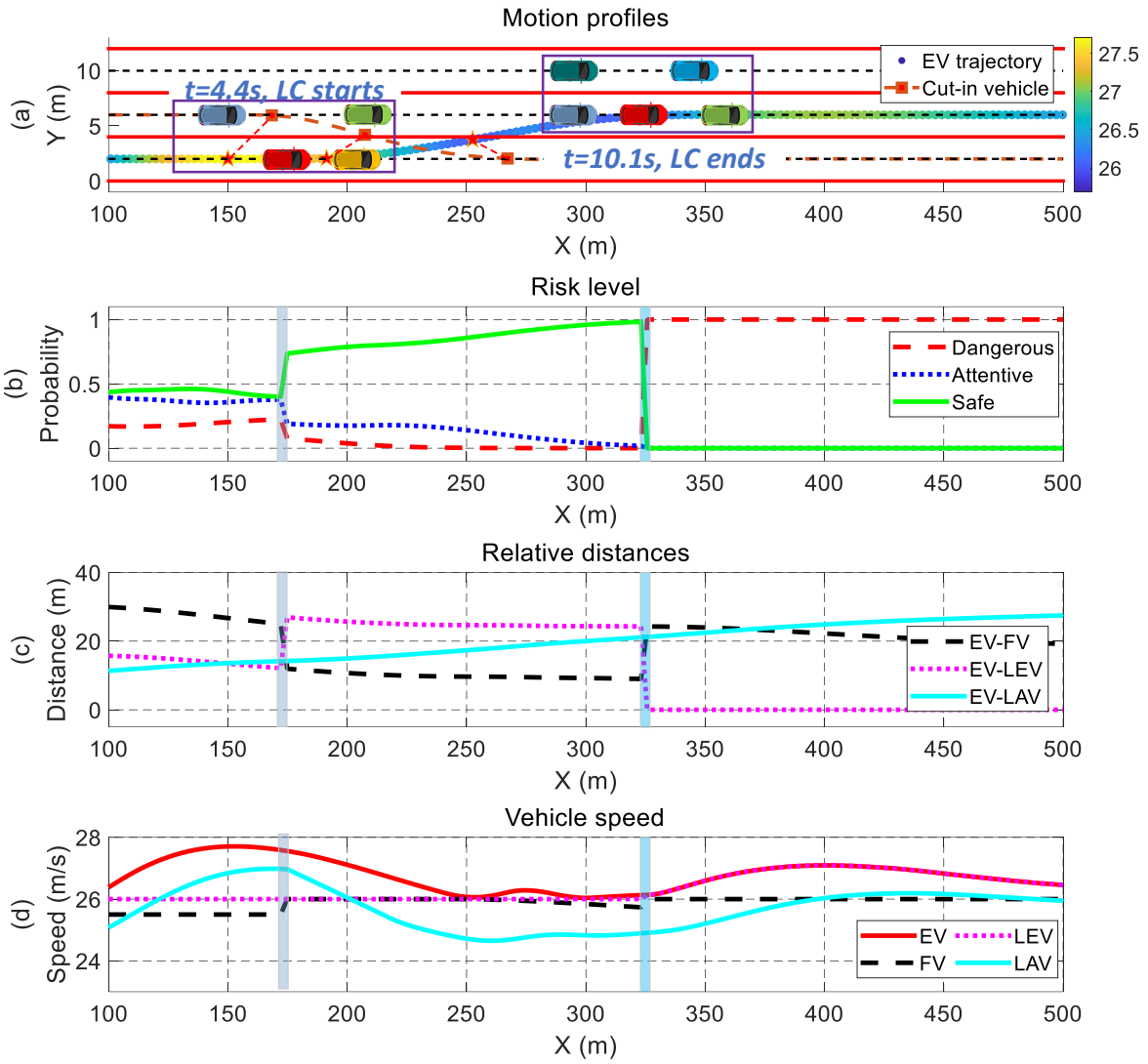

Figure 6.6. The autonomous vehicle interacts with the cautious lag vehicle driver when LEV cuts in. (a) Motion profiles. (b) Risk level. (c) Relative distances. (d) Vehicle speed.

6.2.2 LEV cuts in and LAV accelerates

In this case, the LAV accelerates to compete for the driving space while the driving environment and the motions of other surrounding vehicles are kept the same as the previous one, as is shown in Fig. 6.7. The lane change behavior is conducted at t=4.4 s, however, the EV-LAV distance keeps decreasing and the probability difference declines gradually between being safe and dangerous in the target lane. The EV thus cancels the lane change and gets back at t=6.5 s, when the EV-LAV distance is 10 m. The LAV keeps accelerating and overtakes the EV at t=10.5 s, and the simulation ends.

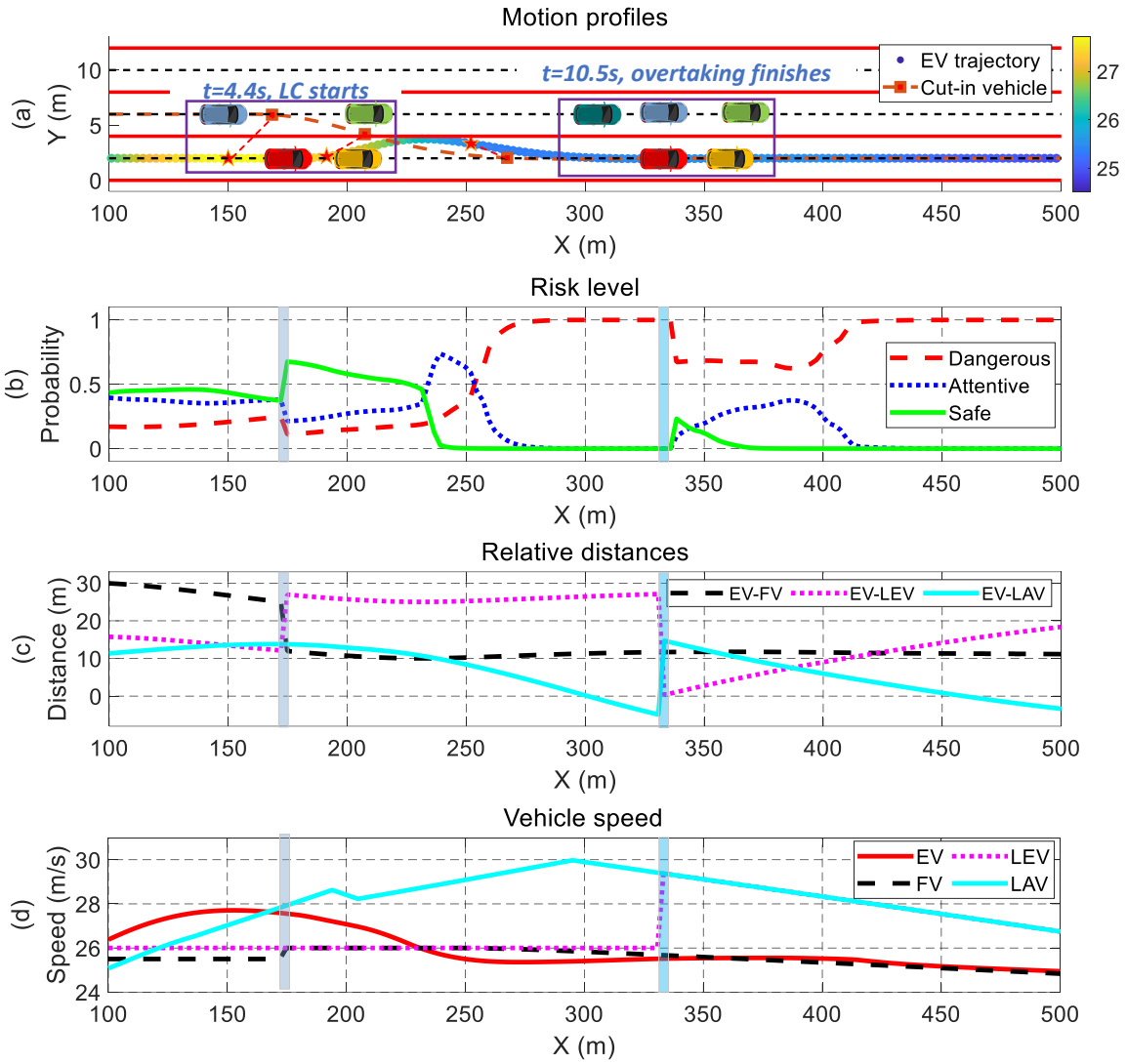

Figure 6.7. The autonomous vehicle interacts with the aggressive lag vehicle driver when LEV cuts in. (a) Motion profiles. (b) Risk level. (c) Relative distances. (d) Vehicle speed.

6.3 Validations based on real driving data

In this section, the proposed decision-making model is validated by comparisons with the motion profiles of real human drivers. Two scenarios are extracted from the naturalistic driving data, i.e., the LEV keeps lane and the LEV cuts in. Thus, two-player game and multi-player game are utilized to model the driving decisions of the EV separately.

6.3.1 LEV keeps lane

When the LEV keeps lane, the EV makes driving decisions based on the two-player game. The

initial positions of EV, FV, LEV, and the LAV are (6.48, -2.12), (55.91, -2.27), (46.09, 2) and (-12.8, 2.2), separately. The initial longitudinal speeds of the EV, FV, LEV, and LAV are 23.57 m/s, 21.85 m/s, 27.52 m/s, and 27.62 m/s, respectively.

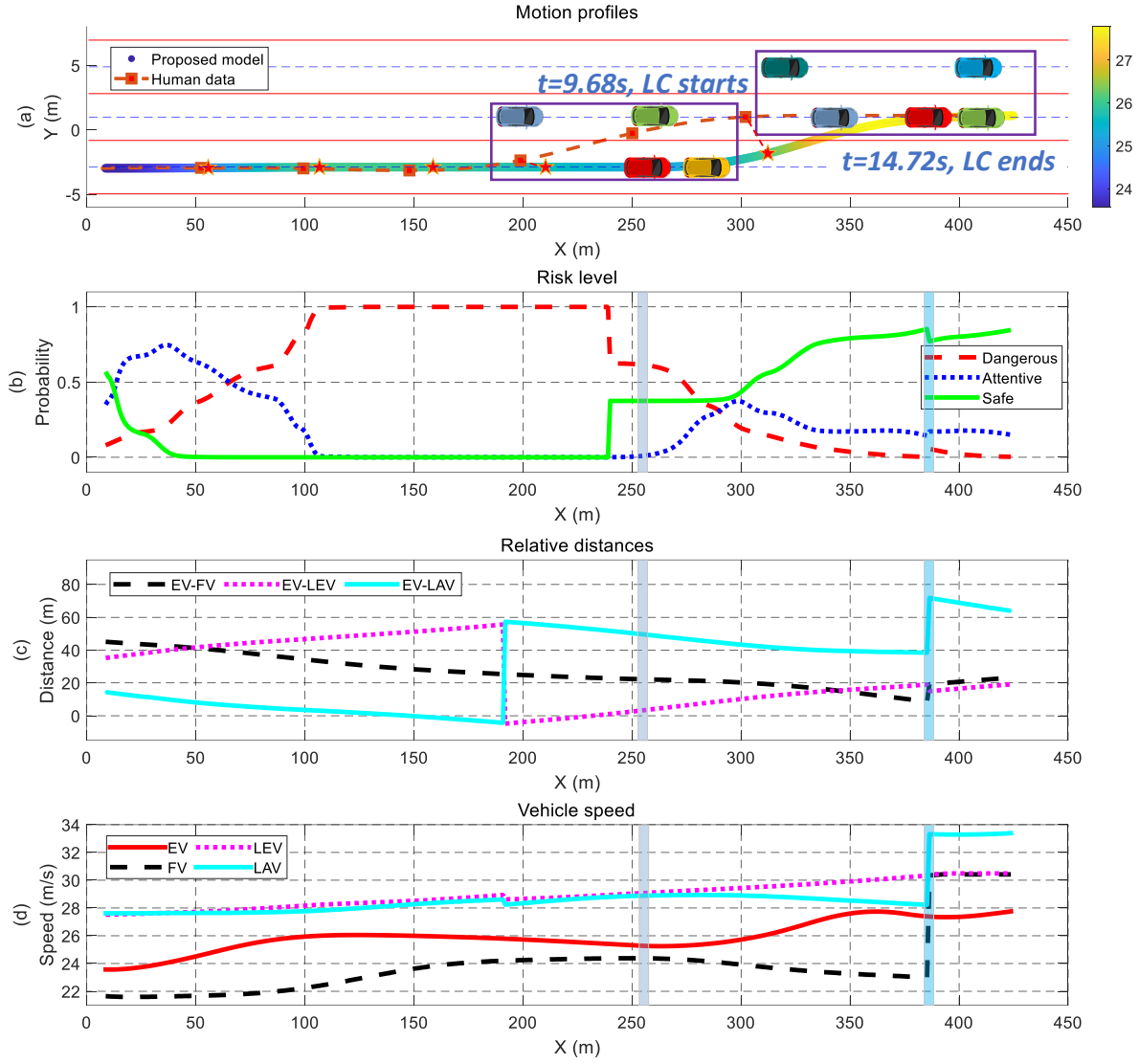

Figure 6.8. The comparisons of the human driving and proposed model when LEV keeps lane. (a) Motion profiles. (b) Risk level. (c) Relative distances. (d) Vehicle speed.

The EV accelerates at the beginning because the EV-FV distance is large, while the human driver adopts a different strategy by waiting and yielding to the LEV in the target lane. Therefore, the EV controlled by the proposed model drives faster than the human driver. When the EV approaches the FV, it decelerates to keep a safe distance without changing lane because the LAV in the target lane is close and the probability of being dangerous is 1. Since the human-

driven EV yields to the LEV at the beginning, it changes lane earlier than the car controlled by the proposed model. The proposed decision-making model tends to keep lane unless the driving space decreases to a threshold value.

In terms of the driving efficiency, the proposed model drives to 424.85 m during the validation, while the human-driven car stops at 413.03 m. The result shows that their driving efficiencies are close.

6.3.2 LEV cuts in

When the LEV changes lane and affects the driving safety and efficiency of the EV, the validation is modelled as the multi-player game. The initial positions of the EV, FV, LEV, and LAV are (17.97, 3.69), (155.34, 2.5), (29.8, 7.59) and (9.07, 7.26), separately. The initial longitudinal speeds of EV, FV, LEV, and the LAV are 18.74 m/s, 18.51 m/s, 19.53 m/s, and 19.64 m/s, respectively. It seems that the EV could accelerate greatly since the EV-FV distance is over 100 meters, however, the LEV near the EV shows its lane change intention and changes lane slowly. Therefore, the EV decelerates and yields to the LEV after it finishes the lane change. Thereafter, the EV starts to change lane without the disturbance of the LAV and LEV.

In terms of the driving efficiency, the proposed model drives to 412.4 m during the validation, while the human-driven car stops at 412.69 m. The result shows that their driving efficiencies are close.

It can be summarized from the validations compared with the human driving that the proposed model tends to explore the driving space in the current lane first and consider the opportunity for lane change. The human drivers can make predictions in the longer term, and consider the driving environment more comprehensively. Moreover, the variations exist among human drivers, and the vehicle trajectories may cover a range if more scenarios are analyzed. Compared with the human driver, the proposed model follows a relatively reasonable decision-making logic, which guarantees the driving safety and achieves similar driving efficiency with real drivers.

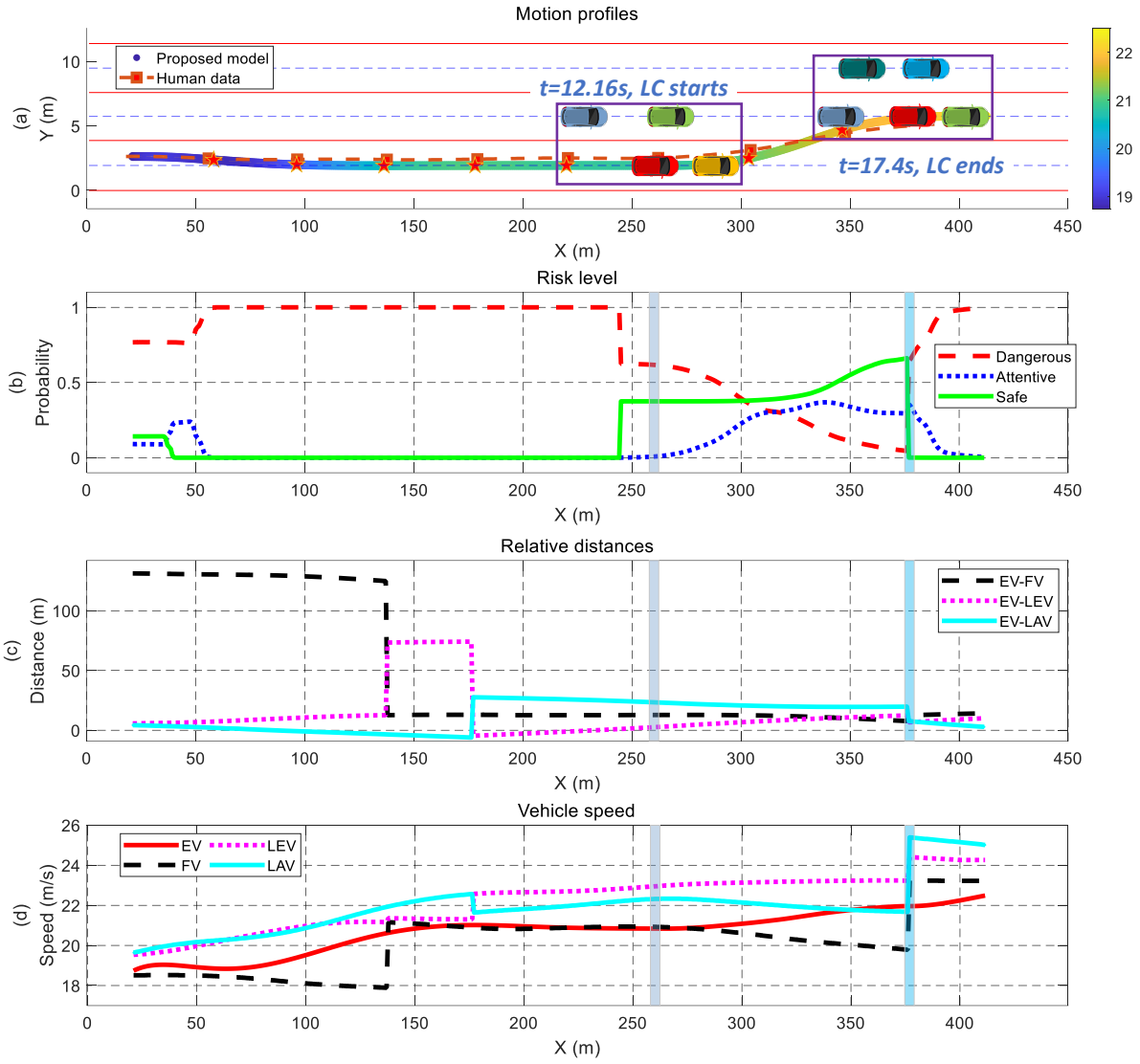

Figure 6.9. The comparisons of the human driving and proposed model when LEV cuts in. (a) Motion profiles. (b) Risk level. (c) Relative distances. (d) Vehicle speed.

6.4 Summary

In this chapter, two simulations and one validation were presented. In the first simulation, three scenarios were designed with the LAV style varying from cautious to overtaking car. Moreover, two other models were introduced for performances comparisons, namely the game model without driver identification and the rule-based model MOBIL. In the second simulation, the LEV cut in to the front area of the EV, and the LAVs responded differently to the EV's lane change. In the validation part, the scenarios were extracted from the real driving data, and the

human driving behaviors were used for comparisons. The simulation and validation results showed that the proposed model could help the ego vehicles make safe and efficient driving decisions in the highway lane change. The human-likeliness is also indicated in the comparisons with human drivers.

Chapter 7.

Conclusions and future work

In this chapter, the findings of this research are concluded, and some future works are pointed out.

7.1 Conclusions

In this research, a game theory based decision-making model was proposed to deal with the strong interactions between an autonomous vehicle and human-driven vehicles in highway lane change scenarios. This research offered some insights to enable autonomous vehicles to make safe and efficient driving decisions and behave in a human-like way in a mixed traffic environment. The performances of the developed model were evaluated under various conditions by assigning different driving styles to the human-driven vehicles, which were learned from the real driving data. The simulation results showed that the proposed lane change decision-making model could identify the types drivers in the surrounding vehicles and make safe and efficient driving decisions adaptively, based on the identification results and driving environment. The comparisons with the human driving data in the validations showed the human-likeliness of the proposed model through the analysis of the lane change decision-making process.

The lane change process was firstly analyzed to identify the components related to driving decision-making. The lane change was modelled to capture the interactions under the framework of game theory. The information was found to be important in the lane change game modeling, and the games with complete information and incomplete information were both discussed. The incomplete information game was more likely to happen in real traffic due to the unavailability of information sharing. Therefore, the probabilistic models were further introduced in the game to estimate the needed information. It was demonstrated that the driver identifications helped the decision-making model evaluate the driving behaviors of other vehicles and make driving decisions more decisively, compared with the one without the driver

identifications.

To model the lane change decision-making in realistic traffic scenarios, the two-player model was extended to the multi-player game model, and the lateral driving behaviors of the surrounding vehicles were considered. Compared with the two-player game, the scenarios in the multi-player game were more complex. The combinations of the behaviors of multiple surrounding vehicles led to the scenarios varieties. It was shown that the game-based decision-making model made driving decisions adaptively according to the types of the lag vehicle when the leading vehicle in the other lane cut in.

The interactive driving data were utilized to model the behavior of the surrounding vehicles, and the simulation environment became more realistic. Moreover, the data were utilized to the decision-making model by introducing driver aggressiveness recognition based on GMM. With the introduction of the real driving data, the surrounding vehicles' motions and the decision-making model were both connected to human driving behavior. The interactions between the ego vehicle and the surrounding vehicles were more realistic, and the generated driving decisions were more human-like.

The decision-making model was evaluated in the dense highway traffic environment with strong interactions, including two-player game and multi-player game. The driver aggressiveness was recognized and transited to the decision-making model. The human-driven vehicles were equipped with various aggressiveness in these scenarios. The simulation results showed that the proposed model could determine the driving styles of the surrounding vehicles, and make safe and efficient driving decisions. The comparisons with the real human drivers in the validations showed that the proposed model generated human-like decisions and trajectories.

Overall, this research developed a game theory based decision-making model for highway driving. T Real-world driving data were used to train the driver identification module and model the behaviour of surrounding vehicles, ensuring interactions in a realistic traffic environment. The evaluations demonstrated that the proposed model made safe and efficient driving decisions in various scenarios. This research offered some insights in the field of

developing a human-like decision-making model when interacting with human-driven vehicles in mixed traffic.

7.2 Future work

In the future work, more validations can be implemented on a real vehicle. Also, the behavior of the surrounding vehicles needs further study. The traffic rules and constraints are not considered in this research, which is worth studying to make the driving decisions comply with traffic regulations.

Copyright Permissions

IEEE, as the publisher of the three manuscripts fully or partly adopted in Chapters 1-6 allow the reuse of published papers in the thesis without formal permissions. Thus, the waivers of copyright from IEEE are achieved by the following statement:

Policy Regarding Thesis/Dissertation Reuse, from IEEE Copyright Clearance Centre

"The IEEE does not require individuals working on a thesis to obtain a formal reuse license; however, you may print out this statement to be used as a permission grant".

References

[1] W. H. Organization, “Global status report on road safety 2018: Summary,” World Health Organization, 2018.

[2] B. of T. S. U.S. Department of Transportation, “Transportation Statistics Annual Report 2018,” Washington, DC, 2018.

[3] N. H. T. S. Administration, “Critical reasons for crashes investigated in the national motor vehicle crash causation survey,” *Washington, DC US Dep. Transp.*, vol. 2, pp. 1–2, 2015.

[4] K. Hurley, “How pedestrians will defeat autonomous vehicles,” *Sci. Am.*, 2017.

[5] M. Richtel and C. Dougherty, “Google’s driverless cars run into problem: Cars with drivers,” *New York Times*, vol. 1, no. September, 2015.

[6] R. J. Aumann and S. Hart, *Handbook of game theory with economic applications*, vol. 1. North-Holland Amsterdam, 1992.

[7] P. Hammerstein and R. Selten, “Game theory and evolutionary biology,” *Handb. game theory with Econ. Appl.*, vol. 2, pp. 929–993, 1994.

[8] T. Roughgarden, “Algorithmic game theory,” *Commun. ACM*, vol. 53, no. 7, pp. 78–86, 2010.

[9] S. Moridpour, M. Sarvi, and G. Rose, “Lane changing models: a critical review,” *Transp. Lett.*, vol. 2, no. 3, pp. 157–173, 2010.

[10] R. Sukthankar, S. Baluja, and J. Hancock, “Evolving an intelligent vehicle for tactical reasoning in traffic,” in *Proceedings of International Conference on Robotics and Automation*, 1997, vol. 1, pp. 519–524.

[11] M. Sivak and B. Schoettle, “Eco-driving: Strategic, tactical, and operational decisions of the driver that influence vehicle fuel economy,” *Transp. Policy*, vol. 22, pp. 96–99, 2012.

[12] Y. Luo, D. Turgut, and L. Bölöni, “Modeling the strategic behavior of drivers for multi-lane highway driving,” *J. Intell. Transp. Syst.*, vol. 19, no. 1, pp. 45–62, 2015.

[13] J. A. Michon, “A critical view of driver behavior models: what do we know, what should we do?,” in *Human behavior and traffic safety*, Springer, 1985, pp. 485–524.

[14] V. Alexiadis, D. Gettman, and R. Hranac, “Next Generation Simulation (NGSIM): Identification Prioritization of Core Algorithm Categories,” Report No. FHWA-HOP-06-008, Federal Highway Administration, US Department of …, 2004.

[15] A. Drogoul and S. Espié, “How to combine reactivity and anticipation: the case of conflicts resolution in a simulated road traffic,” in *International Workshop on Multi-Agent Systems and Agent-Based Simulation*, 2000, pp. 82–96.

[16] C. Urmson *et al.*, “Autonomous driving in urban environments: Boss and the urban challenge,” *J. F. Robot.*, vol. 25, no. 8, pp. 425–466, 2008.

[17] J. Leonard *et al.*, “A perception-driven autonomous urban vehicle,” *J. F. Robot.*, vol. 25, no. 10, pp. 727–774, 2008.

[18] M. Montemerlo *et al.*, “Junior: The stanford entry in the urban challenge,” *J. F. Robot.*, vol. 25, no. 9, pp. 569–597, 2008.

[19] K. Jo, J. Kim, D. Kim, C. Jang, and M. Sunwoo, “Development of autonomous car—Part II: A case study on the implementation of an autonomous driving system based on distributed architecture,” *IEEE Trans. Ind. Electron.*, vol. 62, no. 8, pp. 5119–5132, 2015.

[20] Y. Chen *et al.*, “Terramax^{TM}: Team oshkosh urban robot,” *J. F. Robot.*, vol. 25, no. 10, pp. 841–860, 2008.

[21] B. J. Patz, Y. Papelis, R. Pillat, G. Stein, and D. Harper, “A practical approach to robotic design for the darpa urban challenge,” *J. F. Robot.*, vol. 25, no. 8, pp. 528–566, 2008.

[22] A. Kurt and Ü. Özgüner, “Hierarchical finite state machines for autonomous mobile

systems," *Control Eng. Pract.*, vol. 21, no. 2, pp. 184–194, 2013.

[23] L. Claussmann, A. Carvalho, and G. Schildbach, "A path planner for autonomous driving on highways using a human mimicry approach with binary decision diagrams," in *2015 European Control Conference (ECC)*, 2015, pp. 2976–2982.

[24] I. Miller *et al.*, "Team Cornell's Skynet: Robust perception and planning in an urban environment," *J. F. Robot.*, vol. 25, no. 8, pp. 493–527, 2008.

[25] N. Li, H. Chen, I. Kolmanovsky, and A. Girard, "An explicit decision tree approach for automated driving," 2017.

[26] N. Li, D. Oyler, M. Zhang, Y. Yildiz, A. Girard, and I. Kolmanovsky, "Hierarchical reasoning game theory based approach for evaluation and testing of autonomous vehicle control systems," in *2016 IEEE 55th Conference on Decision and Control (CDC)*, 2016, pp. 727–733.

[27] D. A. Pomerleau, "Alvinn: An autonomous land vehicle in a neural network," in *Advances in neural information processing systems*, 1989, pp. 305–313.

[28] M. Bojarski *et al.*, "End to end learning for self-driving cars," *arXiv Prepr. arXiv1604.07316*, 2016.

[29] C. Chen, A. Seff, A. Kornhauser, and J. Xiao, "Deepdriving: Learning affordance for direct perception in autonomous driving," in *Proceedings of the IEEE International Conference on Computer Vision*, 2015, pp. 2722–2730.

[30] S. Ulbrich and M. Maurer, "Situation assessment in tactical lane change behavior planning for automated vehicles," in *2015 IEEE 18th International conference on intelligent transportation systems*, 2015, pp. 975–981.

[31] R. Schubert, K. Schulze, and G. Wanielik, "Situation assessment for automatic lane-change maneuvers," *IEEE Trans. Intell. Transp. Syst.*, vol. 11, no. 3, pp. 607–616, 2010.

[32] D. Kasper *et al.*, "Object-oriented Bayesian networks for detection of lane change

maneuvers," *IEEE Intell. Transp. Syst. Mag.*, vol. 4, no. 3, pp. 19–31, 2012.

[33] J. Schulz, C. Hubmann, J. Löchner, and D. Burschka, "Interaction-aware probabilistic behavior prediction in urban environments," in *2018 IEEE/RSJ International Conference on Intelligent Robots and Systems (IROS)*, 2018, pp. 3999–4006.

[34] S. J. Russell and P. Norvig, *Artificial intelligence: a modern approach*. Malaysia; Pearson Education Limited, 2016.

[35] A. Furda and L. Vlacic, "Enabling safe autonomous driving in real-world city traffic using multiple criteria decision making," *IEEE Intell. Transp. Syst. Mag.*, vol. 3, no. 1, pp. 4–17, 2011.

[36] F. W. Rauskolb *et al.*, "Caroline: An autonomously driving vehicle for urban environments," *J. F. Robot.*, vol. 25, no. 9, pp. 674–724, 2008.

[37] J. Wei, J. M. Snider, T. Gu, J. M. Dolan, and B. Litkouhi, "A behavioral planning framework for autonomous driving," in *2014 IEEE Intelligent Vehicles Symposium Proceedings*, 2014, pp. 458–464.

[38] Y. Guan, S. E. Li, J. Duan, W. Wang, and B. Cheng, "Markov probabilistic decision making of self-driving cars in highway with random traffic flow: a simulation study," *J. Intell. Connect. Veh.*, 2018.

[39] D. Loiacono, A. Prete, P. L. Lanzi, and L. Cardamone, "Learning to overtake in TORCS using simple reinforcement learning," in *IEEE Congress on Evolutionary Computation*, 2010, pp. 1–8.

[40] X. Li, X. Xu, and L. Zuo, "Reinforcement learning based overtaking decision-making for highway autonomous driving," in *2015 Sixth International Conference on Intelligent Control and Information Processing (ICICIP)*, 2015, pp. 336–342.

[41] D. C. K. Ngai and N. H. C. Yung, "A multiple-goal reinforcement learning method for complex vehicle overtaking maneuvers," *IEEE Trans. Intell. Transp. Syst.*, vol. 12, no. 2, pp. 509–522, 2011.

[42] P. Wang, C.-Y. Chan, and A. de La Fortelle, “A reinforcement learning based approach for automated lane change maneuvers,” in *2018 IEEE Intelligent Vehicles Symposium (IV)*, 2018, pp. 1379–1384.

[43] D. Pomerleau, “An autonomous land vehicle in a neural network. NIPS 1.” Morgan Kaufmann, 1989.

[44] P. Wang and C.-Y. Chan, “Formulation of deep reinforcement learning architecture toward autonomous driving for on-ramp merge,” in *2017 IEEE 20th International Conference on Intelligent Transportation Systems (ITSC)*, 2017, pp. 1–6.

[45] C.-J. Hoel, K. Wolff, and L. Laine, “Automated speed and lane change decision making using deep reinforcement learning,” in *2018 21st International Conference on Intelligent Transportation Systems (ITSC)*, 2018, pp. 2148–2155.

[46] C. Schöller, V. Aravantinos, F. Lay, and A. Knoll, “What the constant velocity model can teach us about pedestrian motion prediction,” *IEEE Robot. Autom. Lett.*, vol. 5, no. 2, pp. 1696–1703, 2020.

[47] A. Polychronopoulos, M. Tsogas, A. J. Amditis, and L. Andreone, “Sensor fusion for predicting vehicles’ path for collision avoidance systems,” *IEEE Trans. Intell. Transp. Syst.*, vol. 8, no. 3, pp. 549–562, 2007.

[48] G. Zhai, H. Meng, and X. Wang, “A constant speed changing rate and constant turn rate model for maneuvering target tracking,” *Sensors*, vol. 14, no. 3, pp. 5239–5253, 2014.

[49] R. Schubert, E. Richter, and G. Wanielik, “Comparison and evaluation of advanced motion models for vehicle tracking,” in *2008 11th international conference on information fusion*, 2008, pp. 1–6.

[50] S. Reisinger, D. Adelberger, and L. del Re, “A two-layer switching based trajectory prediction method,” *Eur. J. Control*, vol. 62, pp. 143–150, 2021.

[51] J. Ji, A. Khajepour, W. W. Melek, and Y. Huang, “Path planning and tracking for vehicle collision avoidance based on model predictive control with multiconstraints,”

IEEE Trans. Veh. Technol., vol. 66, no. 2, pp. 952–964, 2016.

[52] Y. Rasekhipour, A. Khajepour, S.-K. Chen, and B. Litkouhi, "A potential field-based model predictive path-planning controller for autonomous road vehicles," *IEEE Trans. Intell. Transp. Syst.*, vol. 18, no. 5, pp. 1255–1267, 2016.

[53] R. E. Chandler, R. Herman, and E. W. Montroll, "Traffic dynamics: studies in car following," *Oper. Res.*, vol. 6, no. 2, pp. 165–184, 1958.

[54] D. C. Gazis, R. Herman, and R. W. Rothery, "Nonlinear follow-the-leader models of traffic flow," *Oper. Res.*, vol. 9, no. 4, pp. 545–567, 1961.

[55] A. D. May, *Traffic flow fundamentals*. 1990.

[56] G. F. Newell, "Nonlinear effects in the dynamics of car following," *Oper. Res.*, vol. 9, no. 2, pp. 209–229, 1961.

[57] M. Treiber, A. Hennecke, and D. Helbing, "Congested traffic states in empirical observations and microscopic simulations," *Phys. Rev. E*, vol. 62, no. 2, p. 1805, 2000.

[58] D. S. González, V. Romero-Cano, J. Dibangoye, and C. Laugier, "Interaction-Aware Tracking and Lane Change Detection in Highway Scenarios Using Realistic Driver Models," 2017.

[59] D. S. González, V. Romero-Cano, J. S. Dibangoye, and C. Laugier, "Interaction-aware driver maneuver inference in highways using realistic driver models," in *2017 IEEE 20th International Conference on Intelligent Transportation Systems (ITSC)*, 2017, pp. 1–8.

[60] T. Gindele, S. Brechtel, and R. Dillmann, "Learning driver behavior models from traffic observations for decision making and planning," *IEEE Intell. Transp. Syst. Mag.*, vol. 7, no. 1, pp. 69–79, 2015.

[61] T. Gindele, S. Brechtel, and R. Dillmann, "A probabilistic model for estimating driver behaviors and vehicle trajectories in traffic environments," in *13th International IEEE Conference on Intelligent Transportation Systems*, 2010, pp. 1625–1631.

[62] H. Kita, “A merging–giveway interaction model of cars in a merging section: a game theoretic analysis,” *Transp. Res. Part A Policy Pract.*, vol. 33, no. 3–4, pp. 305–312, 1999.

[63] H. Kita, K. Tanimoto, and K. Fukuyama, “A game theoretic analysis of merging-giveway interaction: a joint estimation model,” *Transp. Traffic Theory 21st Century*, pp. 503–518, 2002.

[64] K. Kang and H. A. Rakha, “Modeling driver merging behavior: a repeated game theoretical approach,” *Transp. Res. Rec.*, vol. 2672, no. 20, pp. 144–153, 2018.

[65] K. Kang and H. A. Rakha, “A Repeated Game Freeway Lane Changing Model,” *Sensors*, vol. 20, no. 6, p. 1554, 2020.

[66] H. Yu, H. E. Tseng, and R. Langari, “A human-like game theory-based controller for automatic lane changing,” *Transp. Res. part C Emerg. Technol.*, vol. 88, pp. 140–158, 2018.

[67] H. X. Liu, W. Xin, Z. Adam, and J. Ban, “A game theoretical approach for modelling merging and yielding behaviour at freeway on-ramp sections,” *Transp. traffic theory*, vol. 3, pp. 197–211, 2007.

[68] K. Kang and H. A. Rakha, “Game theoretical approach to model decision making for merging maneuvers at freeway on-ramps,” *Transp. Res. Rec.*, vol. 2623, no. 1, pp. 19–28, 2017.

[69] A. Talebpour, H. S. Mahmassani, and S. H. Hamdar, “Modeling lane-changing behavior in a connected environment: A game theory approach,” *Transp. Res. part C Emerg. Technol.*, vol. 59, pp. 216–232, 2015.

[70] F. Meng, J. Su, C. Liu, and W.-H. Chen, “Dynamic decision making in lane change: Game theory with receding horizon,” in *2016 UKACC 11th International Conference on Control (CONTROL)*, 2016, pp. 1–6.

[71] Y. Ali, Z. Zheng, M. M. Haque, and M. Wang, “A game theory-based approach for modelling mandatory lane-changing behaviour in a connected environment,” *Transp.*

Res. part C Emerg. Technol., vol. 106, pp. 220–242, 2019.

[72] J. H. Yoo and R. Langari, "A Stackelberg game theoretic driver model for merging," 2013.

[73] J. H. Yoo and R. Langari, "Stackelberg game based model of highway driving," in *ASME 2012 5th Annual Dynamic Systems and Control Conference joint with the JSME 2012 11th Motion and Vibration Conference*, 2012, pp. 499–508.

[74] M. Li *et al.*, "Shared control with a novel dynamic authority allocation strategy based on game theory and driving safety field," *Mech. Syst. Signal Process.*, vol. 124, pp. 199–216, 2019.

[75] M. Li, H. Cao, X. Song, Y. Huang, J. Wang, and Z. Huang, "Shared control driver assistance system based on driving intention and situation assessment," *IEEE Trans. Ind. Informatics*, vol. 14, no. 11, pp. 4982–4994, 2018.

[76] W. Schwarting, A. Pierson, J. Alonso-Mora, S. Karaman, and D. Rus, "Social behavior for autonomous vehicles," *Proc. Natl. Acad. Sci.*, vol. 116, no. 50, pp. 24972–24978, 2019.

[77] M. Wang, S. P. Hoogendoorn, W. Daamen, B. van Arem, and R. Happee, "Game theoretic approach for predictive lane-changing and car-following control," *Transp. Res. part C Emerg. Technol.*, vol. 58, pp. 73–92, 2015.

[78] D. Sadigh, S. Sastry, S. A. Seshia, and A. D. Dragan, "Planning for autonomous cars that leverage effects on human actions.," in *Robotics: Science and Systems*, 2016, vol. 2.

[79] D. Arbis and V. V Dixit, "Game theoretic model for lane changing: Incorporating conflict risks," *Accid. Anal. Prev.*, vol. 125, pp. 158–164, 2019.

[80] N. Li, D. W. Oyler, M. Zhang, Y. Yildiz, I. Kolmanovsky, and A. R. Girard, "Game theoretic modeling of driver and vehicle interactions for verification and validation of autonomous vehicle control systems," *IEEE Trans. Control Syst. Technol.*, vol. 26, no. 5, pp. 1782–1797, 2017.

[81] D. Sun and L. Elefteriadou, “Research and implementation of lane-changing model based on driver behavior,” *Transp. Res. Rec.*, vol. 2161, no. 1, pp. 1–10, 2010.

[82] D. J. Sun and L. Elefteriadou, “Lane-changing behavior on urban streets: A focus group-based study,” *Appl. Ergon.*, vol. 42, no. 5, pp. 682–691, 2011.

[83] S. of A. Engineers, “Operational definitions of driving performance measures and statistics.” Society of Automotive Engineers Warrendale, PA, 2015.

[84] G. of Ontario, “Highway Traffic Act.” Queen’s Printer for Ontario, 1990.

[85] S. Shalev-Shwartz, S. Shammah, and A. Shashua, “On a formal model of safe and scalable self-driving cars,” *arXiv Prepr. arXiv1708.06374*, 2017.

[86] C. Wang, Y. Xie, H. Huang, and P. Liu, “A review of surrogate safety measures and their applications in connected and automated vehicles safety modeling,” *Accid. Anal. Prev.*, vol. 157, p. 106157, 2021.

[87] T. Grüne-Yanoff and A. Lehtinen, “Philosophy of game theory,” *Uskali Mäki (Hg.), Handb. Philos. Econ. Oxford*, pp. 531–576, 2012.

[88] A. Geiger, P. Lenz, C. Stiller, and R. Urtasun, “Vision meets robotics: The kitti dataset,” *Int. J. Rob. Res.*, vol. 32, no. 11, pp. 1231–1237, 2013.

[89] P. Sun *et al.*, “Scalability in perception for autonomous driving: Waymo open dataset,” in *Proceedings of the IEEE/CVF Conference on Computer Vision and Pattern Recognition*, 2020, pp. 2446–2454.

[90] M. Montanino and V. Punzo, “Trajectory data reconstruction and simulation-based validation against macroscopic traffic patterns,” *Transp. Res. Part B Methodol.*, vol. 80, pp. 82–106, 2015.

[91] B. Coifman and L. Li, “A critical evaluation of the Next Generation Simulation (NGSIM) vehicle trajectory dataset,” *Transp. Res. Part B Methodol.*, vol. 105, pp. 362–377, 2017.

[92] A. Robicquet, A. Sadeghian, A. Alahi, and S. Savarese, “Learning social etiquette:

Human trajectory understanding in crowded scenes," in *European conference on computer vision*, 2016, pp. 549–565.

[93] D. Yang, L. Li, K. Redmill, and Ü. Özgüner, "Top-view trajectories: A pedestrian dataset of vehicle-crowd interaction from controlled experiments and crowded campus," in *2019 IEEE Intelligent Vehicles Symposium (IV)*, 2019, pp. 899–904.

[94] R. Krajewski, J. Bock, L. Kloeker, and L. Eckstein, "The highd dataset: A drone dataset of naturalistic vehicle trajectories on german highways for validation of highly automated driving systems," in *2018 21st International Conference on Intelligent Transportation Systems (ITSC)*, 2018, pp. 2118–2125.

[95] W. Zhan *et al.*, "Interaction dataset: An international, adversarial and cooperative motion dataset in interactive driving scenarios with semantic maps," *arXiv Prepr. arXiv1910.03088*, 2019.

[96] J. Bock, R. Krajewski, T. Moers, S. Runde, L. Vater, and L. Eckstein, "The ind dataset: A drone dataset of naturalistic road user trajectories at german intersections," in *2020 IEEE Intelligent Vehicles Symposium (IV)*, 2019, pp. 1929–1934.

[97] R. Krajewski, T. Moers, J. Bock, L. Vater, and L. Eckstein, "The rounD Dataset: A Drone Dataset of Road User Trajectories at Roundabouts in Germany," in *2020 IEEE 23rd International Conference on Intelligent Transportation Systems (ITSC)*, 2020, pp. 1–6.

[98] N. Y. S. D.-D. Manual-Chapter, "8: Defensive Driving." .

[99] A. Kesting, M. Treiber, and D. Helbing, "General lane-changing model MOBIL for car-following models," *Transp. Res. Rec.*, vol. 1999, no. 1, pp. 86–94, 2007.

[100] J. Sun, Z. Zheng, and J. Sun, "The relationship between car following string instability and traffic oscillations in finite-sized platoons and its use in easing congestion via connected and automated vehicles with IDM based controller," *Transp. Res. Part B Methodol.*, vol. 142, pp. 58–83, 2020.

[101] J. Wiest, M. Höffken, U. Kreßel, and K. Dietmayer, "Probabilistic trajectory prediction

with Gaussian mixture models," in *2012 IEEE Intelligent Vehicles Symposium*, 2012, pp. 141–146.

[102] O. Morgenstern and J. Von Neumann, *Theory of games and economic behavior*. Princeton university press, 1953.

[103] A. W. Tucker and P. D. Straffin Jr, "The mathematics of Tucker: A sampler," *Two-Year Coll. Math. J.*, vol. 14, no. 3, pp. 228–232, 1983.

[104] J. Nash, "Non-cooperative games," *Ann. Math.*, pp. 286–295, 1951.

[105] J. F. Nash, "Equilibrium points in n-person games," *Proc. Natl. Acad. Sci.*, vol. 36, no. 1, pp. 48–49, 1950.

[106] J. F. Nash, "4. The Bargaining Problem," in *The Essential John Nash*, Princeton University Press, 2016, pp. 37–48.

[107] L. S. Shapley, *17. A value for n-person games*. Princeton University Press, 2016.

[108] B. Hajek, "An Introduction to Game Theory," *Dep. Electr. Comput. Eng. Univ. Illinois Urbana-Champaign*, p. 116, 2017.

[109] M. J. Osborne and A. Rubinstein, *A course in game theory*. MIT press, 1994.

Appendix

In the appendix, the background for the thesis is presented. This section is structured as follows. Firstly, the components of the game theory are introduced, and the classification in terms of the information availability is stressed. Later, the type of incomplete information game is presented in detail. In the last section, the differences between the pure and mixed strategies are discussed.

A.1 Game theory introduction

A.1.1 The components of game theory

The Theory of Games and Economic Behavior systematically introduced the game theory for the first time in 1944 [102]. The noncooperative game theory is well developed with the research of "Prisoner's Dilemma" [103], [104], as well as the definition and existence of equilibrium [105] studied in the Nash's papers. Important results are also found in terms of the cooperative game theory in the papers published by Nash [106] and Shapley [107] in the same era.

Three are four important elements in a game, i.e., **players, actions, payoffs, and information** (**PAPI**). The modeler's goal is to describe an arbitrary situation in terms of these game rules. In order to maximize their payoffs, the players will select the actions based on the information available. The **equilibrium** is the result of each player's mix of actions. The modeler knows the results of the game from the combination of all the players' actions.

Players make decisions in a game. The purpose of each player is to maximize his payoffs through action selection. **Nature** is a pseudo-player who acts randomly with predetermined probabilities at typical points. The decision-makers are supposed to be "rational", which means they choose the strategies to optimize their predefined utilities.

An option made by player i indicated a_i, is an action or move. The action set of player i, $A_i = \{a_i\}$, $(i = 1, \ldots, n)$ is the set of actions.

The utility function $u_i(s_1, \ldots, s_n)$ of player i is a mapping from the measured states to the

real numbers. If the player is unsure about the states, his utility then becomes an expected value by introducing the probability distribution over the states.

If all the players know the information about the game, then the information is **common knowledge**. Furthermore, each player must be aware that each player is aware that each player is aware, and so on.

The **strategy** s_i of player i tells him the action or move to do at each time step during the game. $S_i = \{s_i\}$ is strategies set which is accessible player i. A strategy profile $s = (s_1, \dots, s_n)$ is composed of the strategy of each player in an order. The strategy advises him how to react to other players' activities.

An equilibrium $s^* = (s_1^*, \dots, s_n^*)$ is a strategy profile where each player has the optimum strategy. The equilibrium strategies denote that each player is required to maximize his own payoffs, considering the other players optimizing their payoffs simultaneously.

Player $i's$ best response to the other players' strategies s_{-i} is the strategy s_i^* that generates the greatest payoff for him

$$u_i(s_i^*, s_{-i}) \geq u_i(s_i', s_{-i}), \forall s_i' \neq s_i^* \tag{A.1}$$

The strategy s_i^d is dominated if the payoffs brought by it is lower than another strategy regardless of the other players' strategies, in the sense that his payout is lower with s_i^d regardless of the other players' strategies. If there is a single s_i' such that s_i^d is dominated mathematically,

$$u_i(s_i^d, s_{-i}) < u_i(s_i', s_{-i}), \forall s_{-i} \tag{A.2}$$

The strategy s_i^* is a dominant strategy if it is a player's strictly best response to any strategies the others may choose, when his payoff is highest with s_i^* regardless of what strategies others choose. Mathematically,

$$u_i(s_i^*, s_{-i}) > u_i(s_i', s_{-i}), \forall s_i' \neq s_i^* \tag{A.3}$$

A.1.2 Game types

Game modeling starts with recognizing important components including players, actions, payoffs, and information. After that, the game type should be determined. The classification of games is necessary as the real game related problems are coupled with factors of time, action sequences, information completeness, etc., which makes it complicated to find solutions. A specific problem can be resolved to the combinations of multiple simple games that only contain one dimension of these factors. Then the equilibriums can be solved by the well-studied models and theories.

Although the methods to solve the game vary greatly, the game classification helps to select the optimal algorithm. Considering the importance that influences how the game is modeled, it can be categorized according to, for example, whether the game is simultaneous or sequential, the binding commitments exist or not, the information is complete or incomplete.

Static Games and Dynamic Games

In a static game, both players make decisions at the same time and their moves are one-off. On the other hand, a dynamic game is either repetitive or sequential. A repeated game is one in which players make the same decision in the same situation repeatedly. In a sequential game, one player decides on his strategy before the other. The order of play exists, and the player who makes the initial decision usually has an advantage.

The visualization of a game could be a payoff matrix in the normal form or a decision tree in the extensive form. A payoff matrix lists the players, their strategies, and the payoffs. The rules of the game can be used to create a decision tree, which is a graphical representation of the game's order of play. Therefore, payoff matrix and decision tree are often used to describe static and dynamic game, separately. As the following prisoner’s dilemma example shows, the game can be described using different forms if the action rule is set differently.

Payoffs		Prisoner B	
		Betray	Do not Betray
Prisoner A	Betray	(-5, -5)	(-2, -9)

	Do not Confess	(-9, -2)	(-3, -3)

(a) Normal game

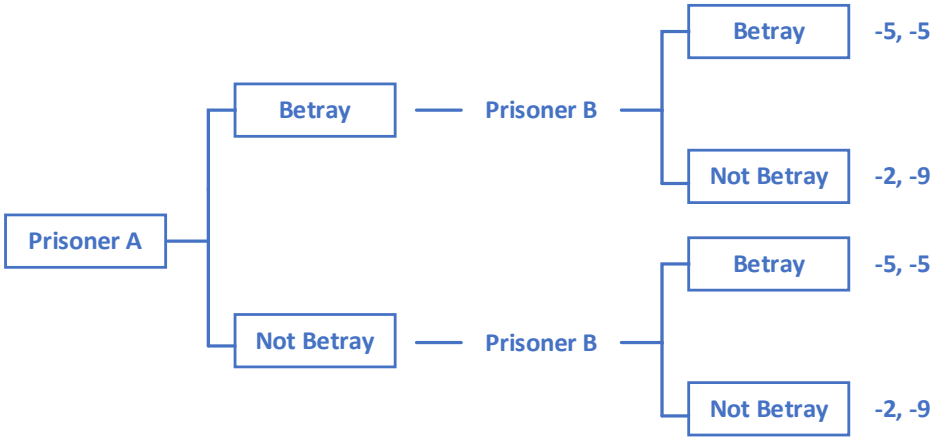

(b) Extensive game

Figure A.1 Examples of the normal and extensive games

Complete and incomplete information games

In the game of complete information, all players know the structure of the game, the fact that the other player knows all of this, the fact that the other knows that he knows, etc. The examples include Game of Chicken, Prisoner's Dilemma, Chess, Checkers etc. In these games, the players know about utility function/payoffs of each other. Incomplete information games were defined as the supplementary set of complete information games.

This ambiguous definition led game theorists to believe that incomplete information games could not be studied until 1967, when John Harsanyi demonstrated that incomplete information game could be turned into complete but imperfect information game by introducing the pseudo player Nature without changing its essentials.

Different from other players, Nature does not have its own payoffs or cost function. Nature moves first and determines the type of other players. The selected player knows his characteristics of which others are not aware. However, the probability distribution of the selected player's characteristics is known to himself and other players, i.e., the probability distribution is common knowledge. This process is called Harsanyi transformation. In this way, if Nature chooses the players' types first, the complex concept of incomplete information can

be transformed to a game of imperfect but complete. The players do not know the exact choice of Nature but the probability distribution of all possible choices. Then each player is assumed to know the distribution of his opponents' types, and the expected utility can be calculated by selecting actions from action set.

Cooperative games and non-cooperative games

The criterion to determine cooperative and non-cooperative games is clear. A cooperative game is a game where the players can make binding commitments, which is externally forced to be protected. If the players cannot form such agreements or need to be self-forcing, the game is non-cooperative. Cooperative game focuses on outcome properties instead of the strategies to achieve the outcome. In a noncooperative game, players are required to maximize their personal utility functions. The Prisoner's Dilemma is a game in which each player attempts to maximize the utility function. It might, however, be modelled as a cooperative game if the players have access to communicating with each other and make binding contracts.

A.2 Incomplete information game

For the lane change in the highway modelled by the game theory, the information is important for the decision-making because the drivers are not homogeneous. The human-like strategies are largely dependent on the interactive objects. Therefore, the incomplete information game is selected to be the target model for the highway lane change.

$G = (I, (S_i)_{i\in I}, (\Theta_i)_{i\in I}, (u_i(s,\theta))_{i\in I}, p(\theta))$ is an incomplete information game, which satisfies [108]

- I is the finite set of players;
- For each $i \in I$, S_i is a set of actions accessible to player i, and $S = \mathrm{X}_{i\in I} S_i$ is the set of action profiles, with a specific element $s = (s_i)_{i\in I}$;
- Θ_i is a set of player i's types and $\Theta = X_{i\in I}\Theta_i$ is the set of all players' types, where a specific element is $\theta = (\theta_i)_{i\in I}$;
- Given s and θ, $u_i(s,\theta)$ is the payoff of player i;
- p is a probability mass function (*pmf*) over set of players' types Θ.

The above definition of incomplete information game shows that nature chooses a type assignment using *pmf* p at the start of the game, and the player i knows its own type, θ_i. The categories of the

other players are not revealed to the players; θ_i is regarded personal information of player i. The conditional probability distribution of the possible types of other players, $p(\theta_{-i}|\theta_i)$, is known by each player i, because all players are supposed to know p, the *pmf* over Θ. The players are required to choose a move that is dependent on their own types, after their types are learned by themselves; The pure strategy s_i for a player i can then be defined as a mapping from the player type to the actions set $s_i : \Theta_i \to S_i$.

If for each player $i \in I$ and each player type $\theta_i \in \Theta_i$ in a game

$$s_i(\theta_i) \in \arg\max_{s_i' \in S_i} \sum_{\theta_{-i}} p(\theta_{-i} \mid \theta_i) u_i(s_i', s_{-i}(\theta_{-i}), \theta_i, \theta_{-i}) \tag{A.4}$$

then $(s_i(\cdot))_{i \in I}$ is a Bayesian (or Bayes-Nash) equilibrium. Given the player i taking strategy s_i', and his type θ_i, the expected payoffs can be calculated by summing up the utilities over all possible strategies in S_i. A randomized pure strategy is a mixed strategy for the player i. The profile of the mixed strategies is a Bayesian equilibrium, if the expected payoff of any specific player i is maximized with the mixed strategy, while the other players also utilize the mixed strategies. The Bayesian equilibrium exists in any finite Bayesian game with the mixed strategies.

A.3 The pure and mixed strategies

In some games, the Nash equilibrium may not exist if there are only pure strategies considered, which is defined as

A **pure strategy** maps the available information sets of each player to one action: $s_i : \Theta_i \to S_i$. Expanding the strategy space to include random strategies is frequently useful and realistic, and in this situation, a Nash equilibrium almost always exists. These random strategies are called "**mixed strategies**."

If the action space of player i is S_i, then the probability distributions space is denoted by Σ_i over S_i. For player i a mixed strategy is a probability distribution σ_i over S_i: To put it another way, $\sigma_i \in \Sigma_i$. Let $f(s_i)$ denote the mapping from the strategy $s_i \in S_i$ to a real number: $f: S_i \to \mathbb{R}$. We typically employ the notational convention $f(\sigma_i) = E_{\sigma_i}[f]$ when σ_i represents a mixed strategy for player i. The probability vector σ_i satisfies $f(\sigma_i) = \sum_{s_i \in S_i} f(s_i)\sigma_i(s_i)$. If the mixed strategies are utilized by the player in a normal form game, we suppose that each player i's random choice of pure strategy is determined using distribution

σ_i, which is independent to the strategies of other players. The expected payoff for player i abbreviated $u_i(\sigma)$, or, equivalently, $u_i(\sigma_i, \sigma_{-i})$ represents expectation of $u_i(\sigma)$ with regard to the product probability distribution $\sigma_1 \otimes \cdots \otimes \sigma_n$ for a mixed strategy profile $\sigma = (\sigma_1, \ldots, \sigma_n)$.

An important proposition regarding to the mixed strategies is that every finite strategic game has a mixed strategy Nash equilibrium [109]. This proposition guarantees that the probabilities of the decisions can be generated in any lane change scenarios at any time.

A.4 Summary

In the appendix, the background knowledges of this study are presented. As a well-developed method to deal with the human-like agent interactions, some basic concepts of game theory are introduced. Compared with other methods, one of the advantages of game theory is that it can list all the possibilities by considering the mutual active interactions in the utility functions. Meanwhile, game theory avoids the heavy calculations that happen in the DBN where the casual relations are represented by the probability graph.